JOURNAL OF APPLIED PHYSICS

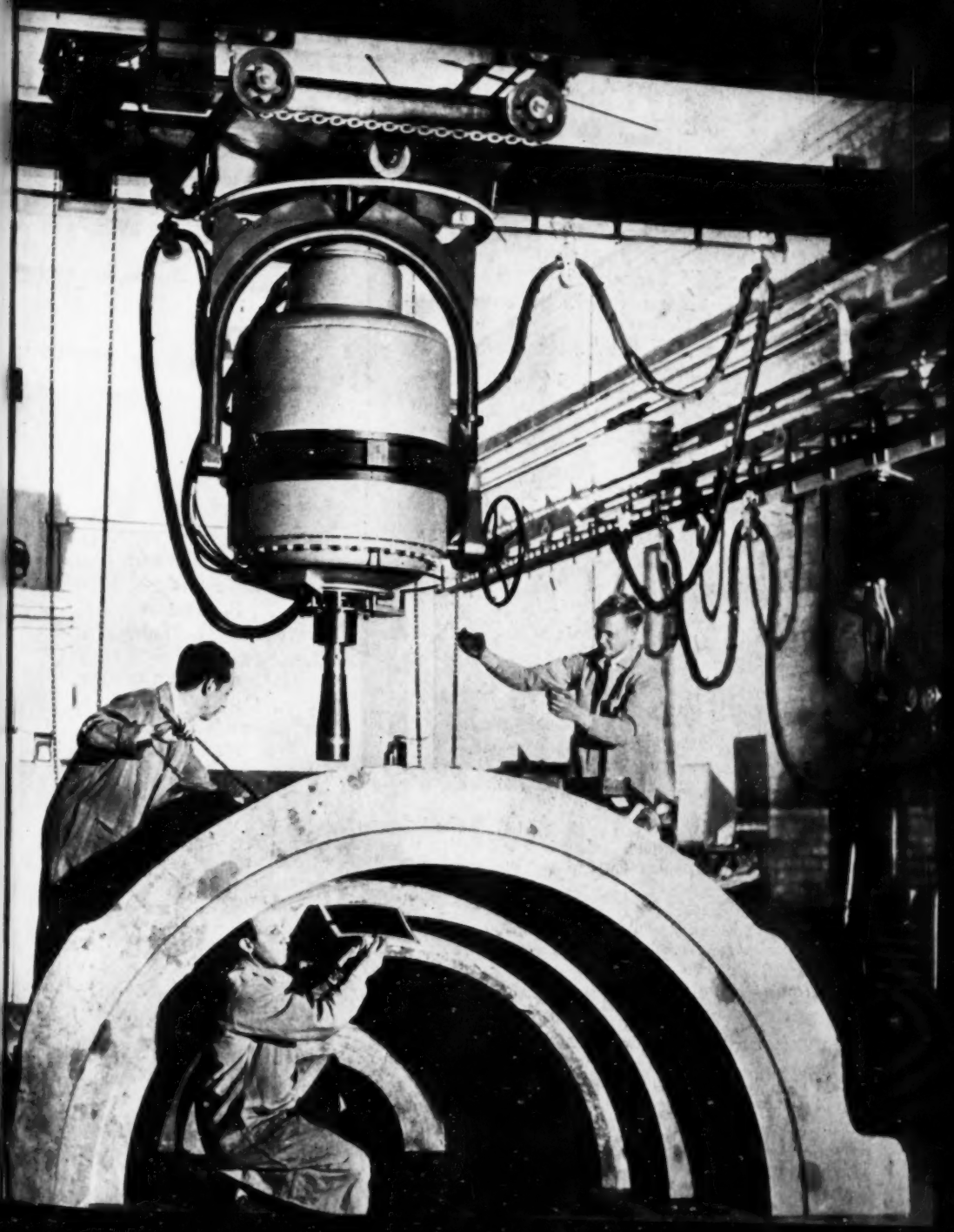

JOURNAL
OF
APPLIED PHYSICS

APRIL, 1942 Vol. 13, No. 4

In This Issue

Page

A Challenge to Physicists P. W. BRIDGMAN 209

Frictional Phenomena. VIII ANDREW GEMANT 210

Résumés of Recent Research 222

Contributed Original Research

Magnetization Near Boundaries JAMES H. WAKELIN, JR. 227

Amontons' Law, "Traces" of Frictional Contact, and Experiments on Adhesion ROBERT SCHNURMANN 235

Model Method of Photographic and Photometric Determination of Heat Radiation Between Surfaces and Through Absorbing Gases MAX JAKOB AND G. A. HAWKINS 246

Diffusion of Heat Through a Rectangular Bar and the Cooling and Insulating Effect of Fins. I. The Steady State MELVIN AVRAMI AND J. B. LITTLE 255

New Approach to the Study of Arcback JOHN E. WHITE 265

In Every Issue

Calendar of Meetings 221

New Books 224

Here and There 226

Innovations in Instruments 274

Index to Advertisers xiv

BOARD OF EDITORS

ELMER HUTCHISSON, *Editor*

Associate Editors

FRANCIS BITTER
W. F. BUSSE
S. H. CALDWELL
ROBLEY D. EVANS
MORRIS MUSKAT
FREDERICK SEITZ
B. E. WARREN
J. B. WHITEHEAD

Publication of the American Institute of Physics

ADMINISTRATIVE STAFF

HENRY A. BARTON, *Director*

MADELINE M. MITCHELL, *Publications Manager*

JOHN T. TATE, *Adviser on Publications*

GOVERNING BOARD

PAUL E. KLOPSTEG, *Chairman*
GEORGE B. PEGRAM, *Secretary*
R. B. DOW
L. A. DUBRIDGE
FLOYD A. FIRESTONE
HARVEY FLETCHER
R. C. GIBBS
K. S. GIBSON
ARTHUR C. HARDY
GEORGE R. HARRISON
HERMANN MARK
A. G. WORTHING
JOHN T. TATE
N. W. TAYLOR
WALLACE WATERFALL

The JOURNAL OF APPLIED PHYSICS, published monthly at Prince and Lemon Sts., Lancaster, Pa., is devoted to physics in its role as the science basic to other natural sciences and to the arts and industries. Previous to 1937 this publication was known as PHYSICS. It aims to be of service not only in physical laboratories, but also in the laboratories of industrial, chemical, geological, geophysical, meteorological, radio, and similar concerns. The JOURNAL OF APPLIED PHYSICS publishes editorials, news of physicists and reviews, as well as technical papers of applied physics.

Manuscripts should be submitted to Elmer Hutchisson, Editor, American Institute of Physics, 175 Fifth Avenue, New York, New York.

Subscriptions and orders for back numbers should be addressed to Prince and Lemon Streets, Lancaster, Pa. or to the American Institute of Physics, 175 Fifth Avenue, New York, N. Y.

SUBSCRIPTION PRICE

	U. S. AND CANADA	ELSEWHERE
To members of scientific societies	$5.00	$5.70
To all others	7.00	7.70

Single copies are $.70 each.

Changes of address and proofs should be addressed to the Publications Manager.

Advertising rates supplied on request. Orders, advertising copy and cuts should be sent to the American Institute of Physics.

Entered as second class matter at the Post Office at Lancaster, Pennsylvania, under the Act of March 3, 1897. Accepted for mailing at the special rate of postage provided for in the Act of February 28, 1925, authorized May 2, 1932.

Copyright 1942, by the American Institute of Physics.

Journal
of
Applied Physics

Volume 13 April, 1942 Number 4

A Challenge to Physicists

By P. W. Bridgman
Harvard University, Cambridge, Massachusetts

THAT physicists are making an important technical contribution in the present crisis is readily conceded; I believe it is in their power however, if they will only seize the opportunity, to make another contribution which ultimately may prove even more important.

From a long-range point of view the deepest issues of the present crisis are intellectual. The failure of this country up to the present has been primarily an intellectual failure—intellectual sloth, lack of imagination, and wishful thinking. The crisis of a totalitarian victory is, from the perspective of ten thousand years, an intellectual crisis. The day when the human race may evolve into a race capable of the intellectual mastery of its fate will be immeasurably postponed by such a victory. The fundamental thesis of the totalitarian philosophy is an intellectual monstrosity; to maintain that the individual is subordinate to the state simply does not make sense, and it is an intellectual affront to be asked to accept it. The only society which can successfully maintain such a thesis is a society intellectually half slave and half free, a society in which compartments of intellectual activity are forever closed to scrutiny by edict. More than this, the totalitarian philosophy is actively anti-intellectual, even anti-intelligent. The totalitarians do not like to have people use their minds, and are committed to produce a society in which it will be impossible.

There is no minimizing the enormous difficulty and complexity of the task of acquiring intellectual mastery of our fate. In fact, to many people the difficulties are so patent that they have no confidence that a solution is possible. There are disturbing signs everywhere, here as well as in the totalitarian countries, of an anti-intellectual movement. There is no will to intellectual survival; there is intellectual defeatism and intellectual appeasement. Even without a totalitarian victory there is danger that Hitler may have done a permanent disservice to the race if the present intellectual defeatism, for which he is largely responsible, persists.

The race will not save itself until it achieves intellectual morale. Perhaps the two chief components of intellectual morale are intellectual integrity and a fierce conviction that man *can* become the master of his fate. The physicist is peculiarly likely to possess the two components of intellectual morale. A lifetime in the laboratory, struggling to make things work, has shown the inexorable need of intellectual integrity. And as a participant in the one most successful intellectual enterprise of the human race to date, that is, the technological mastery of nature to the extent achieved by modern physics, he is in a peculiar position to have won the conviction that not only is there no substitute for using one's mind, but that the problems which confront us are soluble and soluble by us. If physicists will only make others see their own wider vision, their ultimate influence will far transcend that of any possible technological contribution.

Frictional Phenomena. VIII

BY ANDREW GEMANT
The Detroit Edison Company, Detroit, Michigan

Chapter VIII. Structural Viscosity

Abstract

GEL formation in colloidal systems causes the viscosity of such systems to vary with the stress: these are called non-Newtonian liquids. Because the physical cause of such behavior is related to the gel structure, the phenomenon is called structural viscosity. Three particular features are observed with such systems: a non-linearity of the rate of shear *vs.* stress relation in the case of stationary flow; a finite relaxation process for suddenly applied stresses or deformations; and a frequency dependent dynamic viscosity in the case of alternating processes. The chief experimental facts in these three fields are presented, together with certain semitheoretical equations best suited to describe the experiments.

31. Non-Newtonian Behavior in General, and in Particular with Regard to Gel-Forming Colloidal Systems

We now come to a most interesting departure from a general principle found valid hitherto in this monograph. The mathematical theory outlined in Chapter I assumed the viscosity coefficient, as defined by Eq. (6), to be independent of the rate of shear, and thus a characteristic constant of the material. This assumption was fully justified by all the experimental facts known about gases and liquids, and was supported by the physical theories, which indicated a proportionality between stress and rate of shear.

A departure from this general behavior, however, was observed first by Trouton and Andrews during their investigation of certain highly viscous pitch-like liquids. They observed that the viscosity coefficient was not a constant, but decreased with increasing rate of shear. A large number of authors, among others Bingham and Wo. Ostwald, devoted themselves to the study of this intriguing subject.

The fundamental phenomenon is represented schematically by Fig. 48. Here the abscissae indicate stress or pressure, and the ordinates rate of flow measured by means of any of the apparatus described in Chapter VI. Curve 1 shows the relation in cases of complete proportionality, as considered up to now. The reciprocal of the gradient of curve 1 is a measure of the viscosity η. Such liquids are called Newtonian, since it was Newton who originally postulated Eq. (6). Curve 2 indicates the behavior of a liquid that departs from this law. The rate of flow increases more than proportionally with the stress; the viscosity, given by the reciprocal of the differential quotient of the curve, can be seen to decrease with increasing stress or, in other words, the fluidity increases with increasing stress. Liquids exhibiting such behavior are termed non-Newtonian.

Before proceeding further in this matter it will be well worth pointing out that the proportionality as shown in curve 1 of Fig. 48 is possibly a limiting law for "low" stresses, generally valid for all liquids. It might be that in Newtonian liquids the divergence from linearity occurs at high stresses that are not usually met in practical cases. It is also possible that turbulence usually occurs before such a departure is observable, although it should be mentioned that certain very viscous liquids like honey, with practically no tendency to turbulence, show no sign of non-linearity up to the highest stresses applied. The reason for believing in such a general non-linearity is more theoretical than experimental. In Section 20 a brief outline of Eyring's theory was presented, and Eq. (67) was given as a theoretical expression for η. However, Eq. (67) is only a limiting case for "low" stresses, more specifically for stresses S that fulfil the condition

$$S\lambda^3 \ll 2kT, \tag{95}$$

where λ = average distance between neighboring molecules. The equation, derived for η, contains

the factor

$$\frac{S}{\sinh\,(S\lambda^3/2kT)} \tag{96}$$

and if (95) holds, the series expansion of the hyperbolic function can be approximated by the argument. The stress S then cancels out, and finally Eq. (67) is obtained. If, however, (95) no longer holds, the viscosity will contain the factor (96), rapidly decreasing with increasing S. Thus, non-linearity proves to be a general attribute. It appears that in this case, as in a number of other instances in physics, linearity between two

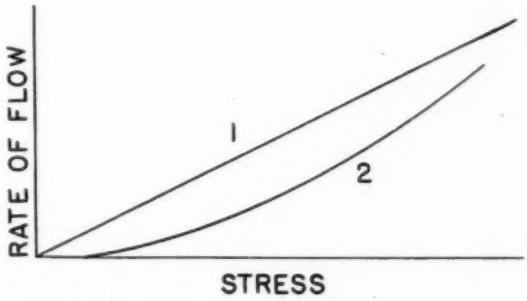

FIG. 48. Diagram of flow curve for Newtonian (1) and non-Newtonian (2) liquids.

measurable quantities is only a limiting case for "low" values of the quantities in question. Even in this monograph several such instances will be encountered in the forthcoming chapters. (Compare, for instance, the section on electrical conductivity in Chapter XII.)

The reason that most liquids obey the linear law can be seen by putting numerical values into (95). With an average shearing stress of $S \sim 100$ c.g.s. units, and $\lambda \sim 5 \times 10^{-8}$ cm, the left-hand side is several orders of magnitude smaller than the right-hand side ($\sim 10^{-13}$ at room temperature). Hence, a deviation from the linear law will not be observable.

The domain of non-Newtonian liquids is not that of homogeneous liquids with which Eyring's theory is primarily concerned. According to all available experimental data non-linearity is observed only on heterogeneous, colloidal systems. Because of the fact that the phenomenon is related to the physical structure of the liquid, it is also called structural viscosity.

Looking for a general characteristic of liquids possessing structural viscosity, it can be stated that the dispersed particles have to be in such a state as to influence each other sufficiently. Thus, a typical sol of low particle concentration (see Section 28) cannot show structural viscosity, since its particles are independent. Gels, on the other hand, are the typical domain for structural viscosity, since the particles not only influence each other, but form a network. There are cases of non-linearity in which the mutual influence does not go quite so far, but even in those (concentrated sols, bentonite suspensions) strong attractional forces must exist between the single solvated particles. In fact, probably all typical suspensions and emulsions will show structural viscosity, if the concentration is high enough for the particles either to touch, or at least to attract each other strongly.

A complete theory of structural viscosity does not yet exist. By a "complete theory," we mean a physical theory that takes account of the actual underlying displacement and motion of the particles of the system. There have been a few attempts to develop general theories on a more abstract, mathematical basis. Such general theories have not proved very fruitful with regard to the interpretation of experimental results which is, after all, the aim of a good theory. Among the several attempts, one by Hencky,[1] and one by Weissenberg[2] should be quoted, both working on the basis of the theory of continua to which certain hypothetical properties are attributed.

The reason that a physical theory is not yet developed will be understandable if one considers the extremely complicated elementary processes occurring in a shearing motion of a gel-like structure. For the sake of illustration, the influence of single elongated particles upon viscosity, as discussed in Section 29, should be quoted. There the elementary process is an orientation of particles, becoming stronger with increasing shear and causing a gradual decrease of the effective viscosity as explained by means of expression (88). Thus it can be seen that the presence of separate sol-like particles also causes a certain non-linearity although, for reasons similar to that in the case of homogeneous liquids, this feature is not generally observable in experiments. The complete mathematical theory of that phenomenon is rather involved,

and part of it exists only in the form of approximations. It is evident, however, that the flow of concentrated sols or gels is incomparably more complicated than that of diluted sols. If, then, the theory of this latter is involved and partly only approximate, our lack of a physical theory in the more complicated case will easily be understood.

The existing more special treatments of structural viscosity are semitheoretical. The equations used for the description of experimental data are based upon certain plausible theoretical assumptions and then empirically adjusted to suit the facts. In the following sections an outline of these basic assumptions will be given, and the equations derived along these lines will be presented. Also, the chief experimental data on a number of representative systems will be given.

32. Physical Basis of Structural Viscosity

As has been stated before, all liquids exhibiting non-linear flow, as shown in Fig. 48, are either concentrated suspensions and emulsions or gels, or else sols in which there is a strong indication of mutual interaction between particles. Before proceeding further it will be useful to point out that there is no strong demarcation line between a typical gel (such as gelatin) and certain sols in which the particles are not independent of each other. In earlier times it was assumed that a sol-gel transition required the change of an essential variable of the system. Such a variable is, for instance, the temperature; its decrease often effectuates the transition of a sol into a gel. The concentration of the dispersed phase is also such a factor: a dilute colloid is often a sol, a concentrated one a gel. In the last two decades, however, certain systems have been discovered wherein the same solution at a given temperature can be either a sol or a gel, the gel-sol transition being brought about by mechanical agitation. When the system is left standing, it is slowly converted into a gel again. The latter appears to be the more stable equilibrium, but it is evident that the two states differ only in the orientation of the particles, and their energy levels do not differ by considerable amounts.

This reversible gel-sol transformation is called thixotropy; it was discovered and further investigated by H. Freundlich[3,4] and his pupils. A typical object is, for instance, an iron oxide sol; later additional research was carried out by E. A. Hauser[5] on bentonite suspensions. Systems exhibiting thixotropy clearly indicate that there is only a difference of degree between a gel and certain sols.

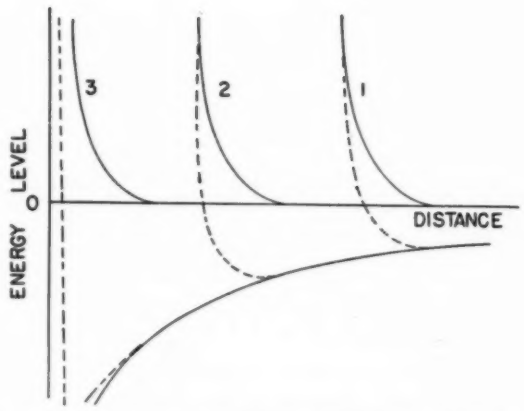

FIG. 49. Diagram of possible equilibrium positions between neighboring particles of a colloidal system (after H. Freundlich).

The difference between a gel and a sol is brought out by the consideration of potential levels, and this will now be explained by means of a potential diagram after Freundlich (Fig. 49). The abscissae show the distance between two particles, and the ordinates the potential energies of repulsion and attraction, the former being positive, the latter negative. Attraction forces are those of the van der Waals-London type, whereas repulsion is due to the ionic cloud, being the outer shell of the electric double layer. The thickness of this layer and thus its sphere of action might vary with conditions; for instance, it decreases with increasing concentration of electrolytes as shown by curves 1, 2, and 3. The dotted lines represent the resultant potentials, obtained by algebraic addition of the two components. In case 1 the whole range of distance is one of repulsion, the particles are kept apart, and the system is a stable sol. In case 2 there is a pronounced minimum in the potential curve, indicating an equilibrium position with a given separation of neighboring particles. This case corresponds to that of a sol with strong interaction between particles. It is as if a network were formed—not a static one however, but a statistical one, changing the

actual configuration continuously with time. Finally, case 3 corresponds to predominating attraction over the whole range of distances, equilibrium occurring when the particles practically touch. If the particles are strongly solvated to prevent precipitation, such a condition will correspond to the formation of a regular static structure, i.e., a gel.

It can thus be seen that a structure in a physical sense is not restricted to a static gel, but can be represented just as well by certain concentrated sols with pronounced equilibrium distances between particles. Whether this distance is only a small fraction of the particle size (gel) or of the same order as the particle size (sol) is not an essential difference, as long as equilibrium positions are present.

It thus appears that the condition necessary for a system to be non-Newtonian is the existence of pronounced equilibrium positions between the dispersed particles. From the theory of elasticity it is known that this is precisely the chief characteristic of an elastic continuum. In other words, non-Newtonian liquids are two-phase systems in which the dispersed phase forms an elastic continuum. For this reason non-Newtonian liquids are called also elasto-viscous, and the whole phenomenon, elasto-viscosity.

A physical theory of elasto-viscosity ought to start from such disperse systems and to explain the different phenomena. Such a theory is still missing, as was pointed out previously. However, the recognition of elasticity as an essential feature has led to the semitheoretical formulas to be explained below. From among the recent literature in this field, a paper by Myers and France[6] may be mentioned, giving an explanation of gel formation, particularly of egg albumin as disperse phase. Arnold and Goodeve[7] have studied the thixotropy of carbon black suspensions in mineral oil, and have tried to interpret the results by means of certain theoretical assumptions. Dube and Dasgupta[8] have considered the van der Waals-London interaction energy between disk-shaped particles when they are parallel to each other. The results can be used for the interpretation of thixotropic substances. Ford, Loomis, and Fidiam[9] have considered the crystal structure of clays and the ionic double layers at the crystal surfaces in connection with the gel-forming properties of their suspensions.

33. Stationary Flow

First, the process of stationary flow under a constant external pressure will be considered. From among the many equations or "theories" only two will be presented, as being the most representative, both operating with the conception of elasticity.

One, suggested by Bingham,[10] also by A. Szegvari—a pupil of H. Freundlich,[11] takes account of the elastic dispersed phase and assumes that at low stresses it opposes the flow of the liquid, and in so doing becomes deformed, like a solid elastic body. At a certain stress, which might be called the rigidity of the system or its yield value, the resistance of this structure is overcome, and the liquid will flow just like any normal liquid that has a constant viscosity. The dispersed phase could then be pictured schematically as in Fig. 50. Here the liquid in a tube is under an increasing pressure head. In *a* the pressure is below the yield value, the particles hold together and only a slight deformation results, and the velocity is zero. In *b* the yield value is exceeded, the structure is broken, and the liquid flows with a parabolic profile. In the middle of the tube the shearing stress is

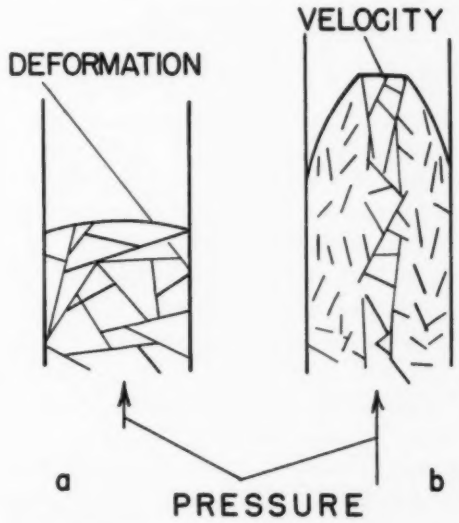

FIG. 50. Deformation and velocity profiles in a capillary tube of a structure-viscous liquid; (a) pressure below yield-point; (b) pressure above yield-point.

so low that it drops below the yield value and the structure is held together; this part of the liquid is extruded like a plug at a velocity independent of the distance from the axis.

Formulating the flow equation one must differentiate strictly between the equations referring to a single volume element and those referring to a complete physical apparatus like a capillary tube or the Couette apparatus. If

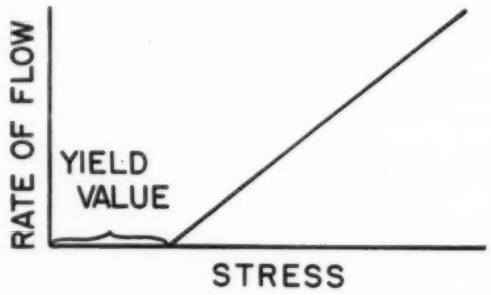

FIG. 51. Diagram of flow curve according to Eq. (97).

the former is known, the latter can be obtained by means of integration, just as Eq. (27), for a complete apparatus was obtained by starting from Eq. (6), which is valid only for a volume element.

Equation (6) can be written in the form

$$S=\eta(du/dy),$$

where S is the shearing stress (denoted by $-X_y$ in Eq. (6)). An extension according to the consideration above involves the introduction of the rigidity, S_0, the equation reading

$$S-S_0=\eta(du/dy) \qquad (97)$$

for $S>S_0$. For $S<S_0$, $(du/dy)=0$. Using Eq. (97) for an apparatus gives the following result, as shown diagrammatically in Fig. 51: up to a certain yield value (proportional to S_0) no flow takes place; for stresses beyond this limit there is proportionality between stress and rate of flow. It can be seen that the line represented by Fig. 51 is a first approximation to curve 2 of Fig. 48.

There is some controversy in the literature as to whether Eq. (97), assuming a definite yield value of stress, or pressure, below which no flow occurs, is an adequate description of experimental results. A large number of observations can be reproduced by means of Eq. (97), since the motion at low stresses is practically zero. However, there is reason to believe that actually no yield value exists, that is, the motion at small stresses is finite though often below the sensitivity of the apparatus. Thus, the equation appears practically useful, but theoretically unsatisfactory. The second equation to be discussed below does not assume a yield value.

Measurements of Wolarowitsch and co-workers[12] on pastes indicate fairly pronounced yield values: 1500 dynes/cm² for a 55 percent kaolin paste and 2400 dynes/cm² for a 25 percent carbon black paste in oil.

The present author has carried out measurements on lubricating and cable oils[13] and has found pronounced structural viscosity in some of them. A modification of the capillary method was used, the time for a given volume to flow through the capillary being measured. Fig. 52 shows the result on a particular cable oil, the abscissae being pressures and the ordinates reciprocals of the time t. It can be seen that at 50°C the oil behaves normally but below that temperature shows structural viscosity; because of the reduced Brownian movement the particles occupy more and more the equilibrium positions shown in Fig. 49, thus gradually forming a gel. The observed data seem to fit Eq. (97) well but, as pointed out, it is quite possible that an intercept of the line with the abscissae is only illusory and that in reality they touch asymptotically. Non-Newtonian behavior is by no means the characteristic of highly viscous systems. The viscosity of the oil in question is about 10 poises at 40°C. In comparison, other oils of a viscosity of 3000 at 0°C behaved perfectly normally.

Breazeale[14] in his study on the structural viscosity of cellulosic solutions forced a pigmented specimen of the liquid through an untreated one. From an observation of the profile he was able to conclude that a definite yield value does not exist. Hobson[15] investigated the flow properties of clay suspensions, particularly the question of the existence of a yield value. Certain observations could be explained by assuming thixotropic properties.

We now turn to another semitheoretical equation that appears to be more reliable than

Eq. (97), although it is far from being a physically founded one. Eisenschitz[16] contends that the equation in question can be deduced on the basis of the elaborate theories of Hencky and Weissenberg.[1,2] However, because of the considerable abstractness of those theories, this is not of much help.

The equation will not be deduced here, but simply explained.

Equation (6) is taken as valid with the extension that η is not a constant but a function of S itself, as can be seen from Fig. 48. Three assumptions are now made.

1. At very low stresses curve 2 on Fig. 48 starts out as a straight line, corresponding to an initial viscosity η_0. This viscosity is that of the undisturbed complex structure (*a* in Fig. 50), since in the general case (curve 2 of Fig. 49) it is understandable that a slow exchange of positions will take place even at lowest stresses.

2. At highest stresses the liquid behaves normally again, corresponding to a viscosity η_∞. The existence of such a value, i.e., the fact that curve 2 of Fig. 48 approaches line 1 asymptotically at highest stresses, was shown in a number of cases by Wo. Ostwald and co-workers.[17] This situation corresponds to the particles broken up and prevented by the shear from occupying equilibrium positions. η_∞ is evidently always smaller than η_0.

3. The transition from η_0 to η_∞ must occur when S becomes of the order of a characteristic quantity, and this quantity evidently has to be identified with the rigidity of the structure,

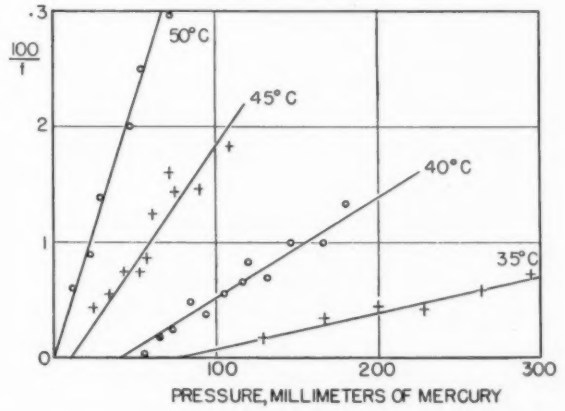

FIG. 52. Flow curves in a capillary tube of a lubricating oil (A. Gemant).

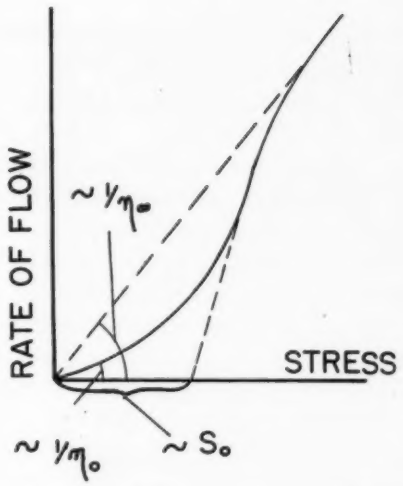

FIG. 53. Diagram of flow curve according to Eq. (98).

previously designated by S_0. Thus the argument of the viscosity function must be S/S_0, so that transition occurs when the argument becomes 1. Since the direction of the stress cannot have any influence on the value of the viscosity, the argument must be $(S/S_0)^2$.

The simplest equation that fulfills the three basic assumptions, derived from the structure as pictured in Section 32, is the following:

$$\eta = \eta_\infty + \frac{\eta_0 - \eta_\infty}{1+(S/S_0)^2}, \tag{98}$$

a form obtained by Reiner.[18] Figure 53 shows the general behavior in an apparatus of a liquid, obeying Eq. (98). The differential quotient of the flow curve is first proportional to $1/\eta_0$, then at a stress of the order S_0 changes and finally settles at a value proportional to $1/\eta_\infty$.

In order to evaluate experimental results from measurements with capillary tubes it first must be ascertained how the Poiseuille law is affected if Eq. (98) for the viscosity is introduced. Philippoff[19] shows that the original Poiseuille law can be used to calculate an equivalent viscosity η_P which is then given by

$$\eta_P = \eta_\infty + \frac{\eta_0 - \eta_\infty}{1+\frac{2}{3}(S/S_0)^2}. \tag{99}$$

From Eq. (99) the constants η_0, η_∞, and S_0 can be computed. If the Couette apparatus is used, again the original Eq. (77) can be used to derive

an equivalent viscosity η_C. An equation analogous to (99), with a numerical factor different from $\frac{2}{3}$, is then used for the computation of the constants.

As an illustration, measurements by Hatschek,[20] by means of the Hatschek-Couette apparatus,[21] on starch suspensions in a mixture of paraffin oil and carbon tetrachloride are reproduced (Fig. 54). The abscissae are stresses on an arbitrary logarithmic scale, the ordinates angular velocities, also on an arbitrary logarithmic scale. Starch concentrations from 2 to 8 percent were measured. The characteristic shape of the curve as shown in Fig. 53 can be seen also in the logarithmic scale. The three characteristic constants as calculated by Phillippoff are shown in Fig. 55 as a function of the concentration. While η_0 and S_0 increase considerably with the concentration of the starch, the variation of η_∞ is only slight, as can be expected from the picture given in Section 32. The dependence on concentration and temperature of η_0 of acetyl cellulose in dioxane after data of Philippoff[22] is given in Fig. 56.

Table IX is a summary of computations carried out by Philippoff on several colloidal systems tested by different authors. Column 1 gives the system, the following columns η_0, η_∞, and S_0 in c.g.s. units. The last column is the ratio $\eta_0/S_0=\tau_0$, the so-called time constant to which reference will be made in Section 34.

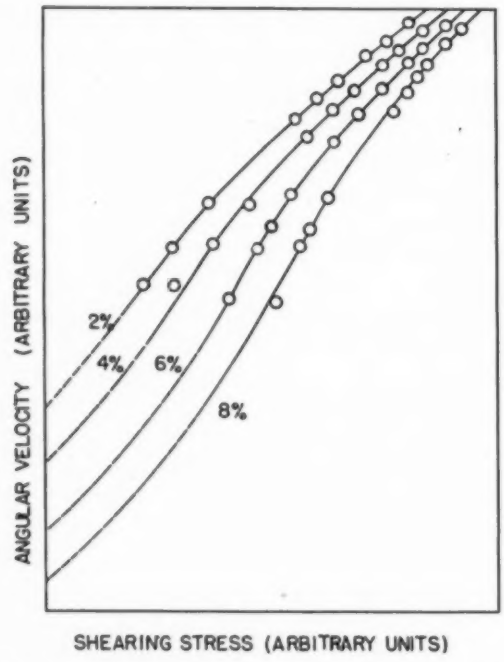

FIG. 54. Flow curves of starch suspensions of different concentration in a mixture of paraffin oil and carbon tetrachloride (E. Hatschek and R. S. Jane).

34. Relaxation Processes

Having reviewed the processes at stationary flow, a second group of observations, the so-called relaxation processes, has to be mentioned. Whereas normal liquids are not able to maintain a static strain because flow immediately sets in, elasto-viscous liquids are able to do so, to a certain extent at least. They occupy a position of transition between liquids and solids in this respect, which is understandable since they exhibit both viscosity (property of liquids) and elasticity (property of solids). If a certain stress is rapidly applied, the structure will not break, but will suffer a deformation, like any elastic body of low modulus of elasticity, rubber, for instance. When now the deformation is maintained, and the stress measured, it will be found that the latter decreases with time, and finally disappears completely. The reason is that the structure slowly breaks up, flow starts, and a new structure, corresponding to the new shape of the body, will be built up. Because the new configuration is a new equilibrium position, no external stress is associated with it. This process is termed relaxation.

TABLE IX. Constants of certain structural-viscous liquids, according to Philippoff.

System	η_0	η_∞ in c.g.s. units	S_0	τ_0 sec.
45% gum arabic sol at 30°C	2.7	0.40	0.09	30
Sulphur melt at 120°C	0.21	0.010	0.07	3.0
Cholesterin butyrate at 100°C	2.4	0.35	1.0	2.3
Hexane 70%, methanol 30%	0.03	0.003	0.05	0.7
Polystyrene 0.4% in tetralin	4.0	1.0	500	0.008
Viscose 4%	4.4	2.2	970	0.004

Although understandable qualitatively, a strict quantitative physical theory is missing, just as in the case of the flow process. However, semi-theoretical equations are used with fair success, here as well as there. One of these equations, suggested by Maxwell, is explained below, although it is only approximately valid.

The theory of Maxwell on elasto-viscosity is purely formal and thus cannot be expected to

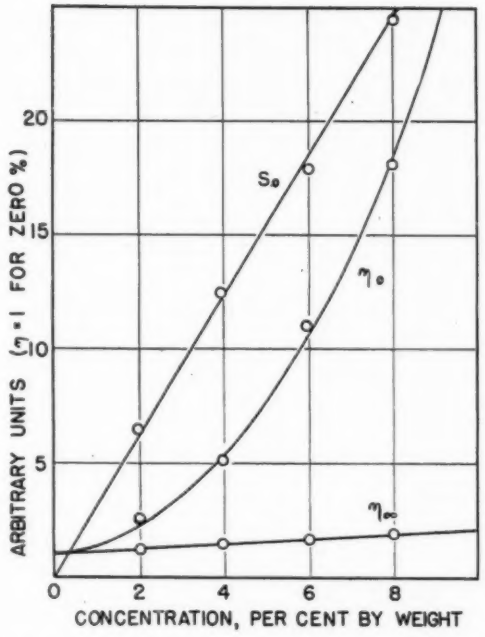

FIG. 55. Characteristic constants of starch suspensions (Fig. 54), computed by W. Philippoff.

hold rigorously. Still it is a useful guide in understanding these phenomena, and besides, has definite connections with the physical picture developed in Section 32. The theory approximates the structure of an elasto-viscous liquid by means of a mechanical model as shown in Fig. 57. The model consists of a piston, filled with liquid, connected in series to a spring. The first element represents a purely viscous resistance (resistance proportional to rate of displacement) and is, therefore, the model of a normal or Newtonian liquid, if the load on the piston is identified with the shearing stress in the liquid, and the displacement of the piston identified with the gradient of displacement in the liquid. The second element is a purely elastic resistance (resistance proportional to displacement), representing a model for an ideal solid.

In a structurally-viscous liquid both elements are present; therefore the two elements are connected in the model. The shearing stress in a liquid acts equally on both the elastic and viscous resistances, but the actual amount of elastic and of viscous displacement (under maintenance or disruption of the disperse network) is generally different. This feature is pictured by assuming a series (not parallel) connection in Fig. 57, since the load on both elements of such a structure is the same; the displacement of both elements, however, is different. The two displacements together form the total displacement.

The fundamental differential equation for a volume element of this nature is obtained by adding together the two displacements. The viscous displacement, i.e., its differential quotient with respect to time, is given by

$$(du/dy)_{vis}=S/\eta_0.$$

The elastic displacement D is given by

$$(dD/dy)_{el}=S/S_0,$$

since the rigidity of the spring has to be identified with the constant S_0 introduced previously. In order to be able to add the two elements together, the second part has to be differentiated with respect to time:

$$(du/dy)_{el}=\dot{S}/S_0,$$

where $\dot{S}=dS/dt$. Consequently the sum will read:

$$du/dy=S/\eta_0+\dot{S}/S_0. \qquad (100)$$

This is the differential equation of the Maxwell body. It is well worth pointing out that the connection between this equation and Eq. (99) used for the stationary flow is by no means direct or conspicuous (even if the latter is simplified by writing $\eta_\infty=0$). Although such a connection supposedly exists via the abstract theories of Hencky or Weissenberg, it was thought more useful to present Eq. (99) simply on the basis of the three assumptions discussed in Section 33 —the more so as the Maxwell model is only a rough approximation of the physical reality,

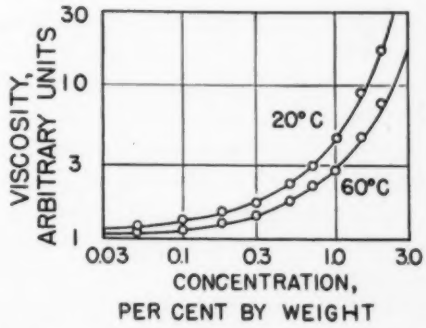

FIG. 56. The constant η_0 of acetyl cellulose solutions of varying concentration in dioxane (W. Philippoff).

and thus any derivation of Eq. (99) on its basis is not quite satisfactory.

Let us see to what conclusion Eq. (100) leads with regard to the relaxation process. If a stress of value A is suddenly released in maintaining the deformation, then its variation with time t can be obtained by integrating Eq. (100). The result is

$$S = Ae^{-t/\tau_0},$$

where $\tau_0 = \eta_0/S_0$, the so-called time constant. This figure is a useful characteristic of elasto-

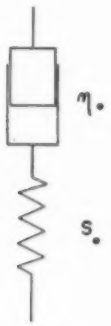

FIG. 57. Mechanical Maxwellian model of a structural-viscous liquid.

viscous liquids. The larger it is, the slower the relaxation process, and the more the system approaches a solid body. For normal liquids it has no significance but for the sake of extrapolation one can assign a time constant to normal liquids as well. It evidently must be very small, since stresses, if any, in such liquids are immediately released.

Even in elasto-viscous systems τ_0 generally is rather low, as can be seen from the last column of Table IX. For this reason experiments of this type are not easy. Flour dough is a system of particularly high viscosity and high time constant (about 500 sec.), and thus is suitable for tests of this type. An experimental relaxation curve obtained by Schofield and Scott Blair[23] is shown in Fig. 58. For the sake of comparison an exponential curve is drawn, and it can be seen that the actual curve is similar, but has a decidedly different slope. This deviation was to be expected from what was said of the Maxwell model. In the next section, after the discussion of alternating processes, reference will be made to this figure. Saal and Labout[24] studied the relaxation of asphaltic bitumens by means of a conicylindric rotating instrument, and interpreted them by model considerations.

35. Vibrational Processes

The third and last group of phenomena to be discussed are those in connection with vibrations of elasto-viscous liquids. In Section 33 it was shown that such a liquid has the viscosity η_0 for stationary processes and low stresses. If the condition of low stress is now maintained, but the process becomes an alternating one with gradually increasing frequency, then the character of the motion will change. Instead of being a viscous flow, as in the stationary case (frequency = zero), it will assume, more and more, the character of an elastic displacement, because with increasing frequency the period of vibration becomes so short that there will be no time for a flow to develop. In the foregoing section it was shown that the time constant of relaxation (order of time required for a flow to develop) is given by the ratio $\eta_0/S_0 = \tau_0$. Thus it is to be expected that the viscous flow will change into an elastic motion in the neighborhood of a vibration period of τ_0, or in the neighborhood of the vibration frequency $1/\tau_0$. In order to describe the influence of frequency on the character of the process, the so-called dynamical viscosity η' can be introduced, the meaning of which is understood from the Maxwell model shown in Fig. 57. In that model the two elements are in series, as explained in the previous section. In mechanics, however, it is customary to describe a vibrating, damped

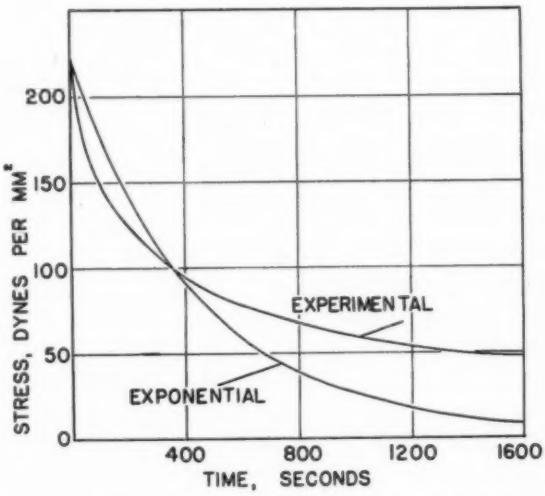

FIG. 58. Relaxation curve of flour dough after Schofield and Scott Blair (exponential for comparison).

element as the parallel connection of a spring and a viscous element. The reason is that in actual membranes with internal damping the displacement of both elements is the same, whereas the stress acting on them is different. As the parallel connection is used to represent such a vibrating body, the problem is to find the elements of a parallel connection equivalent to the series connection of Fig. 57. While we are not primarily interested in the value of the equivalent spring rigidity, the value of the equivalent viscosity is now important. This value should be denoted by η', and the mathematical theory of such connections shows that

$$\eta' = \eta_0/[1+(\omega\tau_0)^2] \qquad (101)$$

with $\omega = 2\pi$ times frequency.

Thus for $\omega = 0$, a stationary process, the viscosity becomes η_0, as it should be. For very high frequencies η' becomes zero. A spring with a parallel piston moving in a liquid of zero viscosity has no damping at all, and this is

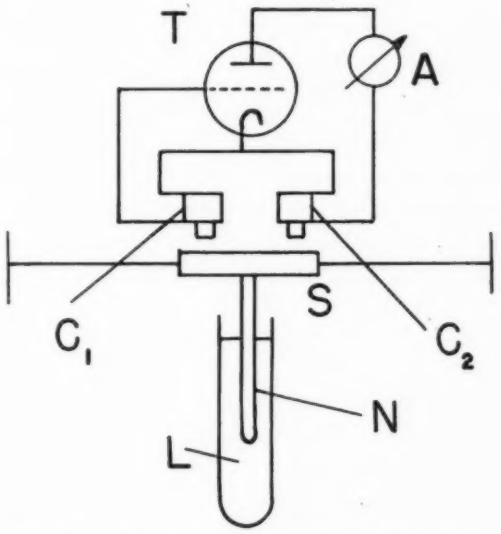

FIG. 59. Vibration apparatus of W. Philippoff for the measurement of the dynamic viscosity of liquids.

exactly what is to be expected when the elastic displacement predominates. Transition occurs, as the equation shows, when $\omega\tau_0 \sim 1$, just as assumed.

Equation (101), being a strict consequence of the Maxwell model, is not expected to hold rigorously. Indeed, it will be shown that, while the general form of (101) is correct, the exponent

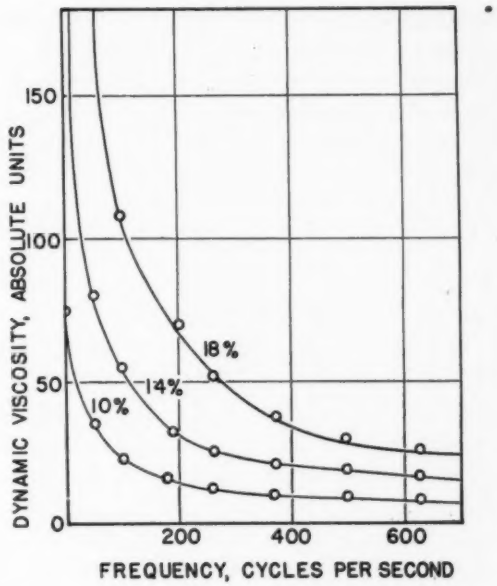

FIG. 60. Dynamic viscosities of Cellit solutions of different concentrations in dioxane (W. Philippoff).

in the denominator as empirically obtained is nearer to 1 than to 2.

Philippoff[25] has carried out an extensive study to check Eq. (101) on solutions of Cellit (an ester of cellulose) in dioxane. The principle of his method is shown in Fig. 59. A steel plate S vibrates in an electromagnetic field and a needle N attached to the plate moves axially in a tube filled with the liquid L, the viscosity of which is to be measured. From among the two coils (four in reality) one C_1 supplies the feed-back current to the grid of a tube T, the other C_2 in the anode circuit supplies the driving current. If the anode circuit is in resonance with the plate (the tension of which is variable) self-excited oscillations will set in. The anode current, the amplitude of the steel plate, and the frequency are measured—the amplitude by means of a mechanical device not shown in the figure. The anode current allows the driving force to be computed, the amplitude and the frequency supply the data for the velocity of the plate. The ratio of driving force to velocity is a measure of the resistance, in this case essentially that of the viscous resistance of the liquid.

The results of some of his tests are shown in Fig. 60 referring to 10, 14, and 18 percent solutions of Cellit. The abscissae are frequencies and the ordinates dynamic viscosities η'. In

checking Eq. (101) by means of these data, it was found that with the exponent 2 the drop of the curve ought to be much steeper than that observed experimentally. The best agreement was obtained when the following relation was used:

$$\eta' = \eta_0/[1+(\omega\tau_0)^{\frac{1}{2}}]. \qquad (102)$$

From the experimental data and this relation η_0 and τ_0, as well as rigidity constant S_0, were calculated, and the values are shown in Fig. 61 as a function of the sol concentration. Viscosity values as obtained from stationary measurements (denoted by + on the η_0 curve) are also included on the graph and are seen to agree well with values derived from the dynamic measurements.

The present author made an attempt[26] to compute the shape of the relaxation curve for elasto-viscous liquids, using Eq. (102) and carrying out the computation by means of the Heaviside operational calculus which generally allows the calculation of transients from impedance data. In this case it was necessary to use fractional differential quotients, the meaning of which is explained in a second paper on this subject.[27]

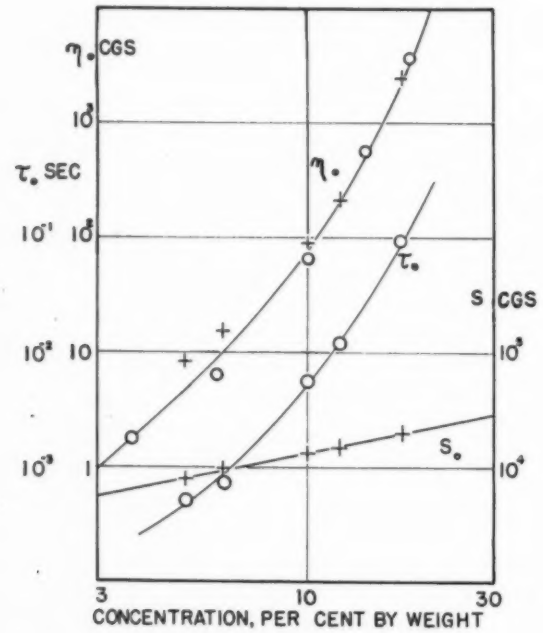

FIG. 61. Characteristic constants of Cellit solutions (Fig. 60), computed by W. Philippoff.

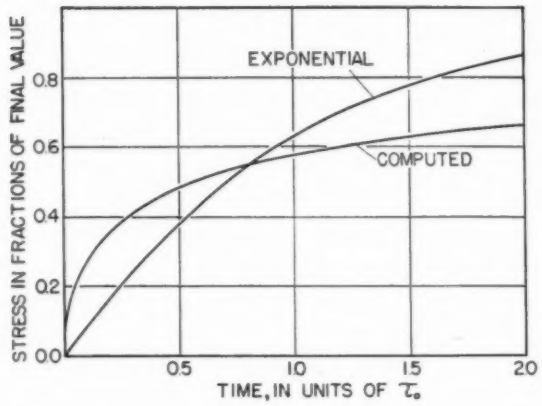

FIG. 62. Relaxation curve of a structural-viscous liquid, obeying Eq. (103), computed by Gemant (exponential for comparison).

In carrying out a numerical computation, the exponent in (102) was taken as unity, as there seemed to be no reason to adhere to the value $\frac{3}{4}$ too literally. Besides, the value 1 seemed in good agreement with certain data obtained from solid materials, to be dealt with in Chapter XIII of this monograph. The specific case was that of a suddenly applied constant rate of shear du/dy. The value of the stress in fractions of the final stress is shown in Fig. 62, the abscissae being the dimensionless number (t/τ_0). The figure also includes an exponential, according to the Maxwell body. Such a body should first show a linear increase of the stress, according to its elasticity. As flow sets in, the curve bends downward and approaches its final value, according to its viscosity. The other curve, calculated after the author's equations, is a relaxation curve for the same case, based on an exponent of unity in Eq. (101). As can be seen, the curve in the first portion is steeper than the exponential, and becomes flatter in the later stages. There is a definite similarity between these curves and those of Fig. 58, indicating that an equation of the form

$$\eta' = \eta_0/(1+\omega\tau_0) \qquad (103)$$

is a good approximation for the dynamic viscosity. Again it is emphasized that Eq. (103), as well as is (101), is of only a semitheoretical nature. A rigorous description of the process from a physical standpoint is missing as yet.

Bibliography for Chapter VIII

1. H. Hencky, Ann. d. Physik **2**, 617 (1929).
2. K. Weissenberg, Abh. d. Preuss Akad. d. Wiss (Berlin, 1932).
3. H. Freundlich, *Thixotropy* (Hermann & Cie, Paris, 1935).
4. H. Freundlich and D. W. Gillings, J. Chem. Soc., p. 546 (1938).
5. E. A. Hauser, *Colloidal Phenomena* (McGraw-Hill, New York, 1939).
6. W. G. Myers and W. G. France, J. Phys. Chem. **44**, 1113 (1940).
7. J. E. Arnold and C. F. Goodeve, J. Phys. Chem. **44**, 652 (1940).
8. G. P. Dube and H. K. Dasgupta, Ind. J. Phys. **13**, 411 (1939).
9. T. F. Ford, A. G. Loomis, and J. F. Fidiam, J. Phys. Chem. **44**, 1 (1940).
10. E. C. Bingham, *Fluidity and Plasticity* (McGraw-Hill, New York, 1922).
11. H. Freundlich, *Colloid and Capillary Chemistry* (Methuen, London, 1926).
12. M. P. Wolarowitsch and W. S. Borinewitsch, Kolloid Zeits. **77**, 93 (1936).
13. Andrew Gemant, Ber. Preuss. Akad. Wiss. (Berlin, 1932).
14. F. Breazeale, J. App. Phys. **11**, 187 (1940).
15. G. D. Hobson, J. Inst. Petrol **26**, 533 (1940).
16. R. Eisenschitz, Kolloid Zeits. **64**, 184 (1933).
17. Wo. Ostwald and H. Malss, Kolloid Zeits. **63**, 305 (1933).
18. M. Reiner, J. Rheology **1**, 251 (1930).
19. W. Philippoff, Kolloid Zeits. **71**, 1 (1935).
20. E. Hatschek and R. S. Jane, Kolloid Zeits. **40**, 53 (1926).
21. E. Hatschek, *The Viscosity of Liquids* (Bell, London, 1928).
22. W. Philippoff, *Chemie der Hochpolymeren* (Verlag Chemie, Berlin, 1937), p. 197.
23. R. K. Schofield and G. W. Scott Blair, Proc. Roy. Soc. **A138**, 707 (1932).
24. R. N. J. Saal and J. W. A. Labout, J. Phys. Chem. **44**, 149 (1940).
25. W. Philippoff, Physik. Zeits. **35**, 883 (1934).
26. A. Gemant, Physics **7**, 311 (1936).
27. A. Gemant, Phil. Mag. **25**, 540 (1938).

Calendar of Meetings

April

10–11 American Physical Society, Southeastern Section, Oxford Mississippi
16–17 National Petroleum Association, Cleveland, Ohio
19 American Ceramic Society, Cincinnati, Ohio
20–24 American Chemical Society, Memphis, Tennessee
23–25 American Philosophical Society, Philadelphia, Pennsylvania
30–May 1 American Physical Society, Baltimore, Maryland

May

11–13 American Institute of Chemical Engineers, Boston, Massachusetts
31–June 5 Society of Automotive Engineers, White Sulphur Springs, West Virginia

June

8–11 American Society of Mechanical Engineers, Cleveland, Ohio
8–12 American Medical Association, Atlantic City, New Jersey
18–20 National Colloid Symposium, Boulder, Colorado
22–26 American Institute of Electrical Engineers, Chicago, Illinois
22–26 American Association for the Advancement of Science, Ann Arbor, Michigan
25–27 American Physical Society, State College, Pennsylvania
29–July 1 Institute of Radio Engineers, Cleveland, Ohio
29–July 1 American Society of Heating and Ventilating Engineers, St. Paul, Minnesota

July

11 American Physical Society, Pacific Coast, Berkeley, California
22–24 American Society of Civil Engineers, Spokane, Washington

September

7– 9 Mathematical Association of America, Ithaca, New York
7–11 American Chemical Society, Buffalo, New York
8–11 American Mathematical Society, Ithaca, New York
9–11 American Institute of Electrical Engineers, Vancouver, B. C.

Résumés of Recent Research

Theory of Adsorption of Gases on Metals

It has been recognized for some time that the forces responsible for the low temperature, non-activated adsorption of gases on solid surfaces have the same origin as the van der Waals forces between gas molecules. In the case of adsorption on metals, Lennard-Jones proposed some time ago that the adsorption force arises from the interaction between the molecule and its electrical image in the metal. Recently H. Margenau at Yale University and W. G. Pollard[1] at the University of Tennessee have studied this type of adsorption by means of the usual theory of dispersion forces. They find that for molecules possessing a permanent dipole moment, the van der Waals potential reduces to the image potential but that the latter leads to too strong an interaction for non-polar molecules. The reason is that the electrons in the metal are able to form images of static or slowly moving external charges but, because of their finite relaxation time, they are incapable of simulating the very rapid motions of the instantaneous dipoles composing a non-polar molecule. These authors obtain a general formula for the mutual energy of a neutral molecule and a solid in terms of the polarizabilities of each system at the resonance frequencies of the other. This energy varies inversely as the cube of the normal distance from the surface to the molecule.

In a companion paper, W. G. Pollard[2] considers the exchange forces between the metal electrons and those of the molecule. This is accomplished by means of a Heitler-London calculation in which the visiting molecule is regarded as one component and the metal crystal as the other of a large "diatomic" system. The exchange interaction is repulsive and varies exponentially with the distance from the surface. Its magnitude depends on the ratio of the radius of a sphere containing one metal electron to the mean radius of the electron cloud in the molecule. This dependence is such that the repulsive forces are large for metals of low electron density and for "small" molecules. The total potential energy of the molecule in the surface field of the solid may be approximated by adding the positive exchange potential to the negative van der Waals potential. The resulting curve for the case of H_2 on Ni is shown in the upper part of Fig. 1. On the same energy scale in the lower part of Fig. 1 is shown a portion of the experimental curve of Eucken and Hunsmann[3] for the heat of adsorption of H_2 on Ni at 20°K as a function of the amount of gas adsorbed. A heat of adsorption equal to the theoretical value was observed in these experiments when 2.2 millimoles of H_2 were already adsorbed. Since, however, the adsorbed layer was clearly in a highly heterogeneous state, it does not seem possible to determine at which stage, if any,

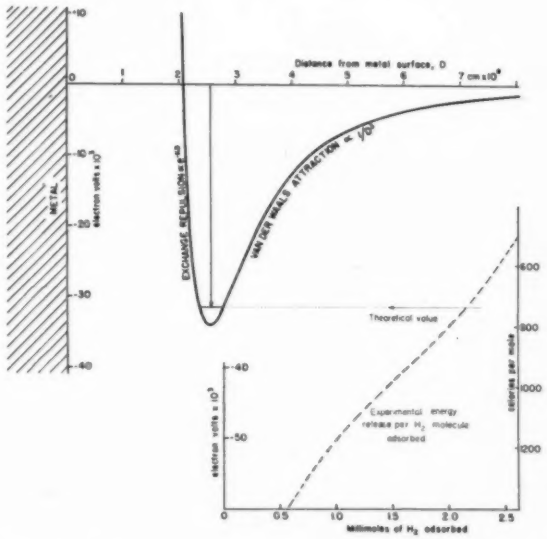

FIG. 1. Upper part: Potential energy curve of an H_2 molecule at the surface of Ni. Lower part: Experimental curve for heat of adsorption of H_2 on Ni at 20°K *vs.* the amount of H_2 already in the adsorbed state plotted on the same energy scale as the upper part. The curve drops to -77×10^{-3} electron volt (1800 calories per mole) at 0 millimoles of H_2 adsorbed. The level marked "theoretical value" is the energy evolution which would have been observed if all the H_2 had been adsorbed according to the theoretical potential energy curve. For convenience the energy scale is also marked off in calories per mole.

[1] H. Margenau and W. G. Pollard, Phys. Rev. **60**, 128 (1941).
[2] W. G. Pollard, Phys. Rev. **60**, 578 (1941).
[3] Eucken and Hunsmann, Zeits. f. physik. Chemie **B44**, 163 (1939).

of the observed adsorption the mechanism corresponds to that contemplated in this theory. Thus it is doubtless only by coincidence that Eucken and Hunsmann's mean value of 800 calories per mole for the whole range of adsorption agrees with the theoretical value.

Electrical Resistance of Metals at Low Temperatures

According to modern theory the electrical resistance of a metal may be thought of as having three components, namely, (1) a temperature dependent term due to thermal oscillation of lattice ions, (2) a temperature independent term due to mechanical strains, and (3) a temperature independent term due to the random scattering of electron waves by impurity atoms in the lattice. At room temperature the last two terms are far outweighed by the first. However, the third component is of considerable interest since a theoretical formula based on quantum mechanics has been derived for it.

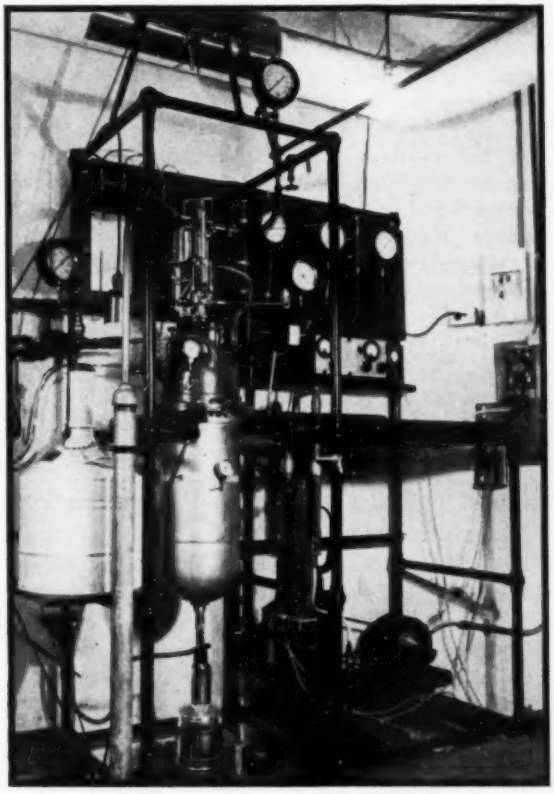

FIG. 1. The equipment used for producing liquid helium.

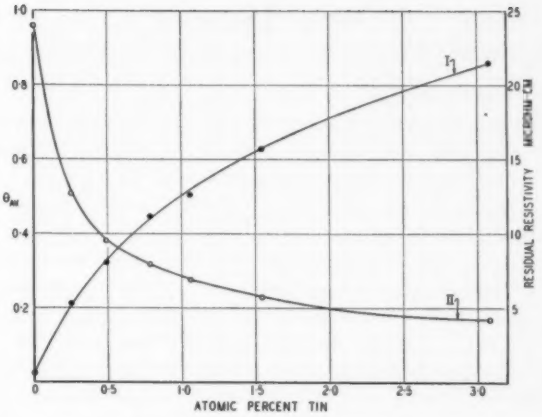

FIG. 2. Curve I. Residual resistivity of antimony-tin alloys as a function of tin content. Curve II. Mean temperature coefficient of resistance for the alloys.

In a recent communication,[1] C. T. Lane and W. A. Dodd have investigated this third component by using strain-free single crystals of antimony with known small amounts of tin in solid solution. In order to suppress the thermal vibration component the measurements were made at the temperature of liquid helium (4.2° abs.). The equipment used for producing liquid helium is shown in Fig. 1.

Figure 2, curve I, is a plot of this "residual resistivity" against the tin content. The curve is nearly parabolic whereas theory shows it should be linear.

The authors suggest that a possible way of resolving this disagreement lies in a consideration of the unusual electronic structure of antimony. Electrical conduction in this metal is supposed owing to a few conduction electrons (about 10^{-2} per atom) and an equal number of vacant electronic states (positive holes). Since tin has only four valence electrons while antimony has five, each atom of tin added removes one electron from the alloy, and this should increase the resistance. However, if the low temperature conduction of antimony is supposed mainly due to positive holes, and if the density of such states increases as electrons are removed, the increase in resistance due to scattering will be partially offset by increase of current carriers and a function more like that observed experimentally would result.

[1] C. T. Lane and W. A. Dodd, Phys. Rev. **61**, 183 (1942).

New Books

Atoms in Action

BY GEORGE RUSSELL HARRISON. Revised edition. Pp. 387+xii, Figs. 19, 15½×22 cm. William Morrow & Company, New York, 1941. Price $3.50.

Two years ago when *Atoms in Action* first made its appearance, I received a thrill from reading it which seldom comes from reading popular exposition in science. Professor Harrison's book seemed to combine in a remarkable degree both accuracy of fact and stimulating style of presentation such as one seldom finds in books written for general appeal. Here is physics written by a physicist in a way that makes the recent progress in atomic research vivid and meaningful. It points out what has been accomplished in a few short years; but, better still, it suggests what still lies ahead when men have learned to control atoms better. I wish that every serious student of physics and engineering might read it for the inspiration it can give, and that every intelligent layman might read it for the clear picture it offers of a progressive field of knowledge that is too frequently allowed to merge indistinctly into chemistry on the one hand and engineering on the other.

Few books that have been written in recent years have accomplished so much for physics as a profession; few have even approached *Atoms in Action* in making physics clear and appealing to the layman. In two years it has already gone through four large printings and it now appears in revised form with a new chapter added under the title of "Science in War and After." A children's edition of the book entitled *How Things Work* has been successfully molded to stimulate the youth of the land to the possibilities of atomic physics, and it is Dr. Harrison's belief that young people *can* become interested in atoms and can understand many things which may still seem strange and unbelievable to their elders. This generation is growing up in an age when it has a right to feel at home with atoms and electrons. In addition to the four American printings, there has been a large British printing, and the book has already appeared in Swedish and Portuguese, while other translations into Spanish, Czech, Italian, and German are now in process.

The first edition of *Atoms in Action* was reviewed in this Journal* just at the time when the book was completed. To that review there is little to add except a few more superlatives. Beyond Dr. Harrison's ability to write with a literary style that is the envy of many who read him, lies his remarkable skill in mustering his facts and relating them in the most telling fashion. Particularly suggestive is his way of showing how difficult problems have been solved by "judicious indirection,"—how physicists sometimes creep up behind some apparently impregnable stronghold of ignorance and take it by assault with *indirect* methods. One cannot help feeling that such a strategic attitude toward the solution of difficulties may help to solve many of our pressing problems, both of war and of peace. Where a frontal attack fails, perhaps a little "judicious indirection" may succeed. Another cogent train of thought is that in which the author emphasizes repeatedly the numerous links between the various fields of physics and how these links have been forged and welded together. He also points out where some of the weaker links are situated, and he thereby opens areas of thought and of investigation which may stimulate the thinking of a coming generation of physicists.

The new chapter (30 pp.) on "Science in War and After" is written to portray "some of the consequences on human welfare of the work of the scientist in so rapidly shrinking our world and expanding our universe." It is a mixture of fact, so far as certain recent applications of physics to warfare are concerned, and of opinion, so far as the author takes a somewhat restrained opportunity to express himself on the social implications of science. On the factual side, the question of the ever-increasing speed of airplanes comes in for consideration; the part played by reconnaissance photography and the scientific methods of detecting camouflage are linked with what the reader has discovered in earlier chapters about light. The successful solution by British physicists of the vital problem of locating airplanes in flight is reported as one of the recent triumphs. Dr. Harrison goes to some length in defining the difference between an idea and an invention, and shows what a vast gap frequently exists between recognition of a problem and its successful solution. It is to be hoped that his remarks may help to deflect some of the well-intentioned but wild ideas that laymen place before the military at times like these, without discouraging the person who is willing to pursue his idea through to a useful solution. In conclusion, Dr. Harrison views the general question of the good and ill that come from applications of science to life in both peace and war, and the problem of the disparity between spiritual and scientific development. He concludes that "we are prone to ignore the 95 percent of blessings that science bestows, and to enlarge upon the 5 percent of discomforts that acceptance of these blessings entails." He blames much of our "war jitters" and the horrors of modern warfare, not so much upon the improvements in the means or effectiveness of destructive agencies, as upon the over-efficiency of our news-gathering agencies! Admittedly, we are in a mess; but for those who hold with Dr. Harrison, "the good old days" do not lie behind us, but are yet to come.

RICHARD M. SUTTON
University of Minnesota

* J. App. Phys. **10**, 667 (1939).

Practical Solution of Torsional Vibration Problems, Volume 2.

BY W. KER WILSON. Second edition. Pp. 694+xxi, Figs. 236, 15×22 cm. John Wiley and Sons, New York, 1941. Price $8.50.

The enormous importance of the internal combustion engine in modern warfare makes this book a most valuable contribution at the present time. The continuous trend toward higher power and speed in aircraft engines has put torsional oscillations in the foreground as one of the major controlling factors in design. Mr. Wilson's book has been known as an invaluable companion to the designer of internal combustion engines for the wealth and accuracy

of its information. The second volume is especially rich in practical data. The important problem of the determination of stresses under conditions of resonance is extensively treated. Quite a thorough discussion is given of the various coefficients by which damping may be expressed. The nature and origin of damping in internal combustion engines are given considerable attention and the conclusions checked against test data are applied to a number of examples. The importance of hysteresis losses is brought out and a comparison is made between various materials. Stress concentration factors are also discussed. The next two chapters take up the subject of vibration recording and the interpretation of the records. A great number of recording devices are reviewed with detailed drawings and photographs of the instruments.

Two other chapters are devoted to the subject of vibration prevention, either by means of vibration damping devices, or the recently developed method of the rotating pendulum vibration absorber. The treatment of the latter subject is very complete and up to date.

In the last chapter, the special problems arising from the direct coupling of internal combustion engines to electric generators are discussed. A simple method of numerical harmonic analysis is explained in the appendix, and the book is supplemented by an excellent bibliography and an extensive list of British patents.

M. A. Biot
California Institute of Technology

Photography, Its Science and Practice

By John R. Roebuck and Henry C. Staehle. Pp. 283+xv, Figs. 96, 22×15 cm. D. Appleton-Century Company, Inc., New York, 1942. Price $5.00.

The Scientific Photographer

By A. S. C. Lawrence. Pp. 180+x, Figs. 83, 14½×22½ cm. The Macmillan Company, New York, and The University Press, Cambridge, 1941. Price $3.75.

The first of these books is intended to provide a summary of the fundamental science of photography for the hobbyist who has mastered the basic techniques and wishes to progress farther. An historical introduction is followed by a discussion of the photographic emulsion and its properties before and after exposure and development. There is a chapter on the color sensitivity of various dye-treated emulsions and their use with filters to obtain particular effects. A concise treatment of photographic chemistry follows. The discussion of the theory of the latent image is modern and shows how one may account for solarization, reciprocity failure, the Herschel effect, and the action of sensitizers. The chapter on positive processes is very brief. In addition to the usual processes, it includes an outline of halftone reproduction. Following this is a chapter on lenses and their aberrations. The properties of some important lenses for special purposes such as copying, enlarging, and air survey are omitted, but the optical discussion is sound. The closing chapter is an instructive outline of those qualities of a picture that make it more than a record photograph.

The book by Dr. Lawrence is intended to furnish "a short account of the possibilities and limitations of photography—primarily for the scientific worker, but also for the serious amateur who has elementary knowledge of chemistry and physics." The book opens with a discussion of the light-sensitive properties of photographic emulsions. However, the scientific worker would certainly require information in regard to the various "effects" associated with the names of Herschel, Eberhard, Becquerel, and others. These have been omitted, while solarization is dismissed with the statement that since it requires an exposure of 10^5 times that of threshold, it has little bearing on photography. To the contrary, in scientific work, some parts of a subject might receive this degree of exposure. Moreover, solarization is the working principle of commercial reversal film.

The chapter on lenses is inaccurate and incomplete. The figures illustrating spherical aberration, coma, and astigmatism are incorrect. For example, the two astigmatic images and an intermediate image are shown produced by three pairs of rays which all lie in the same plane and come from two diametrically opposite points on the lens rim, as if there were a triple refraction at these two places. There is a discussion of the common varieties of telephoto, wide angle, and soft focus lenses, but no reference to special lenses for copying, three-color separation, and aerial surveying. The newly developed methods for reducing reflection losses and flare should have received some attention. Slips have been made in regard to the diffraction theory of resolving power, the variation of light scattering with direction, and the depth of field.

The chapter on scientific applications is only twenty-seven pages long. In addition to straight record work, it contains outlines of high speed photography and photomicrography, including the use of the dark field and polarized light. Photography by radiations outside the visible spectrum receives some attention. There is so little on photographic photometry that it would be of no practical use to the scientific worker. References to supplementary material on this and other applications would be very helpful. Stereoscopic photography is not discussed.

The first book makes no attempt to cover the applications of photography in scientific investigation. Nevertheless, it gives a sound background of photographic science and it includes many references to the specialized literature.

A supplementary laboratory manual gives directions for eighteen experiments suitable for a course in photography. The instructor planning such a course will find the list of necessary equipment and the suggestions for conducting the class work of great value. The equipment needed is no more than that owned by many amateurs.

There are only a few misstatements, one being that color photography is an application of the principles of three color vision. It is better to refer to experimentally verified facts of color mixture than to any theory of vision devised to explain them.

The many halftone illustrations are poorly rendered because of the unsuitable quality of the paper.

Joseph Valasek
University of Minnesota

Here and There

The Physics of Pigments and Glasses

A conference on the physics of pigments and glasses is to be held at the University of Pennsylvania on May 15 and 16, 1942, under the auspices of the Department of Physics.

Friday, May 15, 3:00 P.M.

Chairmen: DR. E. R. ALLEN, *Krebs Pigment Company*
DR. J. T. LITTLETON, *Corning Glass Works.*

Introduction. PROFESSOR G. P. HARNWELL.

1. The Basic Principles Involved in the Preparation of Pigments. MR. R. H. SAWYER, *Krebs Pigment and Color Corporation.*

2. The Basic Principles Involved in the Glassy State. PROFESSOR B. E. WARREN, *Massachusetts Institute of Technology.*

Friday, May 15, 8:30 P.M.

Chairmen: DR. C. GROVE, *United Pigment and Color Company*
PROFESSOR E. C. BINGHAM, *Lafayette College.*

3. The Electron Microscope and the Determination of Particle Size. DR. R. B. BARNES, *American Cyanamid Company.*

4. The Physics of Pigments in Dispersed Systems. H. GREEN, *The Interchemical Corporation.*

Saturday, May 16, 10:00 A.M.

Chairmen: MR. F. C. FLINT, *Hazel-Atlas Glass Company*
DR. J. E. BAILEY, *Plax Corporation.*

5. The Mechanical Properties of Glasses. DR. F. W. PRESTON, *The Preston Laboratories.*

6. Combined Glass-Pigment Systems. DR. C. ROBERTSON, *R & H Division, duPont de Nemours and Company.*

7. Deterioration of Materials by Light. DR. F. SEITZ, *University of Pennsylvania.*

An informal dinner will be held on Friday at 6:00 P.M. in Houston Hall for persons attending the conference.

★

Recent Appointment

Dr. George Russell Harrison, Professor of Physics and Director of the Research Laboratory of Experimental Physics at the Massachusetts Institute of Technology, Cambridge, Massachusetts, has been appointed Dean of the School of Science, to succeed Dr. Samuel C. Prescott who is to retire on July 1, 1942.

★

ESMDT Summer Courses in Acoustics

Brown University will be one of four universities in the United States where special advanced work in acoustics will be carried out this summer to train men needed for research and experimentation in Navy laboratories. The program at Brown is designed to provide fundamental background knowledge and experience on problems related to submarine detection, acoustic mines, sound-insulation and the field of sound transmission.

As a part of the Engineering, Science, and Management Defense Training program of the United States Office of Education, the lectures and laboratory work for the new summer course are to be offered free to qualified students with special ability in physics and mathematics.

Beginning on June 15, the lectures and discussion periods will be held five days weekly for eleven weeks. Two three-hour laboratory periods weekly are also scheduled. The work will cover the equivalent of a year's study.

Other colleges and universities approved by the Navy Department as centers for similar studies are the University of California at Los Angeles, the University of Iowa, and the Case School of Applied Science in Cleveland.

★

Conservation of Scholarly Journals

The American Library Association created last year a Committee on Aid to Libraries in War Areas, headed by John R. Russell, the Librarian of the University of Rochester. The Committee is faced with numerous serious problems and hopes that American scholars and scientists will be of considerable aid in the solution of one of these problems.

One of the most difficult tasks in library reconstruction after the first World War was that of completing foreign institutional sets of American scholarly, scientific, and technical periodicals. The attempt to avoid a duplication of that situation is now the concern of the Committee.

Many sets of journals will be broken by the financial inability of the institutions to renew subscriptions. As far as possible they will be completed from a stock of periodicals being purchased by the Committee. Many more will have been broken through mail difficulties and loss of shipments, while still other sets will have disappeared in the destruction of libraries. The size of the eventual demand is impossible to estimate, but requests received by the Committee already give evidence that it will be enormous.

With an imminent paper shortage attempts are being made to collect old periodicals for pulp. Fearing this possible reduction in the already limited supply of scholarly and scientific journals, the Committee hopes to enlist the cooperation of subscribers to this journal and others published by the American Institute of Physics in preventing the sacrifice of this type of material to the pulp demand. It is scarcely necessary to mention the appreciation of foreign institutions and scholars for this activity.

Questions concerning the project or concerning the value of particular periodicals to the project should be directed to Wayne M. Hartwell, Executive Assistant to the Committee on Aid to Libraries in War Areas, Rush Rhees Library, University of Rochester, Rochester, New York.

★

Physics Laboratory Under Construction

The Trustees of Oberlin College recently awarded contracts for the construction of a Physics Laboratory, for which ground was broken last July 22. The laboratory will cover a space 59 by 194 feet and will consist of two floors and a basement. It will house a well-equipped instrument shop, including glass-blowing facilities, serving all the science departments of the college. This laboratory will be one unit of a proposed science quadrangle to include the Chemistry Laboratory, which is already completed, and a Biology Laboratory now being planned. The estimated cost for both building and furnishings is $390,000.

Contributed Original Research

Magnetization Near Boundaries*

JAMES H. WAKELIN, JR.†
Sloane Physics Laboratory, Yale University, New Haven, Connecticut
(Received February 5, 1942)

Magnetic measurements on ring samples of silicon iron, commercially pure nickel, and low carbon steel, in the thickness range 3.8×10^{-3} to 38.1×10^{-3} cm, indicate that it is possible to detect surface stray flux contributions to the total magnetization by comparing hysteresis loops obtained at a maximum applied field of 4 oersteds. The magnetic quality appears to be insensitive to changes of specific surface though a progression of properties with sample thickness suggests the presence of a low permeability surface layer.

THE magnetization of a ferromagnetic material has long been supposed to be connected intimately with its surface. This supposition arose primarily from the manner in which materials were magnetized before electric currents were used to produce magnetic fields. A piece of iron could be made magnetic by rubbing a permanently magnetized material over its surface. The magnetization, it was thought, was transferred from the surface to the interior of the iron by a kind of chain effect. Examination of thin ferromagnetic wires at ultra-high frequencies by Arkadiew,[1] by Sänger,[2] and their co-workers has made apparent the variation of permeability with frequency which suggested that a magnetic material possessed a surface layer or layers of low permeability. Peterson and Wrathall[3] estimated that a permeability of 250 and a surface layer depth of the order of 10^{-3} cm explained this frequency dependence in silicon steel.

Ballistic measurements indicated that the coercive force was connected with the thickness of thin ferromagnetic films[4] and that Barkhausen discontinuities[5] disappeared in films below a thickness of 1.75×10^{-4} cm. Cioffi[6] has shown with samples of hydrogenized Armco iron between 0.025 and 0.41 cm thick that the maximum permeability is a function of the thickness. More recently Wall[7] has published evidence that the magnetic quality of a material may be controlled by surface treatment. When given a specific heat treatment a non-magnetic layer on the surface of iron and nickel wires greatly enhanced their magnetic quality. In both of these elements Wall found that there was a critical thickness above and below which the maximum permeability declined sharply.

A striking connection between the condition of the surface and the magnetic properties of a material was demonstrated independently by Bitter[8] and by L. von Hamos and P. A. Thiessen studying patterns formed on its surface by a magnetic colloid. This colloidal technique was improved by L. W. McKeehan and W. C. Elmore[9] and extended by them to a variety of ferromagnetic materials. For each element and alloy which they studied, there were character-

* Part of a dissertation presented to the Faculty of the Graduate School of Yale University in candidacy for the degree of Doctor of Philosophy.

† Now in the Physical Research Department, B. F. Goodrich Company, Akron, Ohio.

[1] W. K. Arkadiew, Physik. Zeits. **14**, 561–562 (1913), and subsequent papers.

[2] G. Potapenko and R. Sänger, Naturwiss. **21**, 818–819 (1933); R. Sänger and G. Fejer, Helv. Phys. Acta **8**, 492–493 (1935); R. Sänger, Helv. Phys. Acta **7**, 478–480 (1934).

[3] E. Peterson and L. R. Wrathall, I. R. E. **24**, 275–286 (1936).

[4] S. Procopiu, J. de phys. et rad. **5**, 199–206 (1934).

[5] S. Procopiu, Comptes rendus **208**, 1212–1214 (1939).

[6] P. P. Cioffi, Phys. Rev. **39**, 363–367 (1932).

[7] T. F. Wall, Nature **139**, 928 (1937); **140**, 238 (1937); **140**, 856 (1937); **141**, 205–206 (1938); **141**, 1016 (1938); **142**, 875–876 (1938); **142**, 1039 (1938); **143**, 331–332 (1939); Engineer **163**, 397–398 (1937); **164**, 183–184 (1937); **165**, 667–669 (1938); **165**, 701–702 (1938); **166**, 474 (1938).

[8] F. Bitter, *Introduction to Ferromagnetism* (McGraw-Hill Book Company, 1937), p. 59.

[9] L. W. McKeehan and W. C. Elmore, Phys. Rev. **46**, 226–228 (1934); W. C. Elmore and L. W. McKeehan, Trans. A. I. M. E. **120**, 236–252 (1936).

istic surface patterns observed which were dependent in form upon the magnetic condition of the specimen. These stray flux patterns have been interpreted as resulting from the effort of the magnetization to assume paths of least reluctance at a surface.[10] This concept, therefore, endowed the geometrical boundary of a material with magnetic properties differing from regions of the interior.

The present experiment is a quantitative study of the stray flux leakage responsible for the surface patterns qualitatively described in previous work. It was designed primarily to discover whether ballistic measurements could detect small differences in the distribution of magnetization in a material with change of its specific surface. Hysteresis loops run at low fields on a number of thin smooth rings with their flat surfaces placed together are compared with loops obtained when the same rings are separated by layers of non-magnetic material. In this comparison the former assembly simulates the bulk material, while the latter is indicative of the effect of increasing the specific surface on the same base. If the stray flux is a measurable part of the total magnetization, the hysteresis loops should differ in the two assemblies. Any difference in the curves represents the contribution of the net surface flux to the total measured flux in or against the field; on this hypothesis the net stray flux should be most effective in the region between zero magnetization and saturation. At zero magnetization there are as many lines of flux threading the surface with components along the field as against the field, while at saturation the magnetization has no component normal to the surface.

MATERIALS

All of the experiments were carried out on annular rings of outside diameter 6.350 cm and inside diameter 5.042 cm. The specimens in ring form shared the advantage of possessing no demagnetizing factor with the disadvantage of requiring a new primary and secondary winding for each new test run. The initial measurements were made on rings of silicon iron (3.35 percent silicon) in thicknesses of 5.08, 12.70, 25.40, and 35.56×10^{-3} cm. The 35.56×10^{-3} cm strips were cut from hot rolled material obtained from the Safety Car Heating and Lighting Company in New Haven. The remainder of the rings were cut from material obtained from the United States Steel Company through the courtesy of Mr. Donald S. Miller. The latter were much easier to work because the sheets were cold rolled and had fairly smooth surfaces when received. A second group of tests was run on commercially pure Grade A nickel obtained from the International Nickel Company and cold rolled to thicknesses of 7.62, 10.72, 16.64, 25.70, and 38.86×10^{-3} cm by the Sommers Brass Company of Waterbury, Connecticut. The final tests were run on cold rolled low carbon steel (shim stock) of thicknesses 4.521, 5.742, 10.74, 15.75, 21.40, 26.36, and 38.17×10^{-3} cm, all from one supplier at one time. These materials were chosen because they were the best high permeability sheets available in this range of thickness.

A chemical analysis on low carbon steel and nickel by Dr. W. E. Milligan of the Hammond Metallurgical Laboratory, Yale University, shows that the carbon content in the steel specimens lies between 0.05 percent and 0.15 percent, while the chief impurities are silicon 0.02 percent, manganese 0.3 percent, and nickel 0.04 percent. The analysis on nickel indicates that the impurities are iron 0.1 percent, manganese 0.12 percent, and copper 0.02 percent.

PREPARATION OF THE SPECIMENS

The rings for magnetic testing were cut from sheet material, initially in squares 7.62 cm on a side. These were mounted on a circular casting with a detachable face-plate which held them in a lathe for cutting to the correct inside and outside diameter. A small electromagnet with coplanar concentric pole pieces was designed to support the rings during polishing. To prevent beveling of the edges by loose abrasive a circular groove, 0.025 cm wider than the ring breadth, was cut in the pole pieces. This groove with bottom surface convex upwards, allowed 2.54×10^{-3} cm of the sample to extend above the magnet face. The polishing, done manually, was started on polishing paper; with four different textures in a progression from 0 to 0000 paper, each finer grade

[10] J. Frenkel and J. Dorfman, Nature **126**, 274–275 (1930); L. Landau and E. Lifshitz, Physik. Zeits. Sowjetunion **8**, 153–169 (1935); W. C. Elmore, Phys. Rev. **51**, 982–988 (1937); Phys. Rev. **53**, 757–764 (1938); W. F. Brown, Jr., J. App. Phys. **11**, 160–172 (1940).

was used to eliminate the scratches by polishing at right angles to those produced by the previous grade. The rings were finally lapped on a polishing wheel with a surface of crocus cloth on which levigated alumina in suspension was used as an abrasive. They were then examined under a low power microscope, and those with the best surfaces were chosen for annealing.

The strains due to cutting and cold working were relieved by annealing the rings in a hydrogen atmosphere, the time and temperature of heat treatment being consistent with commercial practice for the strain relief in transformer and dynamo steels.[11] The silicon iron and low carbon

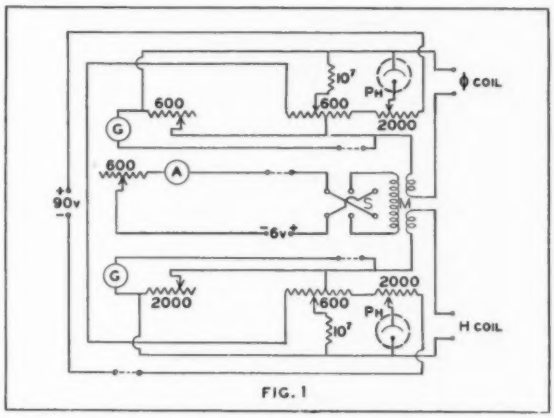

FIG. 1. Fluxmeter circuit diagram.

steel rings were annealed for 4 hours at 800°C, the nickel rings for 4 hours at 900°C, in a Rezistal[12] furnace box. After heat treatment the rings were placed in a toroidal brass case of rectangular cross section within, serving as protection against damage by the primary and secondary windings. A smooth surfaced brass shim stock 0.013 cm thick was chosen for the non-magnetic spacers; rings of the same inside and outside diameter as the magnetic specimens were cut from this stock and annealed in a similar manner at 400°C.

FLUXMETER DESIGN AND CONSTRUCTION

The apparatus employed for obtaining hysteresis loops was an astaticized, photoelectrically compensated fluxmeter of the McKeehan-Haworth type. Figure 1 is a circuit diagram of the fluxmeter. Here a highly overdamped Leeds and Northrup Type R galvanometer G is used to measure flux changes while a Weston A-5 photoelectric cell PH provides a current to compensate the restoring torque of the coil suspension. In principle this is similar to the Grassot fluxmeter since the galvanometer coil has no zero position. The illumination for the photoelectric cell provided by a 50-candlepower lamp is restricted by a thin rectangular slit, then reflected from the galvanometer mirror and focused on a wedge-shaped aperture before the photo-cell. The image of a cross hair illuminated by a second source is reflected also from the galvanometer mirror and is focused on a ground glass screen. As the restoring torque of the coil suspension is a linear function of the angular displacement of the coil for small angles, the wedge-shaped aperture supplies the galvanometer with a current increasing linearly with the coil deflection. Complete compensation is effected by matching the light intensity-current curve of the photoelectric cell to the current-restoring torque curve of the galvanometer. Evidently from Fig. 1, the voltage across the photoelectric cell PH is regulated by the potential across a variable resistance of 2000 ohms. The 600-ohm variable resistor through 10^7 ohms to the photoelectric cell provides compensation for stray light. In practice the current curve of the photoelectric cell is not linear with the illumination nor is the magnetic field of the galvanometer perfectly radial. Proper compensation to eliminate drift requires fitting the two curves across the entire scale.

The galvanometer is connected in series with the secondary of the toroidal test case and that of a standard mutual inductance, M. As the fluxmeter was originally designed to take B and H measurements simultaneously, the standard coil has two secondaries. One, having a mutual inductance of 106.1 millihenrys, was connected to the H galvanometer; the other, with a mutual inductance of 219.8 millihenrys, was connected to the ϕ galvanometer. Throughout this work the H galvanometer alone was used for changes of magnetic induction, while the applied fields were calculated from primary current measurements. Deflections on the scale were reduced to flux

[11] Greiner, Marsh, and Stoughton, *The Alloys of Iron and Silicon* (McGraw-Hill Book Company, 1933), p. 342.

[12] Rezistal 4, a non-hardenable Austenitic Chromium Nickel Steel of composition carbon 0.25 max., chromium 19.00 to 21.00, and nickel 24.00 to 26.00.

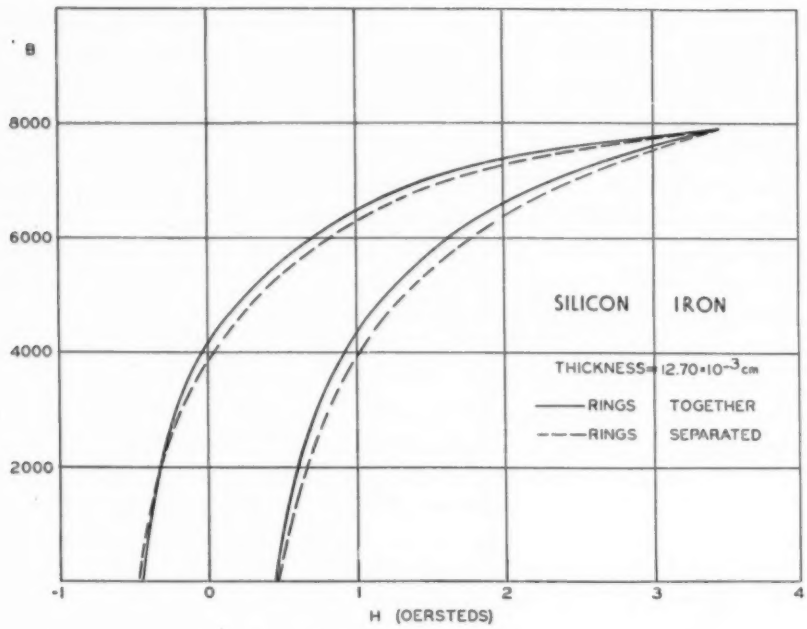

FIG. 2. Effect of ring assembly on the hysteresis loop of thin specimens of silicon iron.

differences by reversing a known current through the primary of the mutual inductance.

Comparisons of the magnetic properties for various thicknesses were made on the basis of weight, as the calculated induction for a ring specimen depended upon its cross-sectional area. Samples of each thickness were weighed while the thickest stock (38×10^{-3} cm) was gauged by micrometer; from the latter an effective thickness for every thinner gauge was calculated. The primary currents for the test coil and the standard mutual inductance were read on a Weston Type 45 milliammeter, calibrated with a Leeds and Northrup Type K potentiometer using a standard cell and a standard ohm.

The greatest sources of error in calibration were those introduced by magnetostrain and demagnetization. In the first toroidal case the ring specimens were subject to varying axial constraints due to thermal expansion and contraction of the primary and secondary windings. This was particularly noticeable with nickel which has a large magnetostriction constant. An improved case design eliminated the effect of temperature variation and constraint differences in packing. Because the maximum applied field did not exceed 4 oersteds reproducibility also depended critically upon the process of demagnetization. Calibration hysteresis curves proved that demagnetization was satisfactory if the current was reversed at the rate of one cycle per second. The whole process required at least an hour to return the specimen to a cyclic condition for the next measurements. With these refinements readings could be repeated to within $\frac{1}{2}$ of 1 percent.

THE AVERAGE APPLIED FIELD

The average applied magnetic field in the toroidal case was calculated in the following manner. Applying Ampere's law in e.m.u.,

$$\oint \mathbf{H}\cdot d\mathbf{l}=4\pi \mathrm{Ni},$$

to the magnetic circuit the field in the toroid at any distance x from the inner wall (radius b) of the rectangular section is

$$H=2\mathrm{Ni}/(b+x).$$

The average field, therefore, in the section of inner radius b and outer radius a is

$$\bar{H}=\frac{2\mathrm{Ni}}{(a-b)}\int_0^{a-b}\frac{dx}{(b+x)}.$$

Or

$$\bar{H}=\frac{0.2N_pI_p}{(a-b)}\ln\frac{a}{b},$$

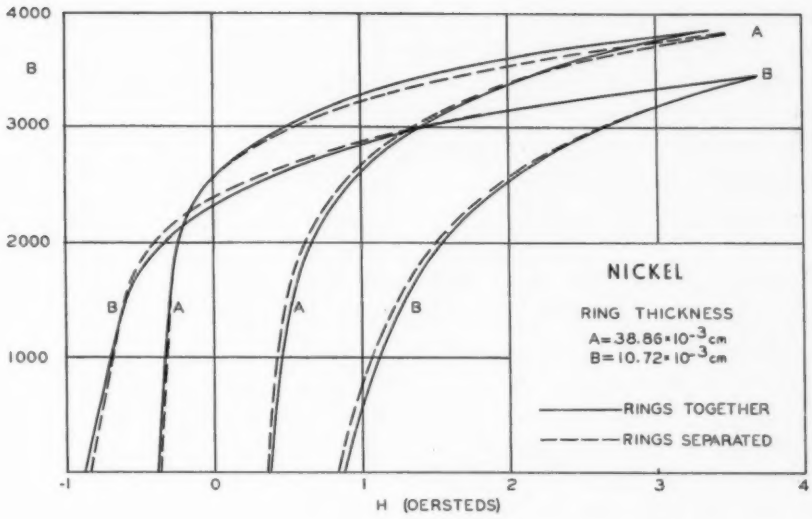

FIG. 3. Hysteresis loops for nickel showing the effect of ring assembly and thickness.

where N_p is the total number of primary turns and I_p is the primary current in amperes. With the values for a (3.175 cm) and b (2.521 cm)

$$\bar{H}=0.0705N_pI_p. \qquad (1)$$

RESULTS

Silicon Iron

The differences in the magnetization curves for highly polished silicon iron rings of thicknesses 5.08, 12.70, 25.40, and 35.56×10^{-3} cm (2, 5, 10, and 14 mils) indicate that there is a very small effect due to the difference in assembly. The hysteresis loops taken with the magnetic rings having their surfaces adjacent are slightly higher and slimmer than those with the rings separated by nonmagnetic spacers. Figure 2 shows the comparison of two hysteresis loops for the thickness 12.70×10^{-3} cm (5 mils). This is the only thickness of silicon iron run under conditions free from magnetostrain and indicates that the maximum permeability is higher and the coercive force slightly lower in the assembly with the magnetic rings together. This is consistent with the stray flux hypothesis as regards the increase in maximum permeability and induction, but not as regards the decrease in coercive force. It is conceivable, however, that the distribution of magnetization near the surface is such that the net flux is not zero at zero measured induction, but at some value near to zero. From Fig. 2 the net flux vanishes at $B=2000$ which implies that at zero measured induction there is a slight contribution of the surface flux to the total magnetization.

Nickel

The measurements on hysteresis loops of nickel rings of thicknesses 10.72, 16.64, 25.70, and 38.86×10^{-3} cm (4, 6, 10, and 14 mils approximately) show no appreciable difference when the two assemblies are compared. It appears from the nickel results that in the thinnest rings the stray flux difference is masked by a small magnetostriction effect which disappears in the thicker samples.

There is, nevertheless, a progression of the magnetic properties for different thicknesses of the nickel rings due to the decrease in specific surface. The maximum permeability and maximum induction both increase with ring thickness while the coercive force decreases. In Fig. 3 are representative hysteresis loops for the thinnest and the thickest nickel specimens, while Fig. 4 summarizes the increase of maximum permeability with thickness. Figure 5 indicates how the maximum induction increases and the coercive force decreases. This progression of the magnetic properties with thickness is consistent with the hypothesis that there is a low permeability surface layer which becomes less important as the ring thickness increases. The manner in which the permeability changes with thickness suggests that the depth of the low permeability layer is

affected by the thickness of the base material. This is in agreement with the conclusions of Peterson and Wrathall[3] who found that the effect of a surface layer became much more pronounced in thin magnetic samples than was consistent with a layer of one thickness.

Low Carbon Steel

Of the three materials tested, low carbon steel is the most favorable for detecting a surface effect due to its high maximum permeability and small magnetostriction constant. In thicknesses of 4.52, 15.75, 21.40, 26.36$\times 10^{-3}$ cm (1.5, 6, 8, and 10 mils approximately) only a small effect was found when the two assemblies for each thickness were compared. The difference between the curves is consistent with the stray flux hypothesis as the magnetization is increased when the magnetic rings are placed together, the hysteresis loops being higher than with the other assembly. An interesting difference between low carbon steel and silicon iron is apparent; the low carbon steel curves for each thickness show little change in coercive force or maximum permeability when the two assemblies are compared. The greatest separation in the hysteresis loops occurs near the knee of the curves, consistent with the proposed hypothesis. That all of the low carbon steel rings did not show this difference in the curves is not surprising as the surface effect is determined mainly by the condition of the surface. In the remaining ring samples, thicknesses of 5.08, 10.74, 38.17$\times 10^{-3}$ cm (2, 4, and 14 mils approximately), the curves repeated themselves to well within the experimental error, providing no contradictory evidence to the stray flux hypothesis.

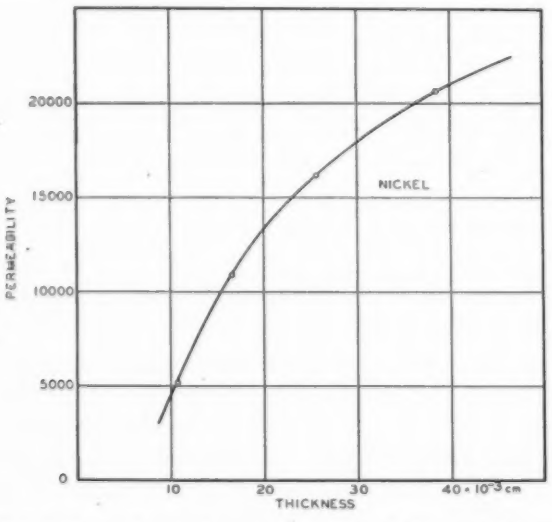

FIG. 4. Dependence of maximum permeability on thickness of nickel.

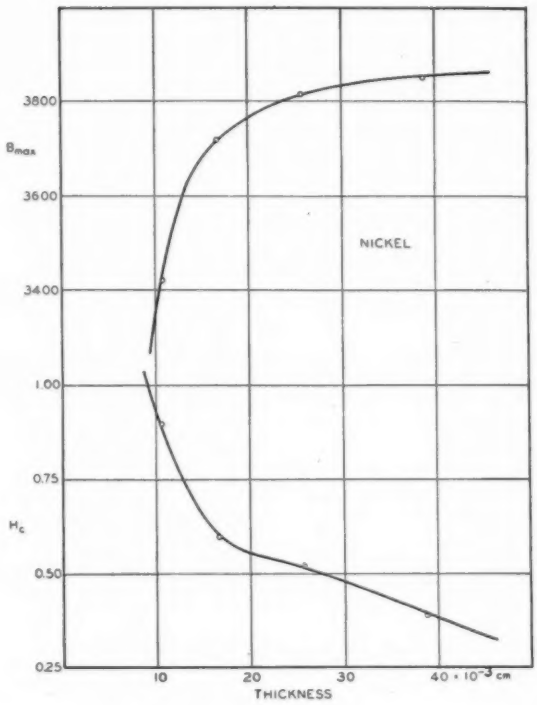

FIG. 5. Dependence of maximum magnetic induction and coercive force on thickness in nickel.

A significant result of the comparison of different thicknesses of low carbon steel is the progression of magnetic properties from the thin to the thicker specimens. Figure 6 shows the difference in the hysteresis loops due to a change of ring thickness. In general, there is a reduction of the coercive force and an increase of the maximum induction (Fig. 7). With the exception of the point at 38.17$\times 10^{-3}$ (15 mils approximately) the maximum induction increases uniformly with thickness. Although the coercive force does not decrease uniformly as in nickel, it shows a general downward trend. The decrease in coercive force and increase in maximum B is consistent with the concept that there is a surface layer of low permeability which becomes less important in the thicker specimens. The maximum permeability, however, is not related simply to the thickness as was found by Cioffi in

much thicker specimens of hydrogenized Armco iron.

Table I summarizes the hysteresis data for nickel and low carbon steel.

DISCUSSION

Magnetic measurements on ring samples of silicon iron, commercially pure nickel, and low carbon steel, in the thickness range from 3.8 to 38.10×10^{-3} cm (1.5 to 15 mils), have indicated that it is possible to detect small stray flux contributions to the magnetization by comparing hysteresis loops obtained at a maximum applied field of 4 oersteds. These results are in accord with the stray flux hypothesis proposed at the outset of the experiment. Although the stray flux effect found was much smaller than originally supposed, there was observed a dependence of magnetic properties upon the thickness of the ring samples, indicating that ballistic measurements can be used to detect the presence of a low permeability surface layer which has been studied mainly with alternating current methods.

The failure to observe large changes in the distribution of magnetization by comparing the two specimen assemblies, surfaces together and separated by non-magnetic material, suggests that the surface flux leakage is no appreciable part of the total magnetization. Essentially the method provides a surface of high permeability or low reluctance for the stray flux of adjacent rings, each specimen serving as a search coil for the surface flux of its neighbors. When the rings are together the flux is allowed then to pass across the surface from one specimen to another and to share the entire group rather than to be restricted to a single thin section.

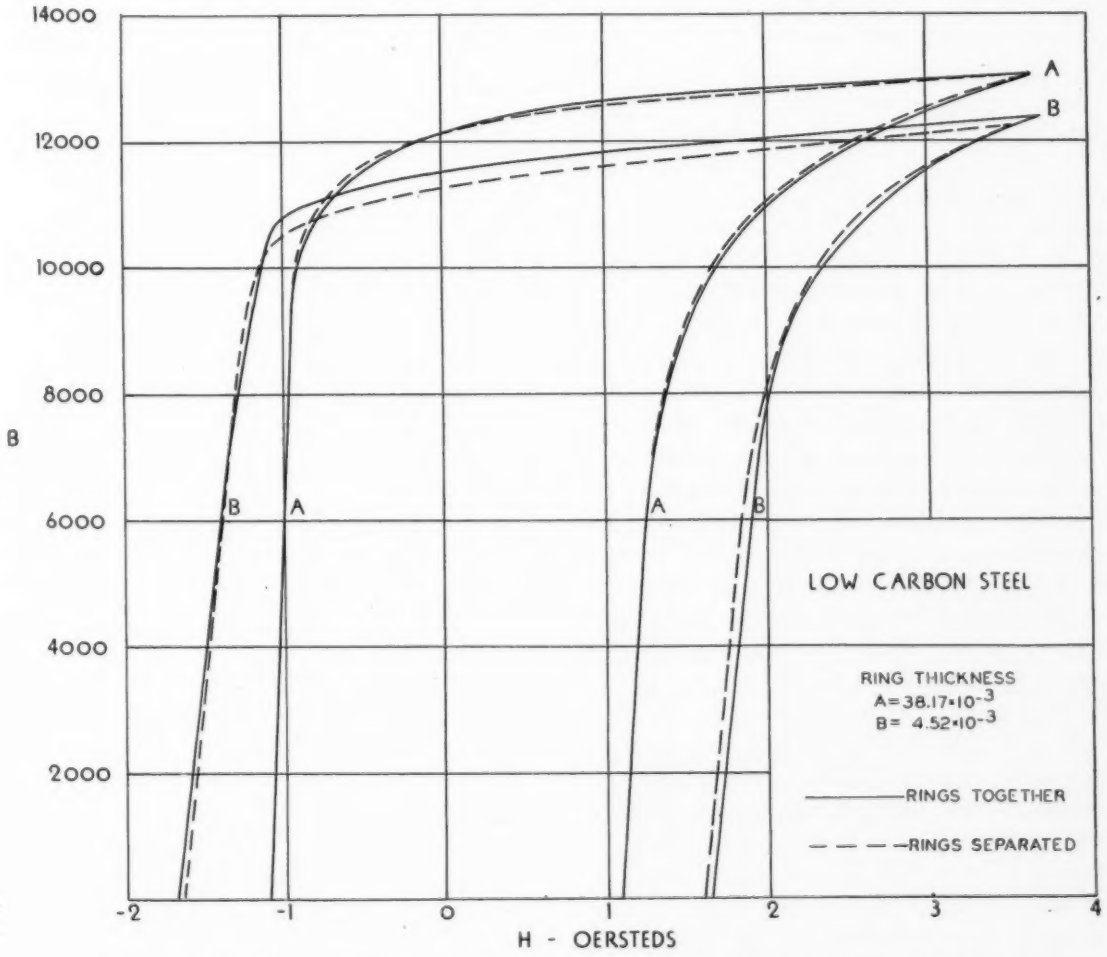

FIG. 6. Hysteresis loops for low carbon steel showing the effect of ring assembly and thickness.

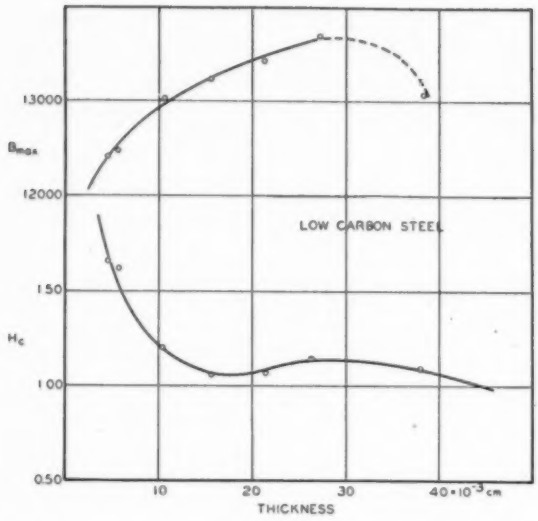

FIG. 7. Variation of maximum magnetic induction and coercive force with thickness in low carbon steel.

Wall[7] has suggested that the surface of a polycrystalline material plays the dominant role in its magnetic quality, that through surface treatment the entire specimen may exhibit large changes in permeability, magnetic induction, and coercive force. The effects which he found by coating a wire with a thin film of a non-magnetic material and heat treating do not appear to be related to a change in the reluctance of flux paths near the surface. In copper coated nickel wires, for example, the diffusion of copper into the nickel base could alter the permeability of the entire specimen rather than act wholly as a high permeability surface layer. If the boundary, however, were subject primarily to strains of a magnetic origin the proximity of a high permeability layer should alter the distribution of total magnetization to a measurable degree. No effect of the distribution of magnetic induction was found which was comparable in magnitude to the variation of field measured by Wall on the inner surface of an iron tube.

The increase of permeability with thickness contradicts Wall's hypothesis that the surface alone controls magnetic quality. The magnetization, he states, proceeds from the surface inwards, and below saturation the magnetic induction is a maximum at the surface decreasing gradually to the center of the specimen. A progression of samples with the same surface layer but varying thicknesses should therefore show a decrease of permeability with thickness. The nickel rings used in this experiment were all rolled from the same parent stock, and were given the same cold working and heat treatment. The maximum permeability increased uniformly with thickness between 10^{-2} cm and 3.8×10^{-2} cm while for uncoated nickel wires Wall found a decrease in permeability from a thickness of 7.6×10^{-2} cm (1/32 in.) to 38×10^{-2} cm (5/32 in.). There appears to be no confirmation of his theory that the magnetization is non-uniform across a sample below saturation or that the process of magnetization is initiated at the surface.

It is evident that more experimental work should be done on this important aspect of ferromagnetism. At present there are two clearly defined problems: to obtain further quantitative information about the effect of surface upon magnetization, and to find the relation between the thickness of a specimen and its magnetic properties. In the study of surface magnetization hysteresis loop measurements should, for example, be compared at lower applied fields, i.e., in the region of 1 oersted. Ideal for this work is a

TABLE I.

Thickness in cm $\times10^3$		μ_{max}	B_{max}	B_r	H_m	H_c	W (ergs/cc/cycle)
L.C. *steel*							
4.52	(t)	27020	12450	11520	3.78	1.67	6392
	(a)	27020	12350	11280	3.78	1.64	6178
5.74	(t)	66260	12440	11720	3.70	1.61	6447
	(a)	66260	12440	11720	3.70	1.61	6410
10.7	(t)	80210	13000	12240	3.70	1.21	5129
	(a)	80210	13000	12240	3.70	1.21	5111
15.8	(t)	66260	13200	12360	3.70	1.06	4768
	(a)	66260	13200	12200	3.70	1.06	4720
21.4	(t)	66260	13400	12600	3.54	1.07	4789
	(a)	66260	13200	12280	3.54	1.07	4676
38.2	(t)	46900	13000	12100	3.70	1.10	4859
	(a)	46900	13000	12100	3.70	1.10	4829
Nickel							
10.7	(t)	5522	3450	2300	3.70	0.89	888
	(a)	5522	3450	2400	3.70	0.85	894
16.6	(t)	10880	3700	2600	3.54	0.59	707
	(a)	10880	3700	2600	3.54	0.59	706
25.7	(t)	16210	3820	2700	3.86	0.54	646
	(a)	16210	3820	2700	3.86	0.57	673
38.9	(t)	20050	3900	2550	3.54	0.39	495
	(a)	20050	3800	2550	3.54	0.38	440

Legend:
μ_{max} = maximum permeability.
B_{max} and B_r = maximum and remanent induction, respectively.
H_m and H_c = maximum applied field and coercive force, respectively.
W (ergs/cc/cycle) = hysteresis loss in ergs per cubic centimeter per cycle.
(t) and (a) = ferromagnetic samples with surfaces together and separated, respectively.

material of high maximum permeability and low magnetostriction constant, properties which are embodied in 80 percent nickel-iron alloys. Unfortunately this permalloy is not yet available in sheet form over a suitable range of thickness. As a second choice electrolytically pure iron, a material slightly inferior to permalloy for this purpose, could be used. Whenever possible the material should be obtained in smooth thin sheets.

The effect of thickness upon the magnetic properties of the ferromagnetic elements should be further investigated. Present results in this field are highly controversial due mainly to the divergence of treatment given the materials before magnetic measurements were made. Wall's work seems to show that there is a thickness below 0.317 cm for which the permeability of a material is a maximum, while Cioffi finds that the permeability for the same material (Armco iron) increases from 0.025 cm to 0.317 cm quite uniformly. The preceding results on nickel, with sheets of different gauges rolled from the same parent stock, indicate that there is a uniform increase in permeability with thickness for the range from 0.010 cm to 0.038 cm.

The writer wishes to express his indebtedness to Professor L. W. McKeehan for suggesting the problem and for many stimulating discussions during the course of the work. His valuable suggestions and keen interest in the problem are sincerely appreciated.

Amontons' Law, "Traces" of Frictional Contact, and Experiments on Adhesion

ROBERT SCHNURMANN
London Midland and Scottish Railway Company, Research Laboratory, Derby, England
(Received December 11, 1941)

AMONTONS[1] measured the tangential frictional force F between the macroscopically plane surfaces of various materials in air and observed that the force was directly proportional to the normal load N and approximately independent of both the nominal area of contact A and the physical properties of the solids. The frictional force was about one-third[2] of the normal load. Coulomb[3] confirmed Amontons' result that the force of sliding was proportional to the normal load,

$$F=\mu\times N \qquad (1)$$

and essentially independent of the velocity of sliding when the surfaces remained undamaged. Coulomb elaborated on de la Hire's[4] hypothesis of the physical mechanism of "unlubricated" friction which assumes that the small irregularities of the surfaces interlock and either elastically deform or abrade each other during relative motion. He remarked that the force of friction might have two physical components, the force of "adhesion" or "cohesion" between the surfaces in contact and the force required to lift the slider over the irregularities of the surface with which it made contact. A criterion as to the mechanism of either solid friction (the friction between the naked surfaces of two solids) or "ordinary friction" (the friction in air between two mechanically clean solids to which no lubricant has been applied intentionally)[5] cannot be based upon Amontons' law which states only that $F=\mu\times N$ when the normal load N assumes such values in air that a limited variation of the nominal area of contact A does not alter appreciably the value of the frictional force. G. Rennie[6] found from experiments in air that the ratio $\mu=F/N$ did not remain constant when the load

[1] G. Amontons, Mém. Acad. Roy. Sci. (1699), p. 206.
[2] Leonardo da Vinci (about 1500) had arrived at the similar result that a slider would move on an inclined plane if the ratio between the tangential and normal components of the gravitational force exceeded one-fourth.
[3] C. A. Coulomb, Mém. Acad. Roy. Sci. (1785), p. 161.
[4] P. de la Hire, Histoire de l'Académie (1699), p. 104.
[5] See for example J. J. Bikerman and E. K. Rideal, Phil. Mag. [7] **27**, 687 (1939).
[6] G. Rennie, Phil. Trans. Roy. Soc. **34**, 143 (1829).

was increased beyond a critical value, and Landsberg[7] pointed out that the matter adsorbed on the surfaces would exclude the action of cohesion forces between the two solids themselves when in contact in air. It is accepted that the range of cohesion forces is extremely small, the force decreasing with the sixth power of the distance if this exceeds a few times 10^{-8} cm.

Experiments are described below to show that the actual area of contact[8] between two solids in air is a very small proportion of the apparent or nominal area of contact if the normal load does not correspond to a contact pressure exceeding the elastic limit of one of the solids, and that monomolecular layers of foreign matter exert adhesive properties between the areas of actual contact of two solids. They will stick together until the applied force assumes a large enough value to shear the weakest part of the joint: solid/foreign matter/solid. And even a metal at a temperature above its melting point can exhibit adhesion to the surface of a solid which it does not wet if a monomolecular layer of water has been condensed on it.

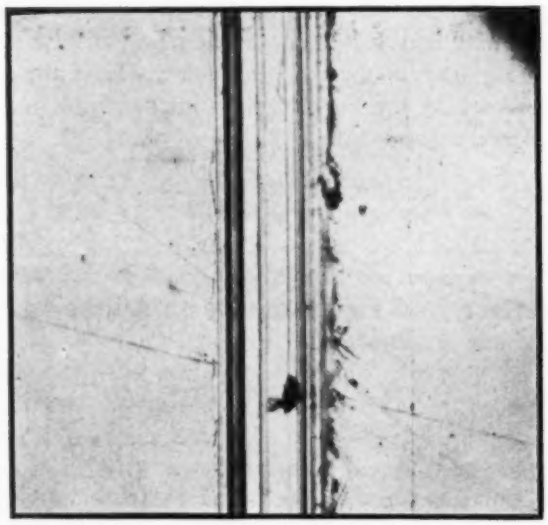

FIG. 1. "Traces" (magnification about 400 times) on the polished surface of a block of silver (weight: about 100 g) which was allowed to slide on an inclined glass plate in air.

[7] K. E. Landsberg, Pogg. Ann. d. Phys. Chem. **1**, 283 (1864).

[8] I.e., the area in which the solid surfaces are separated by not more than a few molecular layers of adsorbed matter.

MECHANICAL CLEANLINESS OF THE SURFACE OF A SOLID IN AIR

Free surfaces are covered with matter which they have adsorbed from the surrounding atmosphere. If the atmosphere is humid and also contains dust and greasy matter in suspension, as air does unless it has been cleaned carefully, foreign matter will condense and settle down in excess of the adsorbed layers. The surface of a solid in air can be made "mechanically clean" by freeing it from visible particles and thick layers of condensed liquid, but it is impossible to remove the whole of the foreign matter so long as it remains in this atmosphere. Even the drastic procedure of removing the contaminated surfaces completely by abrasion does not lead to a physically and chemically clean surface since re-contamination from atmospheric sources begins instantaneously. Nothing better can be done when experiments on supposedly "dry" friction are made in air than to keep the surfaces mechanically clean.[9] Clearly, the force of friction between two macroscopically plane surfaces which form a "dry" and mechanically clean contact must depend upon both the thickness and nature of the layers of foreign matter sandwiched between their load-carrying irregularities and may assume almost any value since it depends upon the shear strength of the weakest part of the combination solid/foreign matter/solid. In cases where the surfaces are separated by a fluid film whose motion is governed by the equations of hydrodynamics the frictional resistance is entirely independent of the nature of the surfaces and dependent only on the characteristics of the fluid. The minimum film thickness in these cases is about 5×10^{-4} cm, and the force of friction transmitted at the actual area of

[9] Sir William Hardy (Phil. Mag. **38**, 32 (1919)) took great care to wash glass plates in a certain way which he described before leaving them to drain and dry in *air*, realizing that contamination from solids touching it would creep over a free surface, but not realizing at the time that contamination from the surrounding air was unavoidable. Sir William Hardy (Proc. Roy. Soc. **A100**, 550 (1922)) mentioned in a later paper that "clean" surfaces as he prepared them were "not the same as surfaces freshly produced by fracture." The author applied Langmuir's (Trans. Faraday Soc. **15**, 69 (1920)) "talc test" to glass plates which after complete immersion for an appreciable time in a solution of chromic oxide in sulphuric acid were either rinsed or left to drain and dry in air. In the latter case they invariably repelled the talc particles, indicating that they were at its best mechanically clean.

contact f is

$$F=(\eta)\partial u/\partial n, \qquad (2)$$

η being the viscosity of the fluid, u the velocity of flow of the film and n the coordinate distance measured in the direction normal to the surface of the solid.

Hydrodynamic flow breaks down when the thickness of the film is smaller than about ten thousand molecules of ordinary size (5×10^{-4} cm)[10] and Amontons' law has been derived from observations on mechanically clean surfaces for which the film thickness has been less than this but large compared with molecular dimensions (a few times 10^{-8} cm). The experiments described below show that Amontons' law breaks down as the thickness of the film tends towards one molecule, and the actual area becomes an appreciable proportion of the nominal contact area.

"TRACES" OF SLIDING

The smoothest physical surface is the cleavage plane of a single crystal. The investigation of the specular reflection of molecular rays of helium of certain wave-lengths from the cleavage plane of a single crystal of lithium fluoride,[11] for instance, showed that the intensity of the reflected beam in a high vacuum decreased steeply when the angle of incidence between the primary beam and the cleavage plane exceeded about 20° and it was calculated from this result that the cleavage plane exhibited irregularities of a height of about two wave-lengths λ of the incident beam (helium, 100°K, and 295°K, wave-length $\lambda=1$ to 2×10^{-8} cm). The plausible assumption was made that these molecular irregularities on a cleavage plane were due to the thermal movement of the ions of the crystal lattice (LiF) and this was supported by the experimental evidence that the reflecting power of the cleavage plane of the crystal increased when its temperature was lowered. Highly *polished* surfaces would appear very rough by these standards, the height of their irregularities being of the order of several hundred molecules. Since light has a much larger wave-length than molecular rays, it is a considerably less sensitive tool for the inspection of surface finish. A surface which is "optically flat" exhibits in fact irregularities of a height of about 10^{-5} cm so that molecular rays which strike it at a glancing angle of more than about 10^{-3} radian are scattered from it but not specularly reflected.[12] The highest of

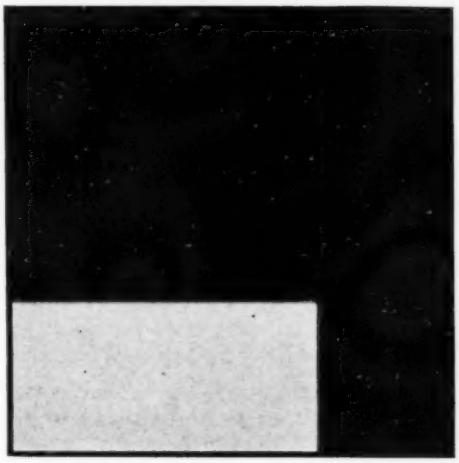

FIG. 2. "Trace" developed by treating a glass plate with a solution of silver nitrate after sliding on a metal surface.

FIG. 3. A portion of the "trace" shown in Fig. 2 magnified 700 times. The white bands consist of numerous parallel lines.

[10] See for instance E. Bodart, Rev. Univ. Mines **14**, 4 (1938).

[11] I. Estermann and O. Stern, Zeits. f. Physik **61**, 95 (1929).

[12] R. Schnurmann, Mech. Eng. **60**, 259 (1938).

these irregularities carry the load when one solid is put on the surface of another, and we imply throughout this paper that the "high points" of the surfaces are in contact when we speak for shortness sake of two surfaces in contact. Clearly, a solid must stand on at least three "legs," and it is easy to demonstrate that between a polished metal surface and a fused glass plate* the number of "legs" is numerous although their integrated area is a small proportion only of the nominal area of contact when the normal load is not sufficient to exceed the elastic limit of one of the components. Amontons' law holds approximately in air within this region.

Observation with the naked eye does not reveal any damage to either surface when the polished surface of a metal block of say 100-g weight has been made to slide slowly along the mechanically clean surface of a glass plate, while microscopic inspection (magnification about 400 times) of the *metal* surface shows some parallel lines on it (Fig. 1). The glass plate has acquired a *latent* image of the actual area of contact, which can be

FIG. 4. A portion (magnification 505 times) of the "trace" produced by a fused glass bead on a mechanically clean glass plate (before silver development).

* Fused glass plates were used throughout these experiments.

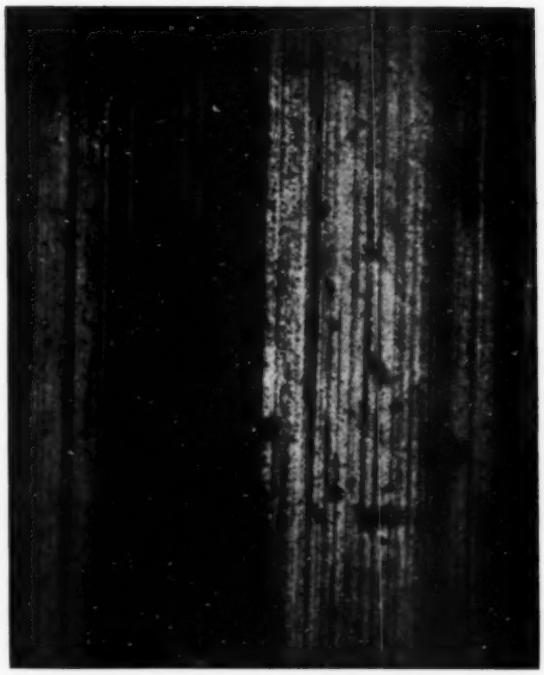

FIG. 5. A portion (magnification 505 times) of a "trace" similar to Fig. 4 after silver development.

developed by treating the glass plate with a solution[13] of silver nitrate to which a reducing agent has been added. The developed "trace" (Fig. 2) appears under the microscope as a number of wide bands (Fig. 3) which higher magnification resolves into multiplets of predominantly parallel lines. The latent image of the "traces" consists of abraded metal, since acid cleaning[14] of a plate carrying developed "traces" destroys both the "traces" and the latent image. Also, a fused glass bead does not produce a "trace" on a glass plate in air unless the applied load is large enough for the bead to "scratch"[15] the plate (see Figs. 4 and 5). The method of obtaining mechanical cleanliness did not alter the appearance of the "traces." The glass plates were either coated with a film of cellulose acetate which was peeled off immediately before establishing fric-

[13] Professor T. R. Merton, F.R.S., at whose suggestion "traces" of frictional contact have been studied, proposed the addition of ammonia to a solution of 11.5 g of silver nitrate in 500 cm³ of water until a faint precipitate was left and then of formalin as a developing agent.

[14] The glass plates had been immersed consecutively in concentrated sulphuric acid, concentrated nitric acid, ammonia, and distilled water.

[15] The "scratches" appear to the naked eye to be single lines while microscopic observation (magnification 505 times) resolves them into numerous lines.

tional contact or washed with xylol and wiped with a cloth.

"Traces" were obtained in air with any kind of metal, silver, copper, steel, lead, and cadmium, provided that the normal load was not appreciably less than 100-g weight, irrespective of whether the glass plates were "dry," or flooded with water or some other lubricant (Figs. 6 and 7). Under "dry" conditions, "traces" obtained with a slider of copper (normal load: 307-g weight) appeared to be fainter than those obtained with a slider of silver (normal load: 257.5-g weight).

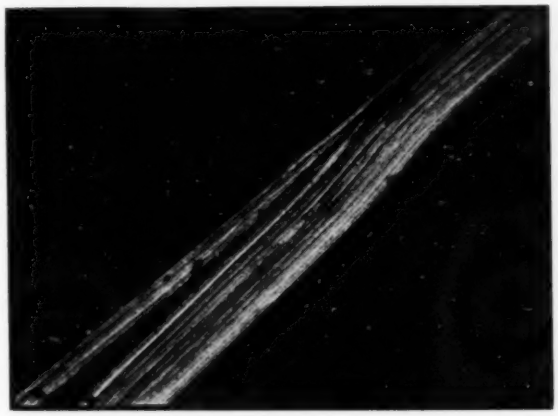

FIG. 6. Developed "trace" (magnification 85 times) produced by a block of copper (normal load, 1726-g weight) which was allowed to slide over an inclined glass plate flooded with distilled water.

Tangential displacement was required for the production of definite "traces." No clear indication of "points of contact" was obtained when a metal block was put on a horizontal glass plate and removed from it without any apparent tangential motion.

"TRACES" OF ROLLING

The force of rolling friction is appreciably smaller than the force of sliding friction, and it has been observed that "traces" of rolling metal spheres of about 700-g weight or more can be developed on glass plates. Viewed with the naked eye they look about the same as "traces" of sliding but, at a magnification of 700 times, the "traces" of rolling appear to be essentially different from those of sliding and to exhibit isolated specks (Fig. 8) instead of more or less continuous parallel lines in the case of sliding. The width of the band of isolated specks obtained with a steel ball of 5.7-cm diameter (759-g weight) was approximately 0.03 cm.

Pre-developing of the glass plates by treating the virgin plates with the solution of silver nitrate made them more sensitive indicators of rolling. The pre-development produced a thin fog of isolated silver grains on the glass plates which then were left to dry, before rolling contact was established. "Traces" of rolling contact with a glass plate prepared thus were visible to the naked eye when the plate was held at the appropriate angle of illumination. The largest sphere produced a line which, of course, was visible most easily, but even the line generated with a steel ball of 8.3-g weight could be seen faintly with the naked eye. The microscope resolved each of these lines into a "milky way" of isolated white dots on a slightly hazy background.

Conditions can be chosen under which either pure rolling, or mixed rolling and slipping, or pure slipping may occur. It was observed that the white dots produced by a sphere were approximately circular when the angle of tilt of the glass plates was very small. They appeared elongated in the direction of rolling when the angle of inclination of the plate was increased. The white dots were larger when a copper roller of 673-g weight was rolled over a glass plate which was

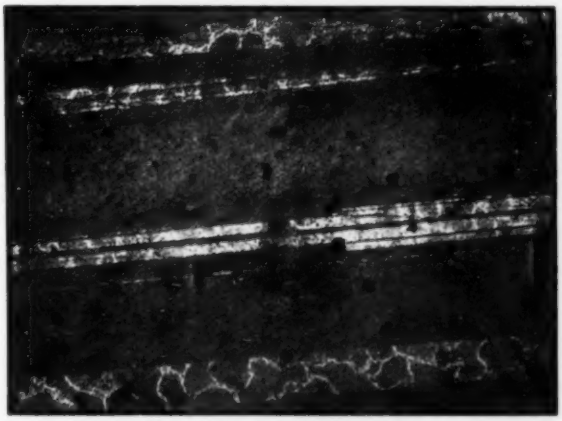

FIG. 7. Developed "trace" (magnification 85 times) on a glass plate after sliding contact with a block of copper (normal load: 1726-g weight). The glass plate had been immersed once in an emulsion of warm water and molten stearic acid. The structure of the "trace" did not exhibit any similarity with the translucent stearic acid crystallites of random orientation observed on the copper surface after sliding had taken place.

FIG. 8. Developed "trace" of rolling (magnification 700 times).

held at an angle of 15° to the horizontal than when it was rolled over the horizontal glass plate. Even a copper roller of 57.3-g weight produced a very faint "trace" on a pre-developed glass plate inclined at about 29°.

THE RATIO BETWEEN THE ACTUAL AND NOMINAL AREAS OF CONTACT

When a metal cylinder is cast on to a glass plate in air the ratio between the actual and nominal areas of contact is of the order of unity and is much larger than in the experiments described above. Professor Merton had observed that a small cylinder of Wood's metal which had been cast on to a mechanically clean glass plate could not be removed by normal or tangential forces applied by hand, but by a normal force of about 15 kg/cm². Experiments[16] were made with Wood's metal and with metals and alloys of higher melting points such as tin solder (m.p. about 183°C), tin (m.p. 232°C), the eutectic cadmium-zinc alloy (82.5 percent Cd, 17.5 percent Zn, m.p. 265°C), cadmium (m.p. 321°C), and lead (m.p. 327°C) which were all found to adhere strongly to the glass plates, provided that the pouring temperature did not exceed appreciably the melting point of the metal or alloy. The casting temperature was rather critical and it was observed that cylinders would crack off from the glass plate, if the casting temperature appreciably exceeded their melting points. Cylinders which had either cracked off or had been levered off exhibited a convex surface.

This strong adhesion is rather surprising at first, because the areas of contact of metals other than Wood's metal have a milky appearance (Fig. 9) and contain numerous blowholes which are not of uniform size although the diameters of most of them are about 10^{-3} cm. The blowholes are caused by water vapor driven off from the glass plate when the hot liquid metal strikes it, and by gas given off from the metal as it solidifies. The initially submicroscopic vapor and gas bub-

[16] The moulds for casting the metals and alloys consisted of hollow copper cylinders of about 1.27-cm internal diameter.

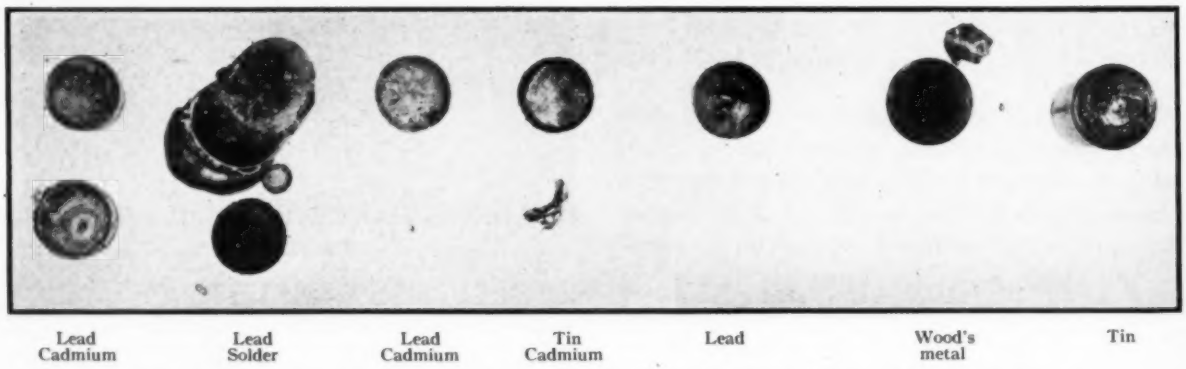

FIG. 9. Apparent areas of contact of cylinders of various metals and alloys which were cast on to glass plates at room temperature in air.

bles collide in the course of their Brownian movement in the interface and unite at a rate which depends primarily upon the rate at which they are generated and upon the viscosity of the medium in which they are suspended,[17] so that finally islands of metal are left between the bubbles. The adhesion between the cylinder and the glass plate must arise at these islands, although they do not form bridges of direct contact between metal and glass. The islands show etched structure under the microscope (Fig. 10) indicating that an extremely thin film of foreign matter (water vapor) remains between them and the glass. The "boiling off" of a large proportion of the humidity which is condensed on the surfaces of solids in air and the consumption of part of the residual humidity for etching the islands leaves a sufficiently thin film between the glass and the islands of metal, to act as an adhesive. The cast-on cylinders would not adhere to the plates unless the poured metal heated the plate sufficiently to drive off a large portion of the humidity condensed on it. For instance cylinders cracked off *metal* plates if they were cast when the plates were at room temperature, since the heat was rapidly conducted away from the contact area. The poured metal however would adhere to a pre-heated metal plate from which most of the humidity had been boiled off by the pre-heating. Evidence that water vapor played an appreciable part in forming the blowholes was obtained when glass plates were heated to 200°C, 250°C and 500°C, respectively, in a furnace with air circulation, and cylinders of lead were cast on to them while they were in the furnace.[18] The contact areas had a mottled appearance even in these cases (Fig. 11) but the blowholes were less numerous and appreciably smaller than when the glass plates were at room temperature.

Easily oxidized metals (for instance cadmium) would not adhere to the glass plates unless a few grains of ammonium chloride had been added to the melt immediately before pouring it. Otherwise, cylinders of such metals and alloys cracked off by tearing apart their oxidized surface layers,

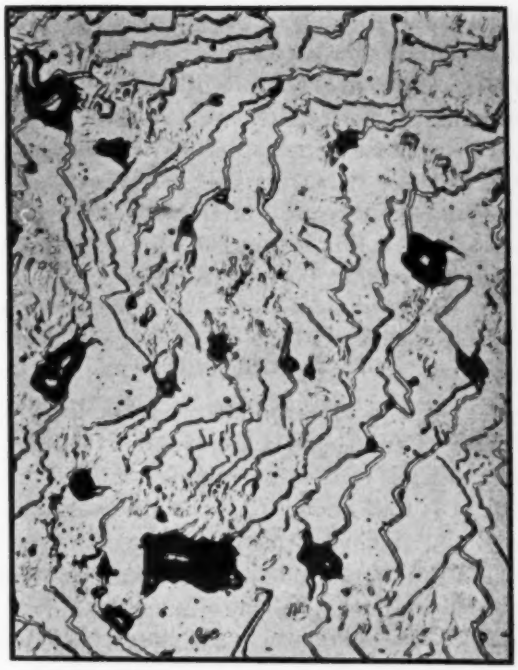

FIG. 10a. Etched structure (magnification 100 times) of an "island of contact" of a cylinder of lead adhering to a glass plate.

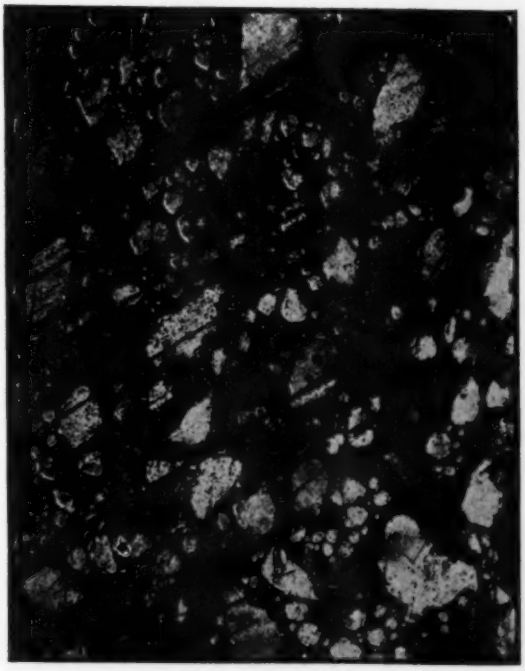

FIG. 10b. A part (magnification 100 times) of the material remaining on a glass plate from which a cast on cylinder of cadmium has cracked off.

[17] R. Schnurmann, Zeits. f. physik. Chemie **A143**, 456 (1929); Kolloid Zeits. **80**, 148 (1937); J. Soc. Chem. Ind. **58**, 172 (1939); Proc. Inst. Mech. Eng. **145**, 183 (1941).

[18] The glass plate which had been heated to 500°C was left in the furnace to cool down to 230°C before the lead was cast on.

part of these sticking to the glass plates (see for instance the center bottom of Fig. 9 and Figs. 10b and 10c). The suggestion is that extremely thin adsorption layers, which are too thin to allow relative motion by internal shear, exert adhesive properties so that relative motion must be accompanied by tearing of the solid of smallest shear strength, for instance of the solid whose surface layers have become oxidized.

THE JERKY MOTION OF MERCURY IN GLASS CAPILLARIES

Evidence has been obtained that the thickness of a film of condensed water vapor is monomolecular when it exerts appreciable adhesive properties. It is well known that the internal diameters of the capillaries of a McLeod manometer should not be smaller than 0.1 cm because otherwise "the surface tension of mercury in conjunction with the friction at the glass walls" gives rise to irreproducible readings of the distance between the two menisci of mercury in the open and the closed capillaries. The mercury columns in the capillaries of a shortened McLeod manometer whose internal diameters are 0.13_8 cm usually appear to ascend and descend steadily, particularly if vapors have been condensed in a liquid-air-cooled trap, and there is then no ambiguity involved in the reading of the difference in height of the mercury levels in the two capillaries. The mercury column in the closed capillary, however, exhibits jerky motion when it reversibly condenses water vapor on the stable adsorption layer adhering at room temperature to the glass wall so that patches of condensate arise of not more than monomolecular thickness, and when the rate of either ascent or descent of the two mercury columns is not very large. The maximum velocity of the change of height of the mercury level was measured in the closed capillary when water at a vapor pressure of $6 \cdot 10^{-3}$ mm Hg was condensed during compression of the volume of gas and vapor from 0.3 cm³ to 0.03 cm³. The nominal area of glass surface available for condensation inside the closed capillary was $A_G = 8.57$ cm². Since the number of condensed molecules was $n \approx 5.10^{13}$ and since $n_0 \approx 10^{15}$ water molecules would cover an area of $A_0 = 1$ cm² with a monomolecular layer in close packing, it would appear that the condensate must have formed either monomolecular patches covering about 1/100 of area A_G, or polymolecular patches covering a correspondingly smaller proportion of A_G. Measurements from a photographic film[19] (16 frames per second) of the ascending and descending mercury columns showed that the one in the closed capillary sometimes stuck to the wall for as much as half a second and then accelerated (Figs. 12a and 12b), and that these "stick-slips" occurred in cycles.

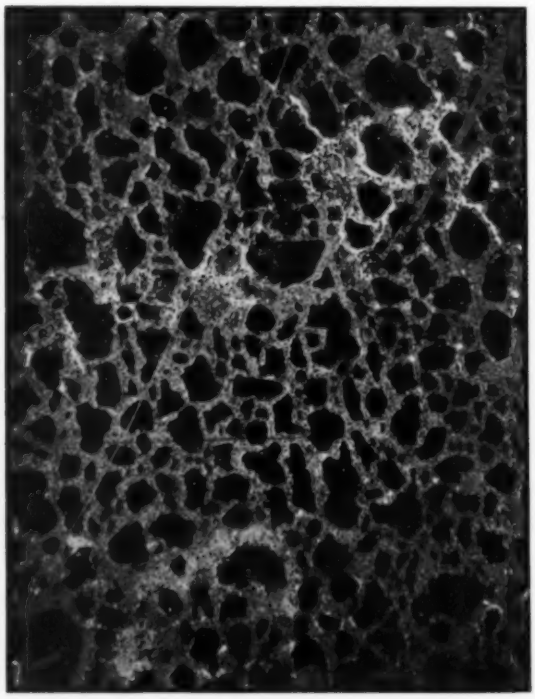

FIG. 10c. A part (magnification 100 times) of the material remaining on a glass plate from which a cylinder of eutectic Cd-Zn alloy has cracked off.

ADHESION DUE TO THE POROSITY OF ONE OF THE FRICTION ELEMENTS

The film of condensed water vapor between the mercury and the glass would not act as an adhesive if it were polymolecular to the extent that the shear strength of adjacent molecular layers of water was small compared with that of water molecules adhering to the surfaces of either the glass or the mercury. The jerky motion of the mercury in the closed capillary tends to vanish at

[19] It is a pleasure to thank Mr. C. W. Newberry for his assistance in making and evaluating the motion picture of the mercury columns.

high water vapor pressures.[20] Any method by which the thickness of the film between two solids is reduced to a monomolecular layer, in the extreme case, makes the two solids stick together. The wringing together of two polished surfaces is one method of achieving the squeezing out of the major part of the film separating the surfaces, and the blotting of the major portion of the

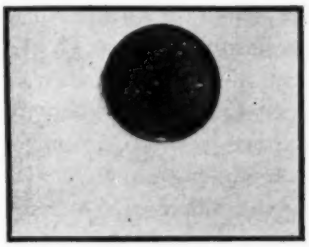

FIG. 11. Apparent area of cylinder of lead cast on to glass plate which had been heated to 500°C and was left in the furnace to cool down to 230°C before the lead was cast on.

intermediate film by a porous material is an alternative method for obtaining adhesion. It is well known that snow adheres to an appreciably inclined base whose temperature is above the melting point of snow. The porous snow blots the major proportion of water formed at the contact area[21] leaving a sufficiently thin layer of melt for adhesion between the snow and the solid with which it is in contact. Thus for instance an appreciable load of snow will adhere to the inclined roof of a house as long as the rate of melting of the snow at the contact area does not exceed the rate at which water can be blotted by the bulk of the snow. The blotted water under these conditions is transferred from the interface, flows through the snow capillaries and forms icicles, if the temperature of the air is below the freezing point of water, so that melting occurs at the area of contact only.

Similar observations can be made with every porous material even if it is far from its melting point and does not provide its own "adhesive." A small amount of water or any other fluid liquid which does not react chemically with either of the solids can be applied at the area of contact. For example, a cylinder of compressed sand (weight: 156 g) was easily stuck on to a fused glass plate with a drop of water and did not slide even at an angle of inclination of the plate of 90°. If it was made to slide by pulling, then the surface of the cylinder was torn, grains of sand remained on the glass plate. Similarly, a piece of lump sugar was stuck on to a glass plate with a drop of alcohol.[22] It was necessary in these cases, of course, for the contacting surfaces of the porous materials to bed themselves down on the surfaces with which they made contact, and it was not possible to stick a cylinder of refractory material (weight: 207 g) onto a glass plate when the surface of the cylinder was not plane.

DISCUSSION

Experiments described in a previous paper have shown that at room temperature the coefficient of static friction (as defined by the ratio of the components of the gravitational force parallel and normal to a plane inclined to the horizontal) of metals cleaned by volatilization in a high vacuum assumes values of the order of unity. No experiments in a high vacuum have been made hitherto with the load varied over an appreciable range.

In air the conditions are very different. If the surfaces are mechanically clean, the coefficient of static friction is almost zero when either the residual film of adsorbed and condensed matter sandwiched between them is very thick (about 5.10^{-4} cm) or in the case of an extremely thin residual film (about 10^{-7} cm) when the ratio between load and shear strength of either component of the joint of solid/foreign matter/solid is very large. In the former case sliding would begin by shearing the sandwiched film, and the surfaces of the two solids would not become torn; in the latter case sliding would begin by tearing one of the solids. On the other hand, the coefficient of static friction would assume an infinite value when the thickness of the sandwiched film (which is usually called the boundary film) was extremely small (about 10^{-7} cm) and the ratio between load and shear strength of either component of the joint were smaller than unity.

[20] See, for instance, E. Warburg, Pogg. Ann. d. Phys. Chem. **21**, 367 (1870).
[21] R. Schnurmann, Nature **145**, 553 (1940).
[22] R. Schnurmann, Engineering **149**, 567 (1940).

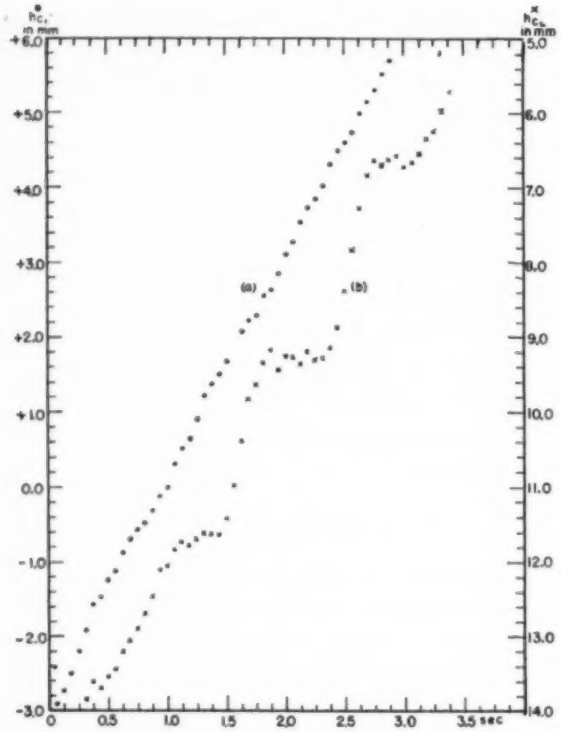

FIG. 12a. The curves (a) and (b) represent the rate of ascent of the mercury columns in the open and closed capillaries respectively of a McLeod manometer, when a given amount of water vapor is condensed on the wall of the closed capillary.

The "traces" described above were obtained when a portion of the surface of a metal suffered tearing in frictional contact with glass. Amontons' law approximately holds as long as the damaged portion is a very small proportion of the apparent area of contact. Definite "traces" of either sliding or rolling contact between any kind of metal and fused glass plates in air could be developed from latent images on the plates, provided that the load had been large enough (about 100-g weight in the case of sliding and about 700-g weight in the case of a rolling sphere). With these loads sufficient metallic matter to form latent images on mechanically clean glass plates was abraded in air, whereas no *clear* indication of "points of contact" between a block of metal and a glass plate in air was found when the load had been increased to as much as 9673-g weight before the block of metal was removed from the glass plate without any apparent tangential motion. Such motion reduces the thickness of the boundary film at a rate directly proportional to the load.

Amontons' law certainly does not hold when the actual area of contact is of the order of magnitude of the apparent area of contact and the boundary film is extremely thin, as in the experiments where molten metal has been poured on to a fused glass plate in air and at a temperature below the melting point of the poured metal. Experiments of this kind indicate the tenacity with which an extremely thin film holds two solids together, since the surface of the solidified metal cylinder assumes convex shape upon being separated from the glass plate. Appreciable adhesion has been found also when mercury at a temperature above its melting point slides over a glass surface on which monomolecular patches of water vapor have condensed. There is no evidence of the formation of "welded bridges" in any of these cases which can all be explained on simple physical grounds.

Speculations about the formation of "welded metallic bridges" between solids in frictional contact in air have played a prominent part in the recent literature on supposedly "dry" friction although no experiment has been published yet to justify such speculations in cases where the bulk of the friction elements was not near their melting points. The generation of friction heat has been known for centuries, and Bowden and Ridler's[23] experiments indicate that the temperature recorded by two friction elements increases with increasing load and velocity of sliding when they are used as the two elements of a thermocouple. The highest temperature which can be recorded is of course the melting point of the lower melting material, which will not necessarily be high enough to remove the last molecular adsorption layer from the higher melting material. If the conditions of thermal equilibrium at the contact area were such that an appreciable amount of material of lower melting point would melt during the motion of a slider acted upon by a constant force and if neither of the friction elements was porous, conditions of hydrodynamic lubrication would arise, and the velocity of the slider consequently would increase. If actual contact were established at a mathematical point, the temperature at this point would assume an

[23] F. P. Bowden and K. E. W. Ridler, Proc. Roy. Soc. **A154**, 640 (1936).

infinite value for any finite value of the load and velocity of sliding. In the physical case, however, the area of actual contact is finite, small though it may be, and the proportion of heat conducted and irradiated from it determines the temperature rise.[24] On account of the high values of the heat conductivity of metals large values of load and velocity of sliding are necessary for obtaining an appreciable rise in temperature.

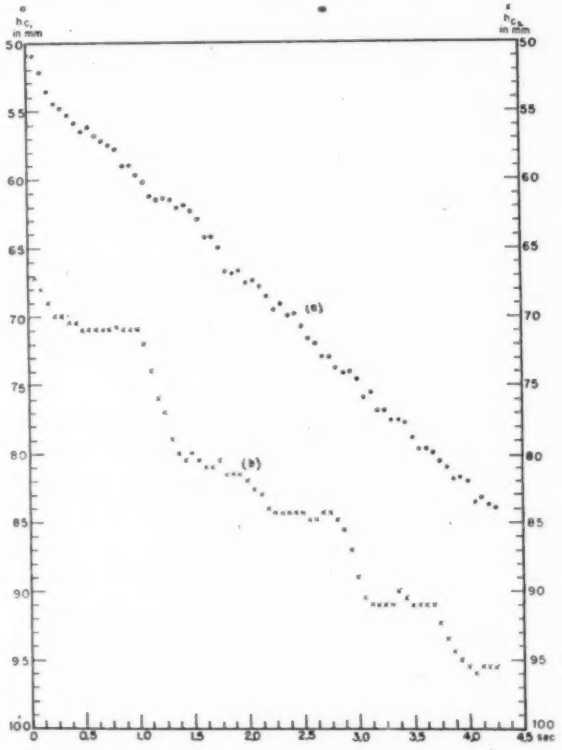

FIG. 12b. The curves (a) and (b) represent the rate of descent of the mercury columns of a McLeod manometer under similar conditions to Fig. 12a.

[24] The friction heat produced per second would be calculated to 0.39 cal. if, for instance, the "coefficient of friction" were 0.33, the normal load 500-g weight and the velocity of sliding 100 cm/sec. Assuming friction elements of copper with large free surfaces and "legs" of a height of 10^{-5} cm and an integrated area of 0.076 cm², the temperature gradient along the "legs" would be $5.6 \cdot 10^{-5}$°C. The thermal conductivity of metals is so large that high temperatures cannot be localized at the irregularities of the surfaces. Assuming alternatively that the emitting surfaces of friction elements of copper were small and, for instance, 9 cm², a temperature rise by 170°C could be calculated for the case in which no heat would be conducted away from the elements by the supports and neglecting radiation losses. High values of load and velocity of sliding are required under actual experimental conditions with metals for producing an appreciable temperature rise by friction heat, as also Bowden and Ridler's experimental results indicate.

SUMMARY

The force of supposedly "dry" friction between mechanically clean surfaces in air depends upon the thickness and nature of the film of foreign matter between them. Amontons' law holds within a very narrow range of film thicknesses considering that hydrodynamic lubrication is not established before the film is at least ten thousand molecules ($5 \cdot 10^{-4}$ cm) thick. It holds approximately when the area which suffers tearing in frictional contact is a very small proportion of the nominal area of contact.

"Traces" of sliding and rolling friction between various metals and glass in air have been studied. They are a measure of the torn proportion of the area of contact. Microscopic examination resolves "traces" of sliding into wide, more or less continuous bands of predominantly parallel lines and "traces" of rolling into isolated specks.

Extremely thin films of foreign matter between the "high points" of two solids in contact act as adhesives. The tenacity of a monomolecular layer of condensed water vapor is very high, as experiments show when various molten metals (of melting points above 100°C) are poured on to mechanically clean glass plates in air. Even mercury exhibits a tendency to stick to the wall of an evacuated closed capillary on which a monomolecular layer of water vapor has been condensed at room temperature. Every method of reducing the thickness of a film of either foreign matter or melt to a monomolecular layer leads to adhesion as observations of snow on a warm base and experiments with porous friction elements far away from their melting points show. Sliding proceeds by tearing the surface of one of the solids whenever the film of foreign matter is not the component of smallest shear strength of the combination solid/foreign matter/solid.

ACKNOWLEDGMENT

The author expresses his thanks to the London Midland and Scottish Railway Company for permission to publish this paper, and to Dr. E. Warlow-Davies for reading the manuscript.

A Model Method of Photographic and Photometric Determination of Heat Radiation Between Surfaces and Through Absorbing Gases

MAX JAKOB
Illinois Institute of Technology and Armour Research Foundation, Chicago, Illinois

AND

G. A. HAWKINS
Purdue University, Lafayette, Indiana

(Received November 26, 1941; revision received January 21, 1942)

Straight analytic determination of the heat exchange by radiation in a device is possible only if the emitting and absorbing surfaces are very simple in shape and configuration. In most practical cases, and particularly if the radiation is partly absorbed on its way by gases, approximative calculations and graphical methods have been used in order to evade the mathematical difficulties. In the present paper an experimental model method with the following characteristic features is described. A model, similar to the device under investigation, is constructed. Light is used instead of the long wave heat radiation, and its absorption by photographic films which cover the surfaces of the model, is measured by the methods of photometry. The case of gases which absorb heat radiation is imitated by using liquids which absorb light rays. The application of the method to radiation through a non-absorbing medium is shown by experiments on a tube bank model. The adaption of the method to heat radiation through absorbing gases is demonstrated by photos of the spectrum of a special combination of light filter, absorbing liquid, and photographic film which are in tune in a narrow wave-length range.

I. INTRODUCTION

SURFACE and gas radiation constitutes an important part, and often is the controlling factor, in high temperature heat exchange devices, such as oil stills and furnaces. In order to calculate the radiative heat transfer, it is necessary to know the laws of radiation, the properties of surfaces and gases occurring in these laws, and the influence of the geometrical configuration of the device. The physical laws are well known, and there exist a good many experimental data relative to the decisive properties of technical surfaces and a few for the respective properties of gases. The principal problem encountered is how to take care of the geometrical configuration.

This is relatively simple for the case of mere surface radiation in geometrically simple arrangements. For the more complex shapes, it is more difficult. For some of these cases, the results of mathematical, graphical, and experimental determinations are available. For more complicated apparatus, it is necessary to make suitable assumptions and simplifications before elementary principles can be applied.

Whereas with surface radiation, the energy is not changed in traveling between surfaces, in the case of radiation through absorbing gases, the intensity of each ray is continually weakened in its path. The influence of geometrical shape has been calculated exactly for only a few simple cases. For complicated configurations, such as combustion chambers, it is very cumbersome and sometimes almost impossible to obtain more than a rough approximation of the influence of the shape.

For the solution of the complex cases, the authors hope that the model method suggested and demonstrated in this paper will be helpful. It is based on the following facts.

Heat radiation is governed by the general laws which apply to all types of radiation. Thus, in a model, geometrically similar to the device under consideration, any photographically active rays will travel in paths geometrically similar to those of the heat radiation in the device.

Also the absorption of photographically active radiation in a suitable homogeneous medium will follow the same law as the selective absorption of heat radiation, i.e., the absorption in some gases at certain wave-lengths.

Finally, the absorption of radiated energy by a photographic film corresponds to the absorp-

tion of heat radiation by a surface, and the degree of absorption can be measured by a photometric method.

So, for an arbitrary engineering device, it is possible to construct a geometrically similar model, in which the emitting surfaces are replaced by light sources, the absorbing surfaces by photographic films, and the absorbing gas, if any, by a light absorbing liquid. The method includes photometric calibration of the films and of the absorbing liquid, exposing the films in the model to the light source, and automatic photometering of the films. The method yields the distribution of the absorbed radiation over any part of the absorbing surface, regardless of its location and shape.

The authors are aware of some of the difficulties encountered by the method, such as the differences of absorptivity between the heat absorbing surfaces and the light absorbing films, and the deviations of the radiation under oblique angles to the surfaces from Lambert's law of diffuse radiation. However, it is hoped that these difficulties can be overcome by proper arrangement and technique, and it is felt that the difficulties are not great in comparison with the advantages of the method, by which calculations of several days or weeks duration and possibly with questionable results, can be replaced by a few photographic exposures, automatic photometering and some routine calculating.

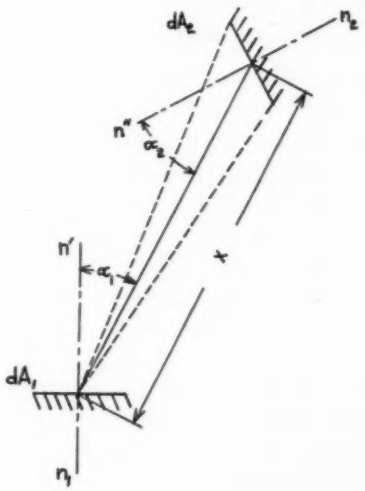

FIG. 1. Radiation between two surface elements.

Experiments have been performed on a model of a tube bank for the case of a non-absorbing medium. By means of photographs of the spectra it will be shown that the absorption of gas radiation can be satisfactorily imitated by the absorption of light by a suitable liquid.

An example of the application of the method to a practical problem will be considered in Section IX. There a procedure will be described by means of which the radiation from flue gases to the superheater tubes of a boiler can be measured.

II. FUNDAMENTAL EQUATIONS OF HEAT RADIATION

The problem is to determine what part of the heat energy, emitted by any element of a radiating surface, strikes any part of a second surface which will be considered as absorbing all of the arriving energy. This assumes that the absorbing surface is black for heat radiation, which is approximately the case with the surfaces inside of furnaces.

In Fig. 1, dA_1 and dA_2 are elements of the radiating and the absorbing surfaces, respectively. Their normals n_1n' and n_2n'' may lie in the same or in different planes. The other symbols are self-explanatory. The energy emitted in unit time by the surface element dA_1 into the hemispherical space above it, is

$$d^2q_1 = \pi I'_\lambda d\lambda \cdot dA_1, \tag{1}$$

where I'_λ is the intensity of radiation at the wave-length λ in the direction n_1n'.

The part of the energy which strikes dA_2 is

$$d^3q_{12} = I'_\lambda e^{-x\delta_\lambda} d\lambda \cdot dA_1 \frac{\cos\alpha_1 \cos\alpha_2}{x^2} dA_2, \tag{2}$$

where δ_λ is defined by the equation

$$dI'_\lambda = -\delta_\lambda I'_\lambda \cdot dx. \tag{3}$$

δ_λ is often called the "coefficient of absorption" of the medium through which the radiation travels, but in order to avoid confusion with "absorptivity," the name "intensity decrement" will be used because δ_λ formally corresponds to the logarithmic decrement of a mechanical damped oscillation. It is well known that only some gases, as carbon dioxide and water vapor,

absorb radiation to an appreciable amount, and that this occurs only in certain wave-length ranges ("bands").

By integrating Eq. (2) the following equation for the radiation which hits the whole surface A_2 is obtained.

$$d^2q_{12}=I'_\lambda d\lambda \cdot dA_1 \int_{A_2} \frac{\cos\alpha_1 \cos\alpha_2}{x^2} e^{-x\delta_\lambda} dA_2. \quad (4)$$

The ratio

$$\varphi=\frac{d^2q_{12}}{d^2q_1}=\frac{1}{\pi}\int_{A_2} \frac{\cos\alpha_1 \cos\alpha_2}{x^2} e^{-x\delta_\lambda} dA_2 \quad (5)$$

is called the angle ratio. This has been determined by exact or graphical integration for different simple configurations, for non-absorbing medium ($\delta_\lambda=0$)[1] as well as for absorbing gases. For gas radiation in a sphere and in an infinitely long cylinder the integration has been performed by Nusselt,[2,3] for the case of infinitely extended parallel planes by Jakob.[4] A table of these values is presented in a recent paper of Johnstone, Pigford, and Chapin.[5] The most comprehensive and practical solutions have been given by Hottel.[6,7] In these also the variation of δ_λ with the wave-length in the range of the band is considered.

It is obvious how difficult, the mathematical solution becomes for complex cases, owing to the fact that Eq. (5) contains not less than 4 independent variables, namely, x, α_1, α_2, and A_2. The method herein presented avoids this difficulty.

[1] H. C. Hottel, "Radiant heat transmission between surfaces separated by non-absorbing media," Trans. A. S. M. E. **53**, 265 (1931).

[2] W. Nusselt, "The heat transfer in the combustion engine," Forschungsarbeiten auf dem Gebiete des Ingenieurwesems, No. 264 (1923). (Title translated by the authors.)

[3] W. Nusselt, "The gas radiation in the flow in a tube," Zeits. d. Ver. deutsch. Ing. **70**, 763 (1926). (Title translated by the authors.)

[4] M. Jakob, "Absorption and radiation of gases free of soot," *Der Chemie-Ingenieur* (Akademische Verlagsgesellschaft, 1933), (Title translated by the authors). Vol. **1**, Part 1, Chap. 5, § 37.

[5] H. F. Johnstone, R. L. Pigford, and J. H. Chapin, "Heat transfer to clouds of falling particles," Univ. Illinois Bull. **38**, No. 43 (1941). Eng. Exper. Station Bull. Ser. No. 330.

[6] H. C. Hottel, "Heat transmission by radiation from non-luminous gases," Trans. Am. Inst. Chem. Eng. **19**, 173 (1927).

[7] H. C. Hottel and R. B. Egbert, "The radiation of furnace gases," Trans. A. S. M. E. **63**, 297 (1941).

III. PHOTOGRAPHIC AND PHOTOMETRIC FUNDAMENTALS OF THE METHOD

A brief discussion of photographic and photometric principles is necessary for a clear understanding of the method suggested. It is a well-known fact that the tiny crystals of silver bromide on a photographic film are affected when exposed to light, and when the film is developed, the bromide is reduced to metallic silver on those spots, where it had been struck by light rays. The amount of this chemical conversion depends on the quality and intensity of the radiation and on the time of exposure.

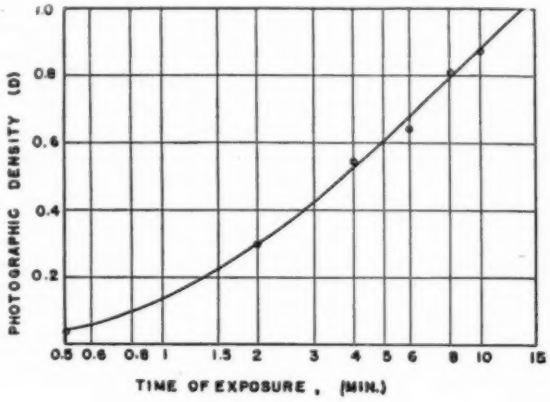

FIG. 2. Film calibration chart.

Thus, the density of the silver deposits or the grade of blackening of the film gives a measure of the absorbed radiation.

The density D of a silver image on a film is defined by the equation

$$D=\log_{10} I_0/I, \quad (6)$$

where I_0 is the intensity of the incident radiation, and I is the intensity of the transmitted radiation. When $D=0$ all of the incident light is transmitted through the film, when $D=1$ still 10 percent is transmitted, and when $D=2$ only 1 percent is transmitted.

It is easily seen that

$$D=(\log e)\delta_s \cdot L=0.4343\delta_s \cdot L, \quad (7)$$

where L is the thickness, and δ_s is a coefficient of absorption or intensity decrement of the silver deposit on the film, defined by an equation similar to Eq. (3). However, following the

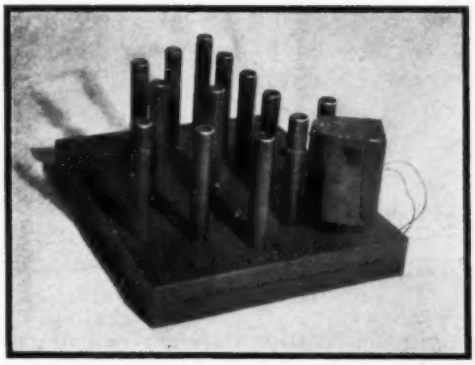

FIG. 3. Model of a bank of tubes with lamp house.

customary use in photographic research, the photographic density D has been retained in this paper.

The ratio I_0/I for any point on the photographic film may be determined by use of a photometer. This consists essentially of a constant source of light, film holder, lens system, sensitive thermocouple, and recording galvanometer. The light passes through the film and is then focused on a thermocouple which is connected to the galvanometer. As the film is drawn across the beam of light, the intensity of light striking the thermocouple will vary with the blackness of the negative. The corresponding deflections of the galvanometer are recorded photographically. Referring to the original film, the ratio of the galvanometer reading for the developed clear base of the negative to the galvanometer reading at a given darkened spot on the film is equal to the ratio of the intensities I_0/I, if the intensity of light transmitted through the clear film base is called I_0 and used as reference intensity.

IV. CALIBRATION OF THE FILM

All films used in the experiments were calibrated by exposing sections of the films for various lengths of time, developing the films, and passing the resulting negatives through a photometer. In all calibrations extreme care was exercised in order to insure as nearly as possible uniform development over the entire surface area of the film. This is absolutely necessary in order to eliminate variables such as differences in solution concentration and temperature, age of developer, and unequal agitation of the solution with respect to the negative. After the negative was properly prepared, it was passed through the photometer. For each section of the film the values for I and I_0 were determined by direct measurement from the photometer record. The density values were then calculated for each section by means of Eq. (6). The resulting density values were plotted against the corresponding exposure time on semi-logarithmic paper to form the calibration chart. Many experiments have been performed in order to select the most suitable film for a particular application. However, a great deal of difficulty was encountered in placing extremely sensitive panchromatic films in the apparatus in total darkness. From the standpoint of ease of manipulation of the apparatus, it was found that films which could be used under safe lights were the most desirable. A typical film calibration chart is given in Fig. 2.

V. DESCRIPTION OF A MODEL

A model of a bank of tubes, Fig. 3, was constructed in order that the radiation from a source of radiation to different curved surfaces could be studied. The model consisted of a

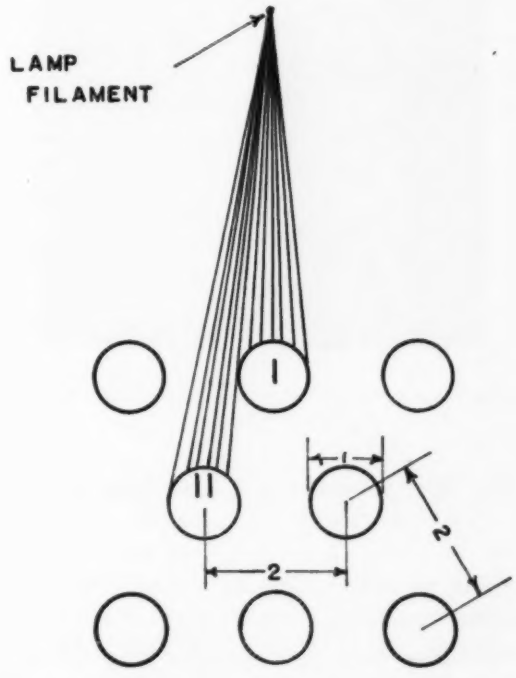

FIG. 4. Arrangement of tubes and rays hitting tubes I and II.

number of pipes, 1-in. outer diameter, 10 in. long, located in an accurately drilled base. In a horizontal cross section through the tube bank, Fig. 4, the tube centers are on the corners of equilateral triangles, and the pitch between the tubes is equal to the outer pipe diameter. The tube surfaces were blackened with flat black mixed with lamp black.

FIG. 5. Print from test negative (tube I illuminated in a horizontal plane).

FIG. 6. Print from test negative (tube II illuminated by vertical filament).

The light source was a single-filament galvanometer-lamp which was located in a lamp house (see Fig. 3) or without that in an adjustable mounting. By horizontal slits in the housing, radiation could be restricted to a horizontal plane. When used without housing, the whole filament, about $4\frac{3}{4}$ in. long, acted as the source of radiation, parallel to the tube axes. By this method an illumination was obtained which was uniform in the vertical direction over a rather great length.

After the apparatus had been clamped into position, pieces of the same film as used in the calibration experiments, were wrapped around the pipes, and the device was ready for exposure.

VI. DETERMINATION OF THE RADIATION WITH A NON-ABSORBING MEDIUM

The films in position were exposed to light for a pre-determined time interval, namely such as always to insure that the results would fall on the straight line portion of the calibration curve (see Fig. 2). The exposed films were then developed under the same conditions as was the calibration film.

A print made from a negative taken on tube I (see Fig. 4) with radiation in a horizontal plane (using the lamp house with slits) is shown in Fig. 5, a print for tube II under illumination from the whole vertical filament is shown in Fig. 6.

It must be remembered that the white portions of the prints actually represent the dark portions on the original negative, and that considerable detail is lost in making a print from a negative used for photometric purpose. However, the characteristic items, particularly in Fig. 6, will be recognized.

It is apparent from Fig. 6 that the blackening was not uniform around the film on tube II owing to the shading effect of tube I (see Fig. 4). While the print is flat, the actual film recorded blackening on the cylindrical surface of the cylinder II. The negative was then placed in the photometer and a record made of the blackening. Since the illumination was constant over the vertical length of the film, the results from only one horizontal line around the cylinder were recorded from the photometer measurements. The actual distance across the blackened portion of the film was approximately 0.8 inch. Owing to the magnification of the abscissa by the photometer the resulting trace was approximately 14 in. in length. A photometer trace for the film shown in Fig. 6 appears in Fig. 7 as the curve reaching the maximum height. The other lines represent different exposure times for films on the same tube. The photometer

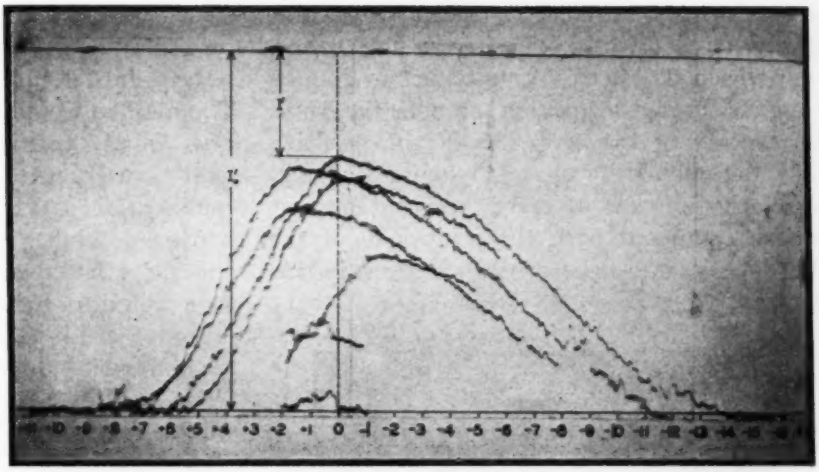

FIG. 7. Photometer traces belonging to Fig. 6. (The left side corresponds to the right side of Fig. 6.)

traces are shifted in order to avoid lines falling one on top of the other. For convenience in recording the results the position on the photometer trace corresponding to maximum displacement from the lower reference line is designated by 0. One-half inch intervals on either side of the zero position are numbered positively in one direction and negatively in the opposite direction. Each interval corresponds to about $0.8/28 \approx 30/1000$ in. on the tube circumference.

VII. DETERMINATION OF THE NORMALIZING FACTOR AND THE RELATIVE RADIATION

The calibration of the films was based on a special location of the film with respect to the light source. In order to use the calibration for arbitrary locations a simple method of reduction of the energy values can be used.

Figure 8 is a schematic diagram of tube I and the light source. For a given time interval t_0 the energy absorbed Q_0 on a small area at reference point 0 would produce a certain density D_0 on the film. This density would correspond directly with the calibration data. At point 3 the energy Q' would produce a blackening which would result in a density D' equivalent to an exposure time t in the normal position. However, for position 3, angle and distance variables are encountered which differ from the normal case. In order to have the results on a comparable basis it is necessary to normalize the results for position 3 to correspond to the normal position at point 0. Since the intensity of the light source remains constant,

$$Q = (t/t_0)Q_0 = NQ_0, \tag{8}$$

where the ratio $N = t/t_0$ may be termed the normalizing factor.

For each of the positions on the various photometer traces for the tubes, other than for the zero position of tube I, directly opposite the light source, the value of the density D' is determined from the measurements of I'_0 and I' and Eq. (6). The corresponding equivalent exposure time t to produce the same density can be taken from the calibration curve. The exposure time t for each position on any one of

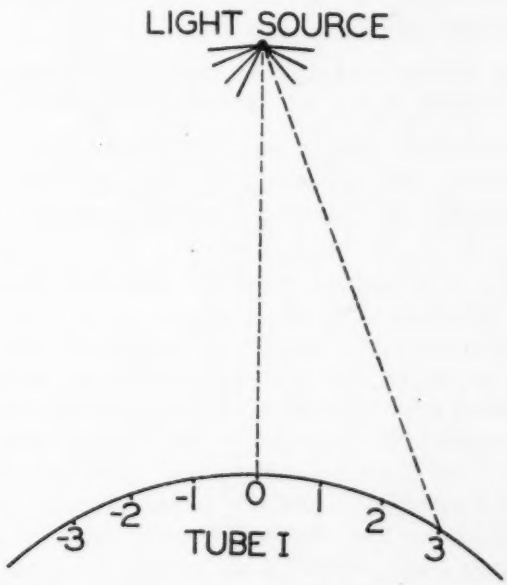

FIG. 8. Schematic diagram of light source and tube I.

the tubes is to be divided by the exposure time t_0 for the tube directly opposite the light source and position 0. The resulting values of N may be plotted against position around the tube. The average of the ordinates of the resulting curve, determined by use of a planimeter, gives the relative amount of energy received by that tube as compared with the position 0 of the tube opposite the light source as the standard reference.

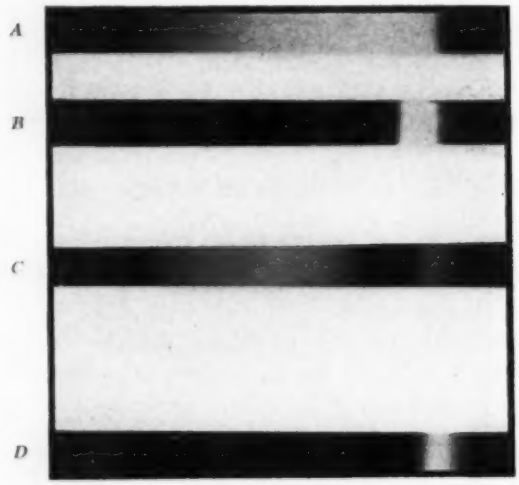

FIG. 9. Typical spectrograms.

The authors feel that this method will prove of value for determining the relative radiation striking various parts of complex radiant heat exchangers.

VIII. DETERMINATION OF THE RELATIVE RADIATION WITH AN ABSORBING MEDIUM

One of the original phases of the program was to study the possibility of using a model to determine the effect of absorbing mediums on the radiation. This, if practical, could be applied later to important industrial problems dealing with radiation through gases.

In general, the method investigated consists in immersing the entire apparatus in an absorbing medium such as water containing a dye. The difficulties encountered were many, and to overcome them a great deal of experimentation was required. It is essential to use a combination light source and filter which will transmit light having a wave-length range in which the liquid will transmit. This is not the only restriction, since it is also necessary to select a film which is sensitive to the wave-length range of light which is transmitted through the absorbing medium. The method would be useless if the film selected was "blind" to the radiation coming from the light source, filter, and absorbing medium combination.

After a number of filters, absorbing solutions, and films had been tried, satisfactory results were obtained using various concentrations of saffron dye in distilled water depending upon the amount of absorption desired, Wratten light filters, and Wratten and Wainwright metallographic plates, and "hyperpanchromatic" cut films. Space limitation does not permit a complete discussion of the various filters and photographic materials used in the investigation.

Figure 9 shows a series of spectrograms made with a Hilger spectroscope. The continuous spectrum of the lamp used is shown in spectrogram *A*. Spectrogram *B* indicates the effectiveness of the filter. *C* is the spectrogram of the lamp and liquid. It is important to note that the liquid transmits light in the same approximate range as does the filter. This indicates that the dye and water combination together with the filter is suited for the experiments. Spectrogram *D* shows the result for one exposure when light passes through the filter and absorbing liquid. In order to change the absorbing property of the medium, it was found necessary to change only the concentration of the dye.

Figure 10 shows the same as the spectrogram

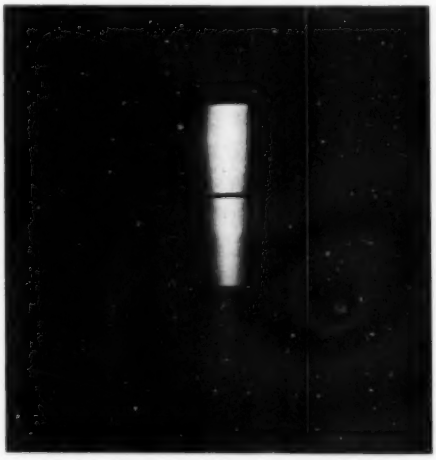

FIG. 10. Spectrograms for three grades of the solution. (Top: weak; middle: medium; bottom: strong.)

D of Fig. 9, for three grades of the absorbing solution (weak, medium, and strong).

Figure 11 contains eleven spectrograms which are explained by Table I. The determination of the relative radiation is the same as described in Section VII.

In practical applications the lengths of the model can have any constant proportion C to the corresponding lengths of the main device, but according to Eq. (5) the following condition of similarity exists:

$$\delta_{\lambda,\,m} = \delta_\lambda / C, \tag{9}$$

where the subscript m relates to the model and

$$C = x_m / x.$$

For only in this case

$$\exp\left[-x_m \delta_{\lambda,\,m}\right] = \exp\left[-x\delta_\lambda\right].$$

This is not a serious restriction of the model method because it is easy to make the concentration of the dye in the absorbing solution weak or strong so that the requirement of Eq. (9) is fulfilled.

IX. CONCLUSIONS

In the present paper the following method for the determination of surface and gas radiation is developed: A small model of the device in which heat radiation occurs is constructed, and its surfaces are covered by photographic films. These are exposed to light sources which imitate the sources of heat radiation. The density of the images produced on the films by exposure is measured by automatic photometry. Gases which absorb heat radiation in the main device are replaced in the model by absorbing liquids. In the latter case, however, a combination of a light filter, an absorbing liquid and a film must be used at such a wave-length range in which the light source yields, the filter transmits, the liquid absorbs, and the film converts into photochemic energy just so much light energy that photometering is sufficiently exact. It required much experimental work to comply with these requirements. As the spectrograms in the paper show, a satisfactory combination has been found and applied.

TABLE I. Explanation of Fig. 11.

Spectrogram No.	Source of light and absorbing bodies	Time of exposure (seconds)
1	Lamp	10
2	Lamp	30
3	Lamp	90
4	Lamp and liquid	90
5	Lamp and liquid	300
6	Lamp and filter	90
7	Lamp and filter	300
8	Lamp, filter, and liquid	180
9	Lamp, filter, and liquid	600
10	Iron arc	3
11	Iron arc	3

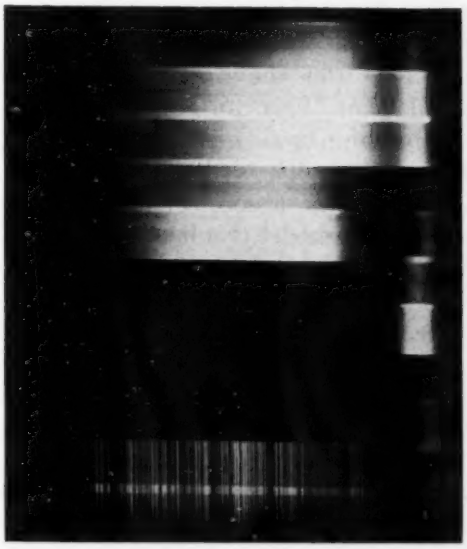

FIG. 11. Spectrograms for different light sources, absorbing bodies, and exposures (see Table I).

So, the authors feel that the underlying experimental problem is solved in principle. However, there are quite a few items requiring further investigation which is underway.

First of all other light sources than a straight lamp filament, as used in the present experiments, must be tried out. There are modern methods of illumination with uniformly and diffusely radiating surface. But either the intensity is not great, or the actual light source has a line spectrum whose photometric treatment is less simple than that of a continuous spectrum. So, their use may be restricted to the case of non-absorbing media. Another possibility is to use filament illumination with several filaments suitably distributed on the surface. It may be simpler to bring one filament to different places

on the surface, expose at each position, and superimpose the results.

It seems even possible to reproduce plane, cylindrical, and conical radiating surfaces in the main device by moving a lamp in the model at a constant small velocity in such a way that the straight filament would describe a plane or the surface of a cylinder or cone during the time of exposure. It is a necessary condition, that if lamp movement is employed the radiation must always come from the same part of the surface of the filament. This can be easily attained by moving the lamp house together with the filament.

Another difficulty is that in heat radiation the same bodies absorb and emit radiation whereas in the model this is not the case. Thus for instance, the method must be modified for the case of a hot radiating gas inside a colder envelope. Consider the example of the radiative heat transfer from flue gases to the superheater tubes in a boiler. The tubes may be arranged similar to the model indicated in Figs. 3 and 4, and all of the tubes may be at the same surface temperature. If a model bank of tubes having a large number of tubes is considered, each tube which is entirely surrounded by tubes will emit and receive the same amount of radiation as any other tube which is entirely surrrounded by tubes. Light sources may be arranged on the surface of any one tube, as previously described, and films placed on the surrounding tubes. The model may then be filled with the absorbing liquid, and after due exposure the films developed properly. The fraction of the emitted radiation which is absorbed by the medium may then be determined by photometering. But according to theory the emission of a gas in an envelope at a constant temperature is equal to its absorption.[4] Thus by means of the experiment the total gas radiation for the system of tubes described may be found, and the difficulty previously mentioned overcome.

In order to study the effect of diffuse reflection for surfaces which are not entirely black, the method may be modified by placing light sources on the surfaces of the model which correspond to reflecting surfaces in the main device, and films on the surfaces corresponding to those hit by the reflected rays in the main device. The distribution of the radiation falling upon the various surfaces may then be determined from auxiliary photometric charts, which are obtained by photometering the films. If the absorptivity ("degree of blackness") of the reflecting surfaces of the main device is known, then it is a simple computation to correct the main photometric distribution charts by means of the auxiliary photometric charts.

A minor difficulty occurs if more than two different surface temperatures occur in the main device, because the model knows only two poles of radiation, one securing emission, the other absorption. In this case the experiment may be split into different experiments each for only two of the temperatures. The results can be superimposed.

The method is restricted to surfaces which can be developed into a plane, i.e., to plane, conical, and cylindrical surfaces, because only these can be covered by ordinary films. In the rare cases where double curved surfaces occur in an actual device, these may be replaced by approximately equivalent developable surfaces in the model, or thin strips of film along greatest circles of equivalent sphere surfaces may be used.

Instead of liquids in some cases solids of appropriate absorptivity can be used. This may also allow the imitation of differences of the decrement of radiation δ_λ of the gas at different places in the main device. With liquids one may try to imitate such differences by arranging a slow flow of the liquid through the model and changing the concentration on the way, for instance by adding more concentrated dye at certain points of the system.

In general, it must be kept in mind that the method is based on, and requires the knowledge of, the decrement of radiation of the absorbing gases under consideration. It is desirable, not only for the present purpose but likewise for other work on gas radiation, that more experimental work be done concerning this physical property, and particularly its variation with temperature.

The authors wish to express their appreciation to Dr. E. P. Miller, Dr. I. Walerstein, and Dr. H. J. Yearian of the Physics Department of Purdue University for their suggestions, criticisms, and interest during the course of this investigation.

Diffusion of Heat Through a Rectangular Bar and the Cooling and Insulating Effect of Fins. I. The Steady State.*

MELVIN AVRAMI, *Columbia University, New York, New York*

AND

J. B. LITTLE, *Bell Telephone Laboratories, 463 West Street, New York, New York*†

(Received January 26, 1942)

Exact solutions for temperature distribution and heat flow through a rectangular fin are rederived in more general and simple form than previously given. These are studied numerically and graphically and shown to yield new results not contained in the approximate formulas hitherto used. Except for the factor of thermal conductivity of the fin material, the cooling effect is a function only of the height-width ratio β of the fin, and of a dimensionless "relative boundary resistivity" μ governing the heat loss to the environment. It is shown that, for any value of this boundary resistivity, there is a fairly sharp optimum value of the height-width ratio beyond which further increase in height will not lead to much improvement in cooling effect. This optimum β decreases with decreasing μ until, at a certain critical value μ^* in the neighborhood of 1, it becomes zero. At the critical μ^*, the cooling effect is altogether independent of β, and the presence of the fin is a matter of indifference. Below μ^*, the cooling effect decreases with increasing β, so that the presence of the fin serves merely to insulate the hot plate. This analysis of a single fin is the basis upon which a study of the conditions for optimal cooling by an array of fins will be carried out in a subsequent publication.

1. INTRODUCTION

A PROBLEM of considerable practical interest is that of the diffusion of heat through a long bar of rectangular cross section placed suddenly upon a hot plate. We suppose this hot plate to maintain the constant temperature T_i on the surface in contact with it while the other three surfaces of the bar (Fig. 1) are exchanging heat with an environment at zero. The initial temperature of the bar is zero. The physical properties, including the surface heat transfer coefficient or transmittivity, are assumed not to change with temperature. For generality, we may take the surface transmittivity h_1 of the sides of the bar different from h_2, that of the top. It is desired to find the complete thermal history of such a bar, i.e., the ultimate steady state and the initial transient condition.

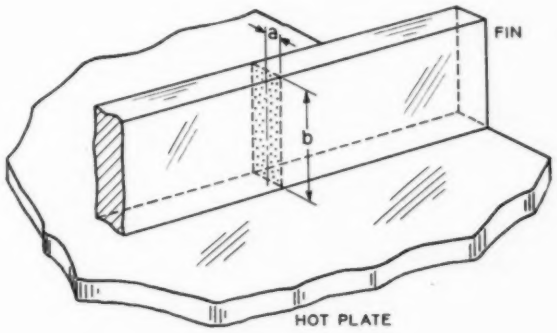

FIG. 1.

There are various practical applications of the solution to this problem,[1] but the one in which we shall be most interested is the application to the cooling effect of a long fin of rectangular cross section mounted on a hot surface. This cooling effect may be measured by the rate of total heat flow through the fin in the steady state since this is the rate of abstraction of heat from the hot plate. One of our primary objects will be to study this cooling effect as a function of height-width ratio of the fin, and of the boundary resistance governing the heat loss to the environment. Physical intuition enables us to foreshadow some of the results of this analysis as follows. The effect of adding a solid fin, such as we are contemplating, to a hot surface is in

* Publication assisted by the Ernest Kempton Adams Fund for Physical Research of Columbia University.

† This work was done at Columbia University.

[1] Certain small scale drawing and tempering operations are carried out by putting the metal bar to be treated on a hot plate. Open pan frying (e.g., of "hot dogs"!) follows the same thermal pattern. Pressing of Bakelite and other materials sometimes presents a similar problem; the mass to be treated is surrounded on three sides by a heavy cold mold and is heated on the fourth side. If the cold mold is so heavy and thermally conducting that its temperature changes can be neglected as compared with that of the heated material, the boundary conditions are similar to those discussed in this paper.

TABLE I. Values of $\mu = k/ha$ for a bar of half-width 1 cm in various circumstances. To get μ for bars (e.g., fins) 1/10 as wide, multiply by 10, etc.

	Very still air $h = 10^{-4}$	Moderately circulating air $h = 10^{-3}$	Rapidly circulating air $h = 10^{-2}$	Quenching medium $h = 10^{-1}$
Good conductor $k = 1$	10,000	1000	100	10
Semi-conductor $k = 10^{-2}$	100	10	1	0.1
Insulator $k = 10^{-4}$	1	0.1	0.01	0.001

two opposite directions. On the one hand, the increase in surface due to the presence of the fin, *increases* the rate of cooling. On the other hand, the interposition of the matter of the body of the fin between the base surface and the new cooling surface (of the fin) increases the resistance to flow of heat, i.e., *decreases* the rate of cooling. For a low boundary resistivity, we may expect the latter "body effect" to predominate, and the cooling effect to *decrease* with *increased height* (=body) of the fin. In this case, the presence of the fin is not desirable unless it is desired to insulate rather than cool the hot plate. For a high boundary resistivity, on the other hand, we may expect the "surface effect" to predominate, and the cooling effect, therefore, to *increase* with *increased height* (=surface) of the fin. These two conclusions are well borne out by the mathematical analysis as may be seen from an inspection of Fig. 2.

The analysis further brings out the fact that the cooling effect, except for the factor of body conductivity (reciprocal of body resistivity), *depends only upon the height-width ratio β and an involvement of the physical properties, μ.* This μ, which we may designate the "relative surface resistivity," is given by the ratio of boundary to body resistivity divided by the half-width of the fin. A remarkable result of the analysis is that, for a certain value of this relative surface resistivity (μ in the neighborhood of $4/\pi = 1.27$), the cooling effect is independent of the height-width ratio, i.e., *the cooling effect remains the same whether we add to the fin or remove it entirely.* Another interesting and practically important result of the analysis is that, for any given value of μ, there is a fairly sharp optimum value of the height-width ratio beyond which increase in height will not lead to much improvement in cooling effect (Fig. 2).

For given height-width ratio β, the cooling effect decreases with increasing μ, becoming inversely proportional at very high values of μ (or low β). The general outcome then is that, other things being equal, the *cooling effect increases with increasing width of the fin and with decreasing boundary resistivity.* The dependence on body resistivity is somewhat more complicated but the relations may be summed up as follows: The effect of decreasing body resistivity is generally smaller than that of boundary resistivity in increasing the cooling effect. For high values of μ (e.g., good conductors in fairly still air), or low values of β (i.e., short stubby fins), the effect of the body resistivity is negligible and *one material will serve as well as another.* For example, consider two fins each 0.1 cm in half-width, one made of copper and one made of cast iron. The values of μ, as well as of the body

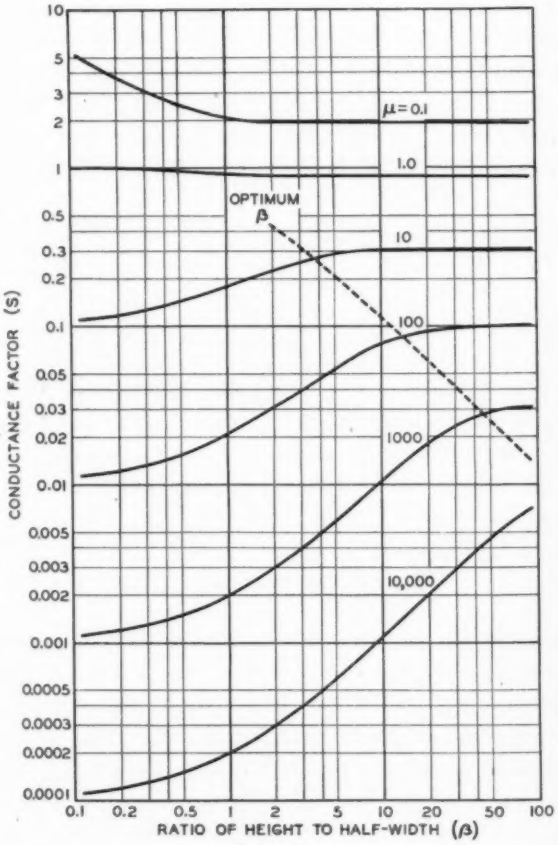

FIG. 2.

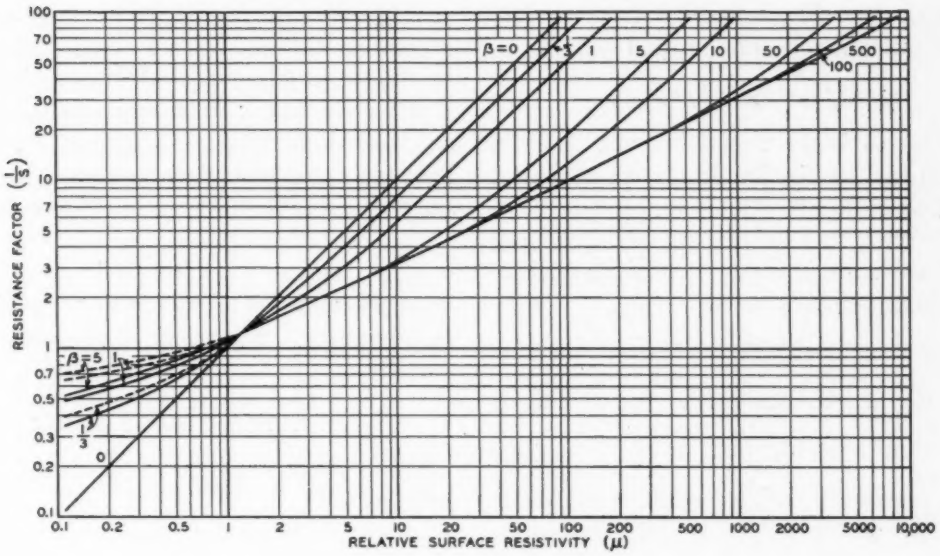

FIG. 3.

conductivities (0.93 and 0.11 cal/cm sec. deg., respectively), are in the ratio **8.5** to **1.** From Table I, Formula (I) and Fig. 3, it can be seen, however, that the ratios of the cooling effects for any reasonable height-width ratio ($\beta \leq 20$) are less than: **1.01** in very still air ($\mu_{Cu}=93{,}000$; $\mu_{Fe}=11{,}000$); **1.14** in moderately circulating air ($\mu_{Cu}=9300$; $\mu_{Fe}=1100$); **1.78** in rapidly circulating air ($\mu_{Cu}=930$; $\mu_{Fe}=110$); **3.15** in quenching medium ($\mu_{Cu}=93$; $\mu_{Fe}=11$). This shows that even under severe conditions of quenching, the effect of the difference in body material of the fin is not very great.

To get some idea of the magnitude of μ in various cases, consider bars 2 cm wide (i.e., $a=1$ cm) made, respectively, of a good metallic conductor like copper, a semi-conducting brick material like fused alumina, and finally an insulating material like wall board. For these, the approximate values of k in cal./cm sec. deg., indicated in Table I, may be taken. For the surface heat transfer coefficient, taking $h=h_1=h_2$, we may consider the four values corresponding to the physical circumstances indicated in the table. The dimensions of h are cal./cm^2 sec. deg. The values of μ resulting from these values of k and h in various combinations are given in Table I.

To turn now to the mathematical treatment of the problem, a simplification can be made immediately by noticing that, since there is no asymmetry in the environment, the flow must be symmetric with respect to the center line of the cross section of the bar. Thus there is no flow across this center line, and the problem is equivalent to one for a bar with one-half the given cross section, and one side insulated. Of the other three faces, one is on the hot plate, and two are losing heat to the environment.

It is always convenient to introduce a set of dimensionless measures of space, time, and thermal resistance to simplify the equations obtained. Such dimensionless measures also facilitate the use of general charts and plots. The linear dimensions are expressed as fractions of the chief linear dimension; thus this chief dimension, expressed in the "dimensionless units" equals one. If a is the half-width and b the height of the bar, the vertical and horizontal dimensionless coordinates, respectively, are:

$$\xi=x/a \quad \eta=y/a.$$

For the height-half-width ratio the symbol β is used:

$$\beta=b/a.$$

The time t (in ordinary units) is replaced by a "dimensionless time"

$$\tau=(D/a^2)t,$$

where D is the diffusivity of the bar material

(in ordinary units). For measures of the boundary resistivities, the dimensionless ratios

$$\mu_1 = k/h_1 a \quad \mu_2 = k/h_2 a$$

are used where k is the thermal conductivity of the bar material. As indicated above, μ_1 and μ_2 may be designated the "relative boundary resistivities." With these notations, the system of differential equation and side conditions governing the diffusion may be written

$$\partial^2 T/\partial \xi^2 + \partial^2 T/\partial \eta^2 = \partial T/\partial \tau, \tag{1.1}$$

$$\partial T/\partial \xi = 0 \quad \text{at} \quad \xi = 0, \tag{1.2}$$

$$-\mu_1 \partial T/\partial \xi = T \quad \text{at} \quad \xi = 1, \tag{1.3}$$

$$-\mu_2 \partial T/\partial \eta = T \quad \text{at} \quad \eta = \beta, \tag{1.4}$$

$$T = T_i \quad \text{at} \quad \eta = 0, \tag{1.5}$$

$$T = 0 \quad \text{at} \quad \tau = 0. \tag{1.6}$$

The dimensionless "fractional temperature," as it may be called, T/T_i is then a function only of ξ, η, τ, β, μ_1, and μ_2; and if in bars of different sizes, conductivities, etc., these quantities have the same values, then the same dimensionless values for temperature, thermal current, and so on, are obtained.

A general procedure for solving diffusion problems of this type is to split the problem into two parts. First we find the steady state temperature distribution T_s under the given environmental conditions. Then we find a solution T_{ts} to the transient (time dependent diffusion) problem with environment temperatures taken as zero and initial distribution equal to T_s. It is clear that the actual solution T of the given problem at any time is the difference of these two, i.e.,

$$T = T_s - T_{ts}, \tag{1.7}$$

since this satisfies the given differential equation and boundary conditions and reduces to zero initially.

2. THE STEADY STATE

The system of equations governing T_s may be written

$$\partial^2 T/\partial \xi^2 + \partial^2 T/\partial \eta^2 = 0, \tag{2.1}$$

$$\partial T/\partial \xi = 0 \quad \text{at} \quad \xi = 0, \tag{2.2}$$

$$-\mu_1 \partial T/\partial \xi = T \quad \text{at} \quad \xi = 1, \tag{2.3}$$

$$-\mu_2 \partial T/\partial \eta = T \quad \text{at} \quad \eta = \beta, \tag{2.4}$$

$$T = T_i \quad \text{at} \quad \eta = 0. \tag{2.5}$$

A particular solution of (2.1) and (2.2) is

$$A \cos \alpha\xi \frac{\cosh [\alpha(\beta - \eta) + \bar{\alpha}]}{\cosh [\alpha\beta + \bar{\alpha}]},$$

where A, α and $\bar{\alpha}$ are arbitrary constants. To

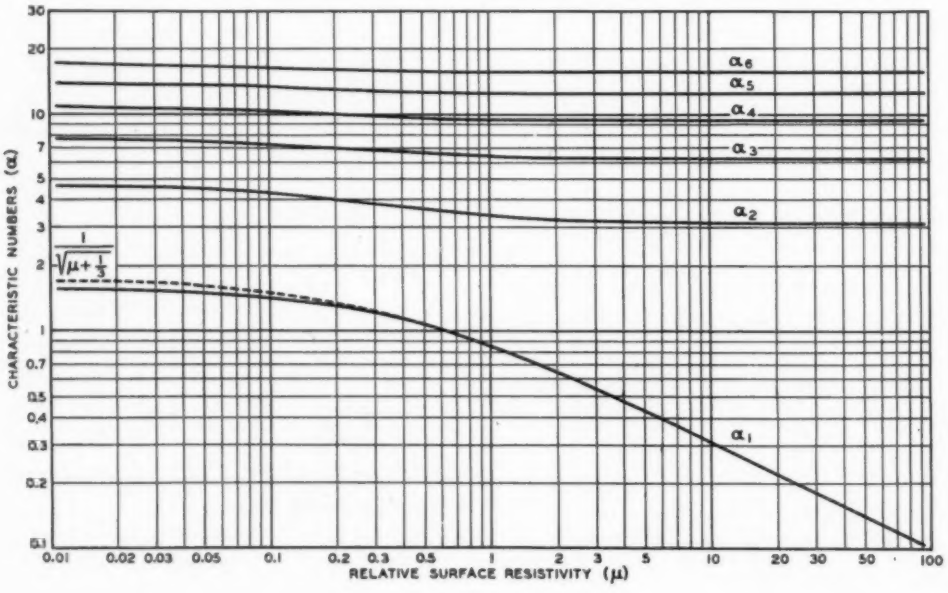

FIG. 4.

satisfy also (2.3) we must have

$$\cot \alpha = \mu_1 \alpha. \tag{2.6}$$

This "characteristic number equation" is satisfied only by a discrete infinite sequence of real positive values $\alpha_1, \alpha_2, \cdots, \alpha_n, \cdots$ and their negatives. Because of the form of our particular solution, we may confine ourselves to the positive α's. The first six of these are plotted as functions of μ in Fig. 4.

It is evident that (2.4) will also be satisfied if

$$\coth \bar{\alpha} = \mu_2 \alpha$$

or, in other words, if

$$\bar{\alpha} = \coth^{-1} \mu_2 \alpha = \ln \left(\frac{\mu_2 \alpha + 1}{\mu_2 \alpha - 1} \right)^{\frac{1}{2}}. \tag{2.7}$$

except for an additional term of the form: integer $\times 2\pi i$, which contributes nothing since $\bar{\alpha}$ always occurs in the argument of a trigonometric function. If, for brevity, we let the real part of $\bar{\alpha}$

$$\ln \left(\left| \frac{\mu_2 \alpha + 1}{\mu_2 \alpha - 1} \right| \right)^{\frac{1}{2}} \tag{2.7'}$$

be represented by $\bar{\rho}$, we may write, in general

$$\bar{\alpha} = \begin{matrix} \bar{\rho} & \text{for} & \mu_2 \alpha \gtrless 1 \\ \bar{\rho} + i\pi/2 & \text{for} & \mu_2 \alpha < 1. \end{matrix} \tag{2.7''}$$

A set of values of $\bar{\rho}$ corresponding to given values of α (for $\mu_2 = \mu_1 = \mu$) is given in Table II. Associated with each characteristic number α_n are then a coefficient A_n and a parameter $\bar{\alpha}_n$, so that our particular solution may now be written:

$$A_n \frac{\cos a_n \xi}{\sqrt{N_n}} \frac{\cosh \left[\alpha_n (\beta - \eta) + \bar{\alpha}_n \right]}{\cosh \left[\alpha_n \beta + \bar{\alpha}_n \right]},$$

where, for convenience, the normalization factor

$$N_n = \int_0^1 (\cos \alpha_n \xi)^2 d\xi = \frac{\alpha_n + \cos \alpha_n \sin \alpha_n}{2\alpha_n} \tag{2.8}$$

has been introduced.

To satisfy also (2.5), we must add up particular solutions so that

$$\sum_{n=1}^{\infty} A_n \frac{\cos \alpha_n \xi}{\sqrt{N_n}} = T_i. \tag{2.9}$$

Now, from the general Sturm-Liouville theory, or by more special arguments, it is readily seen that the functions $\cos \alpha_n \xi / \sqrt{N_n}$ constitute an orthonormal set, so that the number A_n is merely the nth coefficient in the expansion of the constant T_i in this set. Therefore,

$$A_n = T_i \int_0^1 \frac{\cos \alpha_n \xi}{\sqrt{N_n}} d\xi = T_i \frac{\sin \alpha_n}{\alpha_n \sqrt{N_n}} \tag{2.10}$$

and the complete solution[2] for the "fractional steady-state temperature" T_s/T_i is

$$\frac{T_s}{T_i} = 2 \sum \frac{\sin \alpha_n}{\alpha_n + \cos \alpha_n \sin \alpha_n} \times \cos \alpha_n \xi \frac{\cosh \left[\alpha_n (\beta - \eta) + \bar{\alpha}_n \right]}{\cosh \left[\alpha_n \beta + \bar{\alpha}_n \right]}. \tag{2.11}$$

In place of $\bar{\alpha}_n$, its real part $\bar{\rho}_n$ may be written when $\mu_2 \alpha_n$ is greater than 1, and since

$$\cosh (x + i\pi/2) = i \sinh x,$$

$\bar{\rho}_n$ may be written for $\bar{\alpha}_n$ also when $\mu_2 \alpha_n$ is less than 1, provided that **cosh** is replaced both in numerator and denominator by **sinh.**

To study the nature of (2.11) in detail, and to compare with the results obtained in solving the analogous problem experimentally on an electric model,[3] we introduce the following numerical values which would be reasonable for a cast iron bar resting on the hot plate and sur-

TABLE II.

μ	α_1	$\frac{2 \sin^2 \alpha_1}{\alpha_1 + \sin \alpha_1 \cos \alpha_1}$	$\bar{\rho}_1$	$\frac{1}{(\mu + \frac{1}{3})^{\frac{1}{2}}}$	$\frac{1}{\sqrt{\mu}}$	β_{optimum}
0.010	1.555	1.268	.0159	1.707	10.000	.955
0.072	1.466	1.258	.105	1.570	3.725	.951
0.10	1.429	1.250	.142	1.519	3.162	.951
0.72	0.964	0.943	.854	0.975	1.178	.671
1.00	0.860	0.848	1.295	0.867	1.000	.238
7.20	0.364	0.364	0.402	0.364	0.373	3.01
10.00	0.311	0.311	0.333	0.312	0.316	3.75
72.00	0.118	0.118	0.112	0.117	0.118	11.75
100	0.0997	0.0997	0.100	0.0998	0.100	14.05
720	0.0373	0.0373	0.0373	0.0373	0.0373	39.2
1000	0.0316	0.0316	0.0316	0.0316	0.0316	46.4
7200	0.0118	0.0118	0.0118	0.0118	0.0118	126
10000	0.0100	0.0100	0.0100	0.0100	0.0100	149

[2] A more special and complicated form of this solution was first obtained by D. R. Harper and W. B. Brown, *Annual Report National Advisory Committee for Aeronautics*, **158**, 679 (1922). It was not, however, employed in their numerical calculations and applications, which were based upon an approximate one-dimensional treatment, neglecting the transverse differences of temperature through the width of the fin.

[3] See a forthcoming paper by M. Avrami and V. Paschkis, Trans. Am. Soc. Mech. Eng.

rounded by rapidly circulating air:

$k = 0.108$ cal./cm sec. deg.
$(= 313.5$ B.t.u./ft.^{2} hr. °F/inch)
$D = 0.121$ cm^2/sec. $(= 0.455$ ft.^{2}/hr.)
$h_1 = h_2 = 5 \times 10^{-3}$ cal./cm^2 sec. deg.
$(= 36.8$ B.t.u./ft.^{2} hr. °F)
$a = 30$ cm (approximately 1 ft.)
$b = 10$ cm (approximately 4 in.).
Therefore $\mu_1 = \mu_2 = 0.72$ and $\beta = \frac{1}{3}$.

The results of plotting (2.11) up to six terms with these numerical values, for points taken along six equally spaced horizontal lines and eight equally spaced vertical lines, are shown in Fig. 5. The calculated points are indicated by circles, and the theoretical curve is obtained by drawing a smooth line through them. The distribution of points on the lowest level is still a bit wavy due to the slower convergence of the series (2.11) in this region, so that the higher order terms, beyond the sixth still contribute appreciably. Otherwise the points fall closely on the smooth curves. It is interesting to note how rapidly the temperature at the outer corner falls off.

In principle it is possible to set up an electric circuit (model) representing any body in which heat flows subject to initial and boundary conditions.[3] In line with the fact that heat flow phenomena are non-oscillatory, such an electric model is non-inductive. The model consists essentially of a network of lumped resistances and capacities (condensers) so arranged as to simulate the distribution of resistance and heat capacity in the analogous thermal situation. Electric potential (voltage) and current then correspond to temperature and thermal current.

The original body in which heat flows may be thought of as divided up into a number of elements or sections (e.g., by coordinate surfaces), generally, but not necessarily, uniform. Each of these body elements or sections has a certain heat capacity which, in the electric model, is represented by a condenser of suitable magnitude, one plate of which is grounded. These condensers are connected with neighboring ones, representing neighboring body elements, by means of resistances. The resistances are chosen in both direction and magnitude to correspond with the thermal resistances in the body. The individual condenser, together with those parts

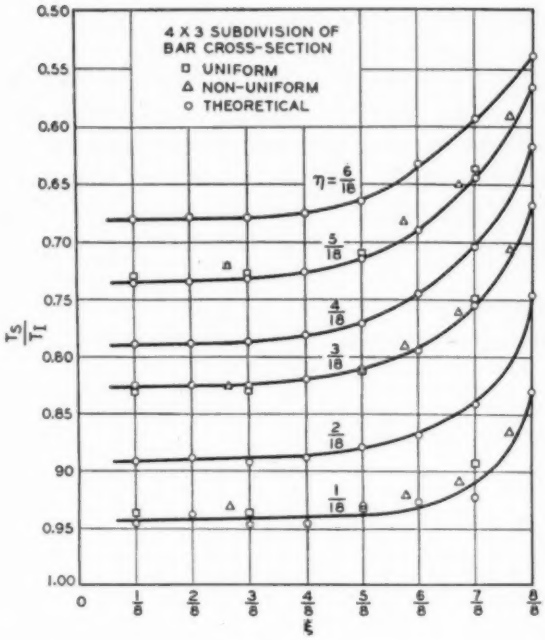

FIG. 5.

of its attached resistances which correspond to a single body element is a "section" of the electric model. Naturally, the larger the number of sections (i.e., the finer the subdivision), the closer is the correspondence between model and reality. It is found[3] that a surprisingly small number of sections, i.e., a fairly coarse subdivision, is sufficient to give excellent accuracy, satisfying any usual engineering requirements. For instance, the experimental points obtained on networks corresponding to two different manners of subdivision (one uniform and one non-uniform) of the bar into 4×3 sections are plotted on Fig. 5. It will be seen that they check each other and the mathematical values very closely. The maximum error by the first subdivision is less than 2 percent, while the root mean square deviation is 1.14 degrees (on the basis $T_i = 100$ degrees). The maximum error by the second subdivision is also within 2 percent, while the root mean square deviation in this case is 1.34 degrees.

The electric model described above is merely an experimental exemplification of a much more general theoretical technique which may be used in solving problems of mathematical physics to any desired degree of approximation. This method consists of (mentally) setting up an approxi-

mating network of any required order (i.e., degree of subdivision of the original system) with appropriate resistances, capacitances, inductances, etc. The network is then solved by the methods of network theory. This procedure, which may be designated the "Method of Approximating Networks," will be studied by the first author in a future publication.

3. HEAT FLOW AND COOLING EFFECT IN THE STEADY STATE

The rate of heat flow through the bar, i.e., the cooling effect, may be measured either by the total inflow or the total outflow which, in the steady state, must be equal. The total inflow to unit length of the bar in the steady state is given by[4]

$$I=\int_0^1 -k\left.\frac{\partial T_\eta}{\partial \eta}\right|_{\eta=0} d\xi$$

$$=kT_i\sum_n \frac{2\sin^2\alpha_n}{\alpha_n+\sin\alpha_n\cos_n}\tanh(\alpha_n\beta+\bar{\alpha}_n) \quad (3.1)$$

[4] If the real part $\bar{\rho}_n$ is written for $\bar{\alpha}_n$, the expression is valid as it stands when $\mu_2\alpha_n>1$; for $\mu_2\alpha_n<1$, the expression is valid when **tanh** is replaced by **coth.**

or, using (2.6) and (2.7), this may also be written

$$I=kT_i\sum \frac{1}{\alpha_n(1+\mu_1+\mu_1^2\alpha_n^2)} \times\frac{\mu_2\alpha_n\tanh\alpha_n\beta+1}{\mu_2\alpha_n+\tanh\alpha_n\beta}. \quad (3.1')$$

Thus, as usual in steady flow situations, we may say that I is given by the applied temperature difference T_i times the conductance, or

$$I=kT_iS,$$

where S, the *conductance*—or *shape-factor*, is defined by the sum in (3.1). A plot of S which, except for the factor kT_i, is the measure of the cooling effect, as a function of the height-width ratio and for various values of μ (taking $\mu_1=\mu_2=\mu$), is given in Fig. 2. It leads to the very interesting and practically useful conclusion that for every value of μ there is a fairly sharp optimum value of β beyond which further increase will not lead to much improvement in cooling effect. A rough graph of this optimum value of β as it depends upon μ is given by the dashed line in Fig. 2 and directly in Fig. 6. The optimum

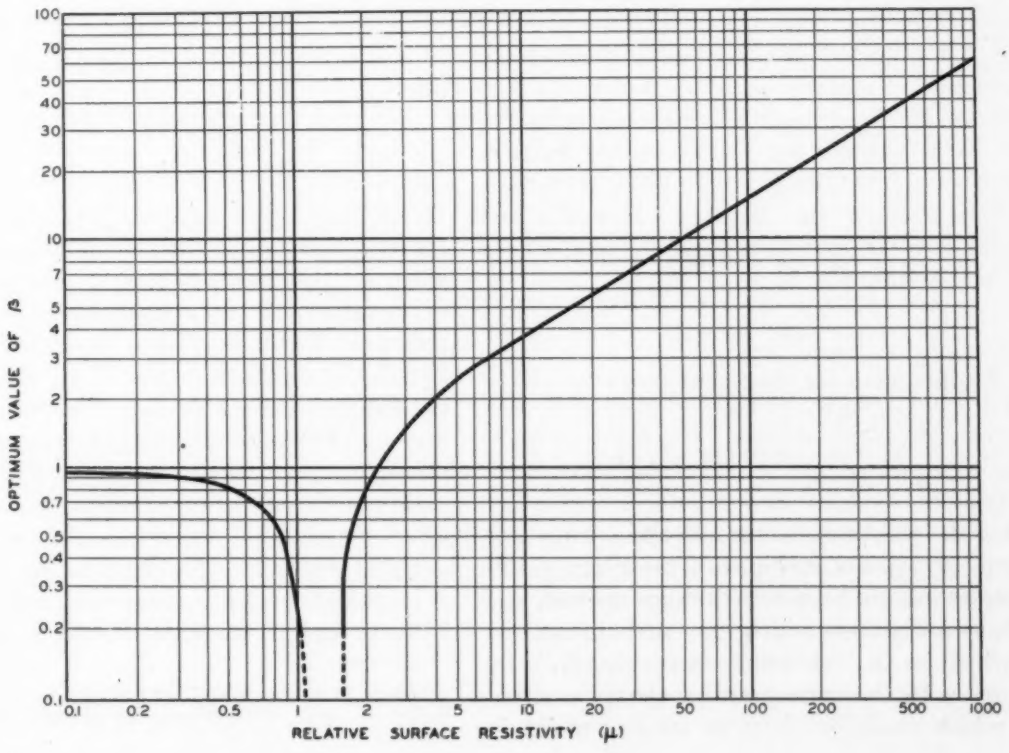

FIG. 6.

β decreases with decreasing μ until, for a value of μ in the neighborhood of 1, it becomes zero. At this critical $\mu=\mu^*$, S is independent of β altogether and, as indicated in the introduction, the cooling effect remains the same whether we add to the fin or remove it entirely. Below the critical value μ^*, the cooling effect actually decreases with increasing β, i.e., the presence of the fin serves merely to insulate the hot plate. Analytic expressions for the optimum β as a function of μ, and for the critical μ^*, will be given below upon the basis of the approximate formulas to be derived.

The reciprocal of the conductance factor is the "resistance factor,"

$$1/S=kR;$$

which, multiplied by the resistivity $1/k$, gives R the over-all resistance of the bar (per unit length perpendicular to the cross section). It is instructive to consider the resistance factor as a function of μ. It is plotted in Fig. 3 in full curves (for various values of β). This is only another mode of representing what is given in Fig. 2, taking the reciprocal of S instead of S, and using μ as abscissae instead of β. But it is useful for certain purposes. The phenomenon of the change at μ^* in the nature of dependence of the cooling effect upon β is reflected in the crossing over of the curves of $1/S$ against μ at μ^* in Fig. 3. The existence of the critical μ^* and this "crossing over effect," as we may call it, do not seem to have been pointed out before in the literature.

Let us examine the limiting values of S and $1/S$ for μ small and large, respectively. For μ very small, from Eq. (2.6)

$$\alpha_n\rightarrow(2n-1)(\pi/2)$$

and S approaches the divergent series

$$\frac{4}{\pi}\sum\frac{1}{2n-1}\coth(2n-1)\frac{\pi}{2}\beta,$$

so that the resistance factor $1/S$ approaches zero with μ, as appears in Fig. 3. Theoretically this means an infinite heat flow through the bar, and we have a situation which may perhaps best be described as a "thermal short circuit," by analogy with the corresponding electrical situation which would obtain if we tried to maintain the bottom of the bar at potential T_i and grounded the sides and top.

TABLE III.

μ	$\beta=\frac{1}{2}$ S-Exact	$\beta=\frac{1}{2}$ S by (I)	$\beta=10$ S-Exact	$\beta=10$ S by (I)	$\beta=50$ S-Exact	$\beta=50$ S by (I)
0.072	3.3	2.76	2.08	1.47	2.08	1.47
0.100	2.996	2.60	1.959	1.43	1.959	1.43
0.720	1.221	1.18	1.031	0.964	1.031	0.964
1.000	0.971	0.936	0.900	0.860	0.900	0.860
7.200	0.176	0.177	0.366	0.364	0.366	0.364
10.0	0.128	0.129	0.131	0.132	0.313	0.312
72.0	0.0183	0.0184	0.101	0.101	0.117	0.117
100.0	0.0134	0.0133	0.0803	0.0798	0.100	0.0998
720	0.00186	0.00186	0.0145	0.0145	0.0358	0.0356
1000	0.00133	0.00133	0.0105	0.0106	0.0292	0.0292
7200	0.000185	0.000185	0.00152	0.00152	0.00634	0.00635
10000	0.000133	0.000133	0.00110	0.00110	0.00470	0.00470

Large μ, on the other hand, corresponds to a large surface resistance compared with the body resistance or, with k/h moderate, to a narrow bar (e.g., a fin with small a). For $\mu\geq0.72$ it may be seen that, no matter what the value of β, all terms after the first in (3.1) may be neglected with an error no greater than 10 percent. Also, it may be seen from Table II that for $\alpha_1<0.964$, i.e., $\mu>0.72$, the expression

$$\frac{2\sin^2\alpha_1}{\alpha_1+\sin\alpha_1\cos\alpha_1}$$

may be replaced by α_1 with an error of about 2 percent. Thus, we have as an approximation[5]

$$S=\alpha_1\tanh(\alpha_1\beta+\bar{\alpha}_1) \qquad \text{(I)}$$

and

$$\frac{1}{S}=\frac{\coth(\alpha_1\beta+\bar{\alpha}_1)}{\alpha_1}. \qquad \text{(I')}$$

It will be seen from Table III that above $\mu=0.72$, for any reasonable value of β, the values of S given by (I) differ less than 5 percent from the exact values. The approximate expression for the resistance factor is plotted in dashed curves in Fig. 3. For values of μ over 0.72 it deviates from the full curves by less than 10 percent and thus may be used as an engineering approximation in this range.

(I) may be used to find the critical value of μ^* where S becomes independent of β, to give simple analytic expressions for the limiting values of S at large and small μ, and the optimum value of β. First, to find μ^*, we notice that S is independent

[5] Here, as above, $\bar{\alpha}$ may be replaced by its real part $\bar{\rho}$ (Table II) provided **tanh** is interchanged with **coth** for $\mu\alpha<1$.

of β if

$$\tanh(\alpha_1\beta+\bar{\alpha}_1)=1,$$

which will be true for all β if $\bar{\alpha}_1=\infty$. This occurs when

$$\tanh\bar{\alpha}_1=\tan\alpha_1=1/\mu^*\alpha_1=1,$$

therefore $\alpha_1=\pi/4$ and $\mu^*=4/\pi=1.27$.

It is immediately evident from (I) that

$$\lim_{\beta\to\infty} S=\alpha_1 \qquad \text{(Ia)}$$

also

$$\lim_{\beta\to 0} S=\alpha_1\tanh\bar{\alpha}_1=1/\mu. \qquad \text{(Ib)}$$

Furthermore, let the optimum β, for any μ, be defined as that value where the cooling effect differs only by 10 percent from its asymptotic value α_1 (for $\beta=\infty$). This condition is achieved when $\tanh(\alpha_1\beta+\bar{\alpha}_1)$ differs from 1 by less than 10 percent, and this will occur when

$$\alpha_1\beta+\bar{\rho}_1\geq 1.5$$

or

$$\beta_{\text{optimum}}=(1.5-\bar{\rho}_1)/\alpha_1 \qquad \text{(Ic)}$$

as may be seen from a table of hyperbolic tangents and cotangents. A plot of β optimum as a function of μ is given in Fig. 6.

S may be expressed more explicitly in terms of μ and β as follows: An approximate expression for α in terms of μ may be found from (2.6) by using the first two terms in the expansion of cot α.

$$\mu\alpha_1=1/\alpha_1-\alpha_1/3, \quad \alpha_1=1/(\mu+\tfrac{1}{3})^{\frac{1}{2}}. \qquad (3.2)$$

This is valid within 2 percent for $\mu>0.72$ (see Table II), and may be called the "higher first approximation" for α_1. If μ is still larger, we may write

$$\alpha_1=\bar{\alpha}_1=1/\sqrt{\mu} \qquad (3.3)$$

and these may be called the "lower first approximations" to α_1 and $\bar{\alpha}_1$.

Using the higher first approximation to α_1 we have

$$S=\frac{1}{(\mu+\frac{1}{3})^{\frac{1}{2}}}\tanh\left[\frac{\beta}{(\mu+\frac{1}{3})^{\frac{1}{2}}}+\frac{1}{\sqrt{\mu}}\right] \qquad \text{(II)}$$

with limiting values

$$\lim_{\beta\to\infty} S=\frac{1}{(\mu+\frac{1}{3})^{\frac{1}{2}}}, \qquad \text{(IIa)}$$

$$\lim_{\beta\to 0} S=\frac{1}{(\mu+\frac{1}{3})^{\frac{1}{2}}}\tanh\frac{1}{\sqrt{\mu}}\backsimeq\frac{1}{\mu} \qquad \text{(IIb)}$$

and

$$\beta_{\text{optimum}}=\frac{1.5-1/\sqrt{\mu}}{1/(\mu+\frac{1}{3})^{\frac{1}{2}}}. \qquad \text{(IIc)}$$

For larger $\mu(>7.2)$, we may use the lower first approximations for α_1 and $\bar{\alpha}_1$ with an error less than 10 percent, giving

$$S=\frac{1}{\sqrt{\mu}}\tanh\frac{1+\beta}{\sqrt{\mu}}, \qquad \text{(III)}$$

$$\lim_{\beta\to\infty} S=\frac{1}{\sqrt{\mu}}, \qquad \text{(IIIa)}$$

$$\lim_{\beta\to 0} S=\frac{1}{\sqrt{\mu}}\tanh\frac{1}{\sqrt{\mu}}\backsimeq\frac{1}{\mu} \qquad \text{(IIIb)}$$

and finally

$$\beta_{\text{optimum}}=1.5\sqrt{\mu}-1. \qquad \text{(IIIc)}$$

It follows from (IIIa) and (IIIb) that, on the double logarithmic plot of Fig. 3, all the curves for large μ lie between the straight lines of $\frac{1}{2}$ and slope 1. As will be shown below, (III) is equivalent to the expression found by Harper and Brown upon the basis of their approximate treatment in which the variation of temperature through the thickness of the fin is not taken into consideration, and the problem is reduced to one-dimension.

Again, if μ is very large ($\sqrt{\mu}$ large compared with β), we may confine ourselves to the first term in the expansion of $\tanh(1+\beta)/\sqrt{\mu}$. We then get for the resistance factor

$$1/S_{\text{lim}}=\mu/(1+\beta), \qquad (3.4)$$

which is exactly what we should get when the volume resistance becomes negligible compared with the surface resistance, and the latter is then proportional to the relative boundary resistivity μ divided by the surface area $1+\beta$. The condition for the validity of this approximation is that $\tanh(1+\beta)/\sqrt{\mu}$ may be replaced by $(1+\beta)/\sqrt{\mu}$, i.e., to get a result accurate within 10 percent, we should have

$$(1+\beta)^2/\mu<0.3.$$

We may now consider the application of our results to the cooling effect of fins, and compare with the results of previous studies in this field.[2] The value of the conductance factor in the limiting case (3.4)

$$S_{\text{lim}}=(1+\beta)/\mu \tag{3.5}$$

is evidently a measure of the cooling effect which the area of a fin surface would have if it were at the base temperature throughout. The ratio of the actual conductance factor to this limiting value is equivalent to what Harper and Brown have defined as the "effectiveness" of a fin which in our terms is then

$$f=\frac{S}{S_{\text{lim}}}=\frac{\mu}{1+\beta}S. \tag{3.6}$$

In terms of approximations (I), (II), and (III), respectively, the fin "effectiveness" is given by

$$f=\frac{\mu\alpha_1}{1+\beta}\tanh(\alpha_1\beta+\bar{\alpha}_1), \tag{Id}$$

$$f=\frac{\mu}{(1+\beta)(\mu+\frac{1}{3})^{\frac{1}{2}}}\tanh\left(\frac{\beta}{(\mu+\frac{1}{3})^{\frac{1}{2}}}+\frac{1}{\sqrt{\mu}}\right), \tag{IId}$$

$$f=\frac{\tanh(1+\beta)/\sqrt{\mu}}{(1+\beta)/\sqrt{\mu}}\equiv\frac{\tanh u}{u}. \tag{IIId}$$

where $u=(1+\beta)/\sqrt{\mu}$. (IIId) is exactly the expression obtained for the fin effectiveness by Harper and Brown, as may be seen by substituting the corresponding symbols in their expression for u:

$$u=w'(2q/kt)^{\frac{1}{2}},$$

since

$$k\rightarrow k,\quad q\rightarrow h,\quad t/2\rightarrow a,\quad w'\rightarrow(1+\beta)a.$$

The expressions (III), corresponding to the Harper-Brown approximations, are found to adhere fairly closely (for all β) to the exact solution in the range $\mu>7.2$. For values of μ less than this, but greater than 0.72, the approximate expression (I), here given, may be used. It may, in fact, be used even for values of μ down to 0.1, but the error here becomes of the order of 20 percent. For any sort of rigor, it therefore becomes necessary to use the exact expression (3.1).

In conclusion, it is worth while to emphasize the "crossing-over" effect which seems to have been overlooked hitherto, though, as pointed out in the introduction, it is obvious upon intuitive considerations alone. It implies that, below μ^*, the function of the fin is to *insulate* rather than dissipate the heat in the hot plate. In this range, optimum values of β for insulation may be obtained from formula (Ic) or Fig. 6. It is of great interest to note that, insofar as we may rely upon the approximate formula (Ic) in this range of low μ, it indicates that β_{optimum} approaches the asymptotic value $1.5/(\pi/2)\backsimeq 1$ as μ becomes very small, i.e., *at low values of the relative surface resistivity μ, the optimum height-width ratio for insulation is in the neighborhood of* $\frac{1}{2}$. From this point of view it would seem that the height-width ratio of from $\frac{1}{2}$ to 1 inherent in sweater-like materials, loosely woven or knitted from yarn, is just about the optimum value for insulation.

A New Approach to the Study of Arcback*

JOHN E. WHITE
University of Pittsburgh, Pittsburgh, Pennsylvania
(Received January 17, 1942)

The generally employed methods of investigating arcback in mercury arc rectifiers are incapable of uncovering some of the important characteristics of the phenomenon. A new method of study has shown that arcback probability varies with time after the appearance of negative voltage, in a surprising and hitherto unsuspected manner. Theoretical implications of this effect are discussed.

I. INTRODUCTION

EARLY studies of mercury arc rectifiers were based on the assumption that, with other conditions fixed, arcback occurs at a definite voltage. Slepian,[1] however, showed that arcback is a random phenomenon, and may occur over a wide range of voltages and other conditions. This led to the acceptance of "arcback rate" (the number of arcbacks per unit time) as a criterion for the condition of a rectifier. It was thought that incipient arcback "causes" occur at random intervals on the surface of an anode, and that a portion of these develop into power arcs during normal operation. A "bad" rectifier would have more "causes." It should thus be possible, by applying a voltage higher than normal to the anode, to develop a larger portion of these causes than normally give arcback, and in this way obtain a measurable arcback rate; the latter, in turn, would define the condition of the rectifier. This is the basis of the so-called "accelerated testing," which has provided the most extensive information so far available on the subject of backfiring.

While perfect confidence was perhaps never felt in the absolute independence of "causes" and applied voltage, tests of this author[2] showed that such accelerated testing may give very misleading information. Thus, a test at one voltage may show that condition "*A*" gives a higher arcback rate than "*B*"; while a test at another voltage may indicate that "*B*" gives a higher rate than "*A*." This author then proposed to test rectifiers at their rated voltages, obtaining the large arcback rate needed for statistical data by increasing the ion density at the tested anode. A method was developed,[3] in consultation with Dr. Slepian, based on application of an oscillatory condenser discharge to the tested anode. Other investigators[4, 5] have since independently developed and used similar methods for studying arcbacks. Unfortunately, it can hardly be expected that if increased voltage introduces new arcback causes, increased ionization will not do likewise.

This author believes that all arcback causes should properly be divided into two classifications: "crude" causes, and "fundamental" causes. Into the former classification would fall mercury droplets striking or leaving the anode; contamination on the surface of the anode; vacuum leaks; insulators lightly touching the anode; etc. Fundamental causes comprise only the effects of interaction of inverse current and voltage on a clean, homogeneous anode surface. To a limited extent, crude causes can be investigated by either of the methods of accelerated testing. Fundamental causes, on the other hand, are called into being by raised voltage and ionization, and their existence under conditions of exceptional stress gives no clue as to the behavior to be expected under normal stress.

What appears to be an example of the occurrence of both fundamental and crude causes is

* Part of a thesis presented to the University of Pittsburgh in partial fulfillment of the requirements for the degree of Doctor of Philosophy, January, 1942. The experimental work was carried out at West Virginia University.

[1] J. Slepian and L. R. Ludwig, Trans. A.I.E.E. (March 1932).

[2] J. E. White, Westinghouse Research Report R-6152-E (April 1931).

[3] J. E. White, Westinghouse Research Report R-8782-A (May 1932).

[4] Y. Watanabe and T. Takahasi, Electrotech. J. (March 1939).

[5] K. H. Kingdon and E. J. Lawton, G. E. Rev. (Nov. 1939).

given in a recent article.[6] In a rectifier operating under practically normal conditions, 40 arcbacks were found to occur near the instant of maximum inverse current, while the remaining 34 of those recorded occurred at random through the inverse period. It seems almost certain that the 34 which occurred at random, when the inverse current was low, were of the crude classification. Of the other 40, some may have been due to fundamental causes, or they may all have been due to a different type of crude cause, especially subject to "amplification" by inverse current.

Regardless of the interpretation of the tests just mentioned, they demonstrate forcibly one fact: At least until more is understood of the nature of arcbacks, investigations must be carried out with inverse current which varies with time; the effects of both instantaneous and previous values of ion current must be taken into account. It was with the purpose of developing an experimental technique for accomplishing this result, that the present work was undertaken.

II. EXPERIMENTAL METHOD

A. Description of Apparatus

The rectifier used in these experiments was a six-anode, Allis-Chalmers laboratory model, with control grids.

For complete flexibility in the tests, it was intended to apply negative voltage as desired to the anode, and furnish ions to produce arcback by means of a discharge to the grid. Due to the thickness of the grid and the narrowness of its openings, however, it was found impossible to produce arcbacks in this manner, so both ionization and negative voltage had to come from a circuit connected to the anode. It is highly desirable in future tests to provide a more open grid, so that the test voltage and ionization may be separately controlled.

Further extension of these tests will also require temperature control of the anode, which was not provided in this investigation. The tested anode was degassed in the normal manner at rated conduction current, and also by ion bombardment, but its temperature was low during all tests.

B. Functions Required of Circuit

It is clear from remarks in the introduction that, in order to obtain the desired results, statistical data must be taken throughout the negatively-charged interval of a periodically-stressed anode. Negative voltage and varying ion current must be applied to the tested anode at, say, commercial frequency, and during the negative period instantaneous observations of voltage, ion current, and arcback probability must be made. A single test should consist of a large number of observations of time of arcback occurrence, with "inverse" current and voltage repeating every cycle. (Ion current to the anode is called "inverse" current in agreement with terminology accepted for normally operating rectifiers.) In order to convert observations on the number of arcbacks occurring at any time to "arcback probability," it is likewise necessary to provide means for counting the total number of arcbacks which occur.

[6] W. E. Pakala and W. B. Batten, A.I.E.E. Tech. Paper 40–73 (Dec. 1939).

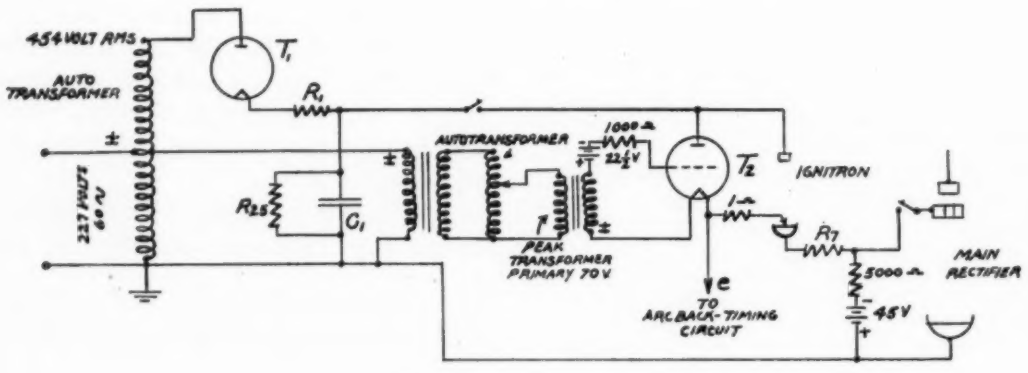

FIG. 1. Ionizing circuit.

C. Operation of Circuit

Aside from ignition and excitation circuits of the tested or "main" rectifier, which will not be described here, the connections used in making

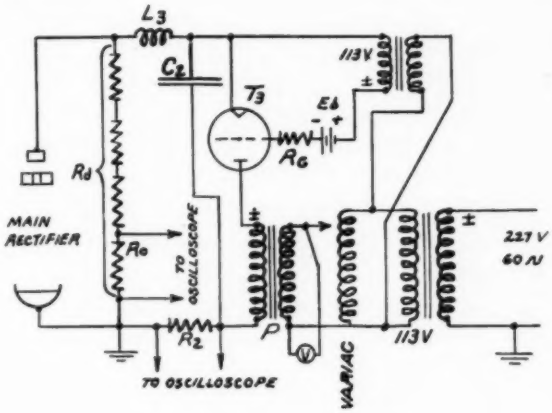

FIG. 2. Main anode circuit.

these experiments have been divided into three circuits, for greater clarity. The first of these is the so-called "ionizing circuit," Fig. 1.

The function of the ionizing circuit is to provide an impulse to the grid of the main rectifier, once per cycle, so that conduction from the tested anode is initiated. Condenser C_1 is charged from the line through an auto transformer and auxiliary phanotron, and discharges through the grid of the main rectifier when the thyratron T_2 is ignited by its peak transformer. With a differently designed grid on the main rectifier, it would be possible to control the magnitude and decay time of ion current to the tested anode by varying the magnitudes of C_1 and R_7. In these tests, however, very little ion current reached the tested anode from the discharge of C_1, and the magnitude and time constant of this current had to be changed by adjusting the constants of the main anode circuit and by controlling the vapor pressure in the rectifier.

The main anode circuit is shown in Fig. 2. The tested anode is held positive by the charge on C_2 until the rectifier grid is energized. An oscillatory discharge then flows from C_2, and at the end of the discharge the tested anode suddenly becomes negative, V_n volts with respect to the cathode. An arcback may occur at the instant of appearance of negative voltage on the anode, or at some "delay time" thereafter. The grid on T_3 prevents the voltage on C_2 from changing until a long enough time after negative voltage application for the arcback probability to have fallen essentially to zero. The resistance of R_d is so large (3.4 megohms) and of R_2 so small (0.4 ohm) that they did not affect the oscillatory discharge appreciably. Anode voltage before ignition, V_p, and after the oscillation, V_n, were measured using a cathode-ray oscilloscope with its plates directly connected across part of R_d. An oscillogram of these voltages is shown in Fig. 3, where time advances from right to left. The zero-voltage time during oscillation is not shown on this picture because of the low frequency timing used. (Several faint traces on the picture show abnormally low voltages. This was caused by occasional failure of the auxiliary ignitron to fire, and consequent ignition of the main anode when its voltage was not a maximum. This did not occur often enough to distort the data. The picture shown was taken with a 20-second exposure, and included 1200 cycles.)

Connection of the oscilloscope across R_2 made possible the measurement of the discharge current of C_2; the time of discharge of C_2; and the magnitude and wave shape of the inverse current.

Most complicated of the circuits employed is that used for timing and counting arcbacks, shown in Fig. 4. At the instant current begins to flow to the tested anode, thyratron T_8 ignites and

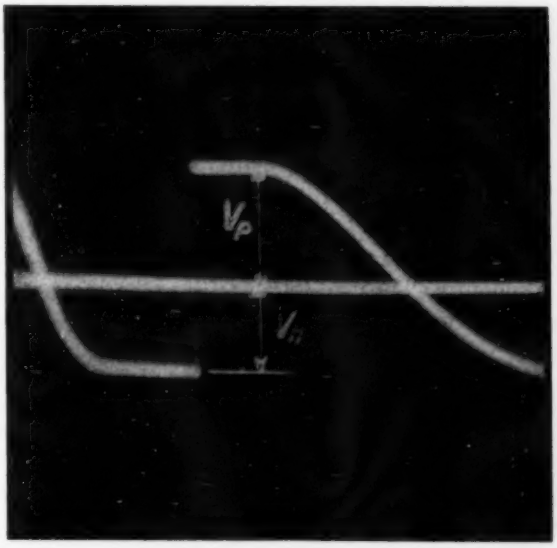

FIG. 3. Oscillogram of anode-cathode voltage.

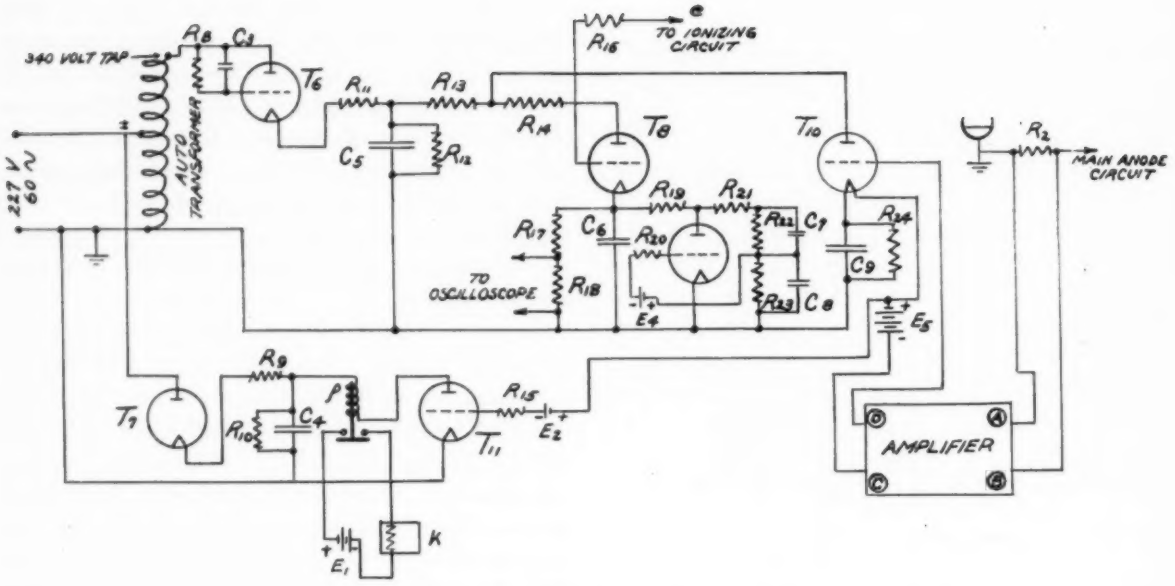

FIG. 4. Arcback-timing circuit.

condenser C_6 begins to charge from the ready-charged C_5. The voltage across C_6 continues to rise until an arcback occurs, at which time the current from C_5 instantly transfers from T_8 to T_{10}. The magnitude to which the voltage across C_6 rises is thus a measure of the "delay time" at which the arcback in question occurs. Thyratron T_9 is arranged as a "spark-gap," to ensure that the voltage across C_6 will always be zero when the main anode discharge begins, even if no arcback occurs.

Figure 5 shows the form of the voltage curve across C_6. The arrow at the top of the curve indicates the voltage at which T_9 ignites, if no arcback occurs.

From the "total delay time," between ignition of T_8 and T_{10}, must be subtracted the time during which conduction current flows to the main anode (9 to 16 μsec.), in order to find the actual amount by which arcback is delayed from the instant of negative voltage application. Further correction must be made for delays in amplifier response and firing times of T_8 and T_{10}. The firing time of T_8 and T_{10} were estimated from the data of Harrison,[7] and found to be small, and approximately to cancel; the amplifier response time was found to be negligible. Counter checks finally established the fact that the corrected delay time used in plotting curves, really gives the time elapsed between application of negative voltage and the occurrence of arcbacks, to within about one microsecond.

The counting function of the latter circuit is performed simply, and hardly requires explanation. Thyratron T_{11} ignites on arcback, and counter K responds to the accompanying closing of relay ρ.

D. Experimental Details

In order to obtain measurable deflections on the oscilloscope from the flow of inverse current through resistor R_2 (Fig. 2), the voltage across R_2 had to be amplified by a 2-stage amplifier. To test the applicability of the amplifier for this service, its output curve was investigated with an exponential input curve of time constant considerably less than the shortest used in subsequent measurements. Even under these conditions, input and output curves agree fairly well.

The inverse current magnitude corresponding to a given beam deflection depended on the time constant of decay of the current, because of the effect of the latter on the voltage amplification.

Inverse current-time measurements were made for widely differing tank temperatures and rates of current decay. A semilog plot of the results is

[7] A. E. Harrison, Trans. Elec. Eng. Supp., p. 747 (Dec., 1940).

shown in Fig. 6. The curves show that inverse current in these tests decayed exponentially, to a first approximation, until it reached 40 percent or less its initial value. Since subsequent arcback tests demonstrated that all arcbacks occurred before the inverse current fell to half its initial value, it was assumed that ion current always decayed exponentially. The time constant of decay was thenceforth determined by measurement of the peak value of the inverse current, and the slope of the curve at half maximum amplitude.

The maximum value of the inverse current is a function of the circuit parameters and of the positive anode voltage. Vapor pressure apparently affected the peak value of the ion current but little.

III. TEST RESULTS

A. Discussion of Curves

It is well known that statistical arcback data is difficult to repeat from day to day, and that a period of ion bombardment should precede any attempt to take such data.[8,9] After temperatures have been stabilized, application of voltage to the tested anode leads to an arcback rate which varies with time. A typical example of this is shown in Fig. 7. Data for comparison were always taken, as is customary, after the arcback rate had more or less stabilized.

The falling portion of such "stabilization curves" has been explained[9] as due to de-gassing of the anode. The rising portion represents a

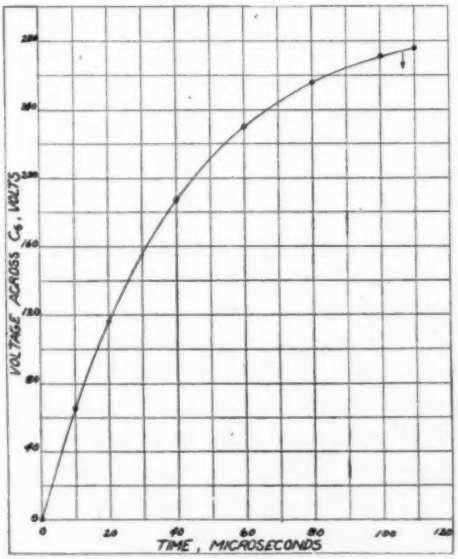

FIG. 5. Arcback-timing voltage.

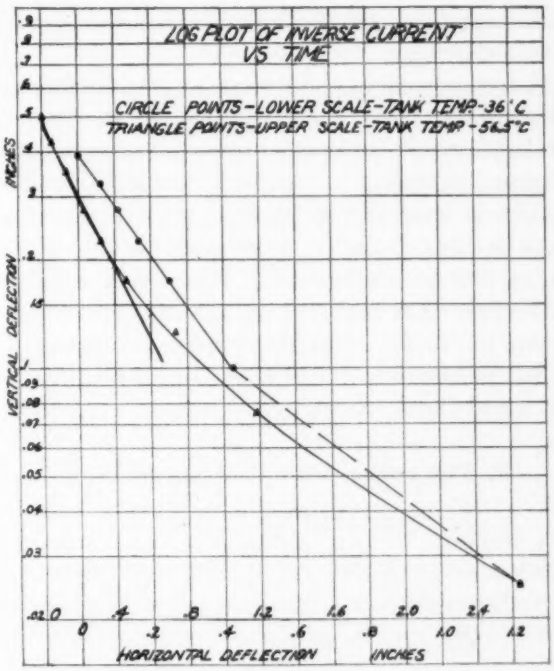
LOG PLOT OF INVERSE CURRENT VS TIME
CIRCLE POINTS-LOWER SCALE-TANK TEMP-36°C
TRIANGLE POINTS-UPPER SCALE-TANK TEMP-56.5°C
VERTICAL DEFLECTION INCHES
HORIZONTAL DEFLECTION INCHES

FIG. 6. Semi-log plot of inverse current *vs.* time.

phenomenon which, so far as I know, has never before been mentioned in published articles, although it was observed some years ago.[2] In the latter tests,[2] with all controllable conditions stabilized and anode temperature at 400°C, no arcbacks were observed for 4 minutes after applying voltage to the tested anode, although about 800 arcbacks occurred in a similar interval after the voltage had been on for some time. An explanation for both the rising and falling portions of the curve of Fig. 7 will be offered in the next section.

The variation of arcback rate with time constant of inverse current decay is shown for two different anode voltages, in Fig. 8. The peak value of inverse current was the same for all points on these two curves.

The probability of arcback occurrence at various intervals after the appearance of negative voltage on the anode was determined experi-

[8] J. E. White and W. Rigrod, Research Reports at V.E.I., Moscow, U.S.S.R. (1936–38).
[9] F. A. Maxfield and G. L. Fredenhall, J. App. Phys. **9**, 600 (1938).

mentally for a variety of conditions. Curves obtained for two conditions are shown in Figs. 9 and 10. For both of these curves, negative voltage appeared on the anode at $\tau_c=0$, and remained constant throughout the extent of the curves. In both, inverse current had its maximum at $\tau_c=0$. For Fig. 9, the inverse current decayed with a time constant $k=87\times10^{-6}$ sec.; for Fig. 10, $k=51\times10^{-6}$ sec.

Since arcbacks are produced under the influence of inverse current, one might expect the largest probability at $\tau_c=0$, when inverse current is the largest. Actually, a smaller probability exists here than later, in Fig. 10; and the "first peak" is even smaller in Fig. 9. Some distribution curves taken showed *no* first peak. It seems reasonable to suppose that many, if not all, arcbacks represented by the first peaks were due to fundamental causes; while those in the later, higher portions of the curves were due to crude causes.

B. Theoretical Interpretation of Data

1. Background for Assumptions

Since most of the arcbacks in these tests occurred considerably after the appearance of negative voltage on the anode and were apparently

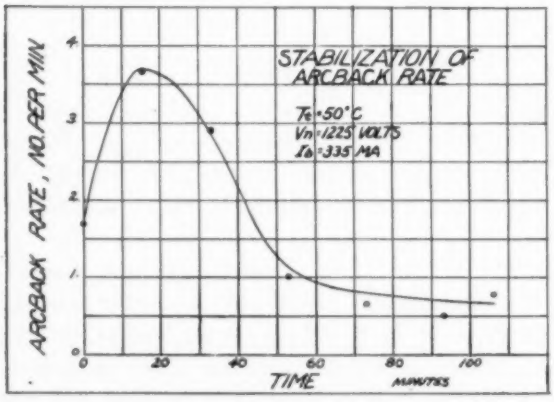

FIG. 7. Stabilization of arcback rate.

due to crude causes, only these delayed arcbacks will be considered theoretically. It is hoped that similar investigations will be carried out later under conditions in which crude causes are eliminated, so that fundamental causes can be studied to better advantage.

This author hesitates strongly to attribute to any one phenomenon the bulk of arcbacks occurring in commercial rectifiers. On the contrary, his experience has shown that the effects of operating conditions and design changes indicate that a number of factors may be responsible for these occurrences. Nevertheless, he believes that a given rectifier which consistently gives trouble usually does so primarily because of one predominating fault. Likewise in these tests, the decided similarity, and regularity, of the probability distribution curves emphatically suggest a single phenomenon as the instigator of most of the observed arcbacks.

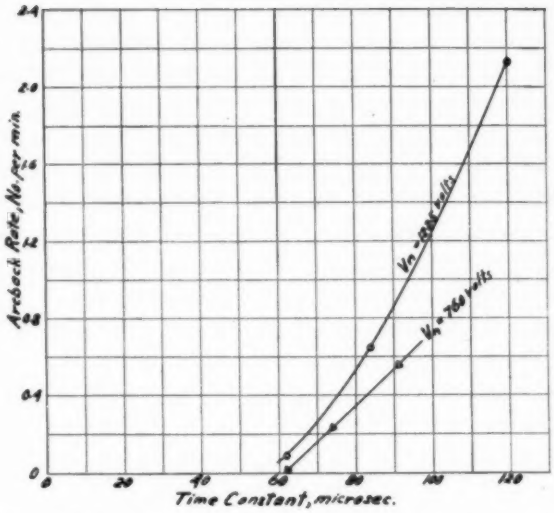

FIG. 8. Arcback rate as a function of the time constant of decay of inverse current.

Langmuir[10] suggested that insulating patches on the surface of an anode bearing negative voltage might cause arcback, and recent investigators[5] have also explained their results by the same mechanism.

While Kingdon and Lawton[5] infer that arcback may be caused by field emission of electrons from the surface of an anode under the action of gradient in a patch charged to as low as 2.8 volts with respect to the anode, this author believes that no patch can cause arcback unless the voltage across it is equal to or greater than the cathode drop of an arc in mercury vapor, which is of the order of 10 volts. This view is confirmed by the recent work of Fett.[11]

[10] I. Langmuir, Zeits. f. Physik **46**, 271 (1927).
[11] G. H. Fett, J. App. Phys. **12**, 436 (1941).

Stewart[12] showed that minute quantities of organic vapor are acted upon by high speed electrons or ions to form an insulating film on any solid material present. The films found by Stewart had puncture voltages of 4 to 14 volts, which is the correct order of magnitude to lead to arc formation. Rigrod and White[8] showed that vapor emitted by rectifier seal rubber operating at temperatures as low as 40°C produced a semi-permanent effect on the arcback rate of an experimental rectifier, as if films similar to those of Stewart had been formed. This evidence points to the likelihood that the rectifier tested here had an insulating organic film, or "patches," on the surface of its anode, since its rubber seals often reached temperatures of 60°C or more.

2. *The Patch Theory*

The mechanism suggested for arcback initiation, then, is as follows: The tested anode was partially covered with a thin, continuous or discontinuous, film of insulating organic material. "Patches" of this material may have been formed either by cracks or spaces, or merely by the limited mobility of ions on its surface. In the conducting direction, electrons can easily pass around the patches—or even go through them, since they will be shown later to be very thin and semi-conducting.* When the anode becomes negative, ions left in the plasma from the conducting period begin to charge up the patches. At first, the patch voltage is low, and no arcbacks occur. Later in the cycle, the gradient in the patches become large enough for puncture, and some of them begin to break down. Thin patches, which break down at low voltages (less than 10 volts) will not cause arcback, but thicker patches may do so. It is shown in the thesis from which this article is condensed, that if all patches have the same resistivity and dielectric constant, the gradient in all of them, regardless of area or thickness, is the same at all times. Arcbacks due to this cause should begin, then, when the gradient in the patches, G, first becomes equal to the minimum breakdown gradient in the patch material, G_0. As G becomes larger, arcback probability P should become larger, and P should reduce to zero when G has fallen again to G_0.

3. *Calculation of Gradient in Patches*

In order to calculate G, it is not necessary to know the area or thickness of the patches; the only information required is the resistivity ρ and the dielectric constant ϵ of the material which forms them. If ρ were a known function of ϵ, G would be absolutely determined from the fact that it must have identical values for two known delay times: t_1, when arcbacks begin, and t_2, when arcbacks cease. An independent determination of G could be made without the knowledge of t_1 and t_2, by merely assuming that G must reach a maximum at the same time as P does. In Fig. 9, G has been calculated by assuming t_1 and t_2 as the times when the central part of the P curve approaches zero. The maxima of G and P are seen to occur at nearly, but not quite, the same time. For Fig. 10, G was determined by making the maxima of the curves coincide. In both figures, G_0 is taken as a horizontal line intersecting G at t_1 and t_2, as nearly as these can be estimated. P does not fall quite to zero at t_1

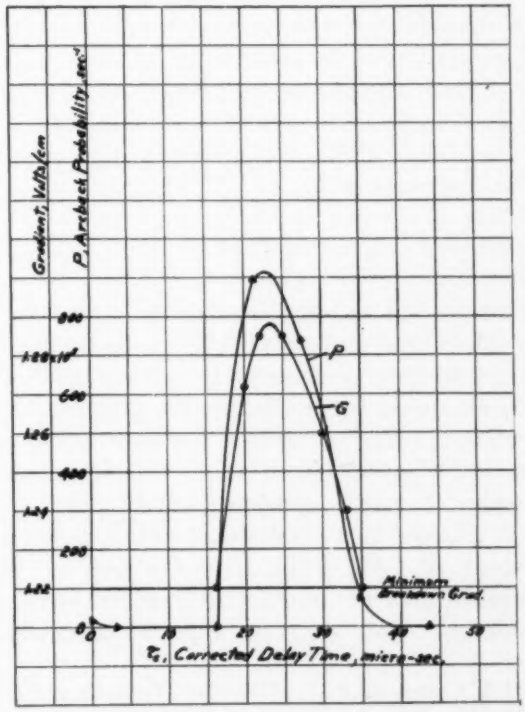

FIG. 9. Arcback probability, and calculated gradient in patches, *vs.* time after appearance of voltage on anode.

[12] R. L. Stewart, Phys. Rev. **45**, 488 (1934).

* Thin, semi-conducting films on conductors frequently have a rectifying property.

and t_2. This is no doubt due either to the presence of other arcback causes, or to the presence of patches with other than the prevailing resistivity and dielectric constant.

Since the exact nature of the patch material is not known, but ρ must be known as a function of ϵ in order to calculate G, it was assumed that ρ is the same function of ϵ as in the case of rubber with a carbon filler.[13] This assumption makes quantitative values doubtful; but patch material must surely be very like the material used as a model, since rubber vapor is the source of the patches, and carbonization under ion bombardment and in contact with a graphite anode is very likely. In the case of Fig. 9, 44.3 percent carbon filler gives the required results, with a resistivity of 1.087×10^7 ohm cm, and dielectric constant of 9.98. For Fig. 10, 45.05 percent carbon is required, with $\rho=7.75\times10^6$ ohm cm, and $\epsilon=10.1$.

4. *Size of Patches*

The thickness of patches involved in arcback production can be estimated from the calculated gradient. No patch with puncture voltage less than 10 volts can give arcback, which determines the minimum thickness; if no patches thicker than those observed by Stewart[12] are formed, the thickest patches may puncture at 14 volts. Using the minimum breakdown gradient from Fig. 9,

$$\frac{14 \text{ volts}}{1.22\times10^5 \text{ v/cm}}=11.47\times10^{-5} \text{ cm},$$

thickness of thickest patches.

The initiation of backfires here is very similar to that studied by Jurriaanse and Druyvesteyn,[14] who found that arcbacks could not be produced by a condenser discharged in contact with an electrode unless the condenser was charged with a certain minimum of energy. The figure given by them is $CV^2 \geqslant 18\times10^4$ cm volt^2. This figure, and assuming a patch condenser 11.47×10^{-5} cm thick, charged to 14 volts and with a dielectric constant of 9.98, leads to 0.133 cm^2 as the minimum area of patches involved in arcback production. This estimate may be somewhat high, as in the tests cited,[14] the authors made only 50 trials to determine whether arcback could be produced, while the tests made here usually included 40 or 50 thousand cycles. Nevertheless, it seems reasonable to suppose that patches of much less than 0.1 cm^2 area would not produce arcback on puncturing.

5. *General Expression for Arcback Probability*

A general expression for arcback probability per unit time, P, has been derived in the original thesis, and is of the form

$$P=(G-G_0)fn(GV_n^2). \tag{12}$$

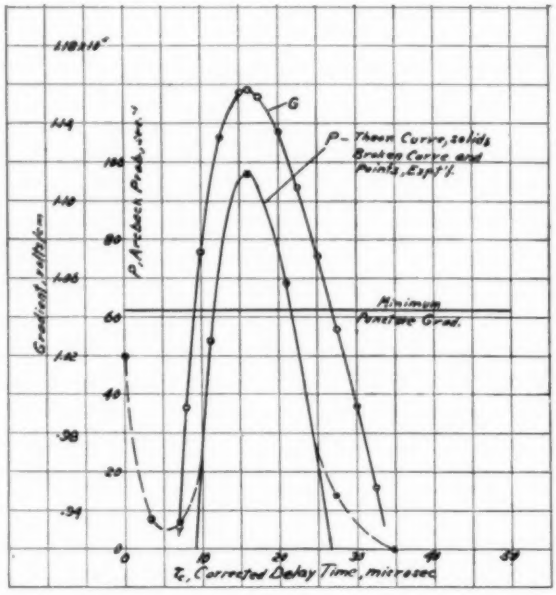

FIG. 10. Experimental and calculated arcback probabilities, and gradient in patches, *vs.* delay time.

Here, G_0 is the minimum breakdown gradient of the patch material, and V_n is the value of the negative voltage applied to the tested anode. This equation applies only to arcback caused by patch breakdown, and the form of $fn(GV_n^2)$ would be changed for different patch materials and patch size distributions.

The simplest form of Eq. (12):

$$P=KV_n^2G(G-G_0) \tag{13}$$

has been plotted on Fig. 10, with $K=8.34\times10^{-14}$ sec.$^{-1}$ volt^{-4} cm^2 and $G_0=1.044\times10^5$ v/cm. This curve is of the shape one would expect, from the

[13] H. L. Curtis and A. T. McPherson, Tech. Papers Bur. Stand. (Oct. 1925), p. 299.
[14] T. Jurriaanse and M. J. Druyvesteyn, Physica **3**, 825 (1936).

experimental points, for arcback due to patches of the predominating characteristics.

Equation (13) shows that arcback *rate* should be proportional to V_n^2, if K and G_0 are independent of V_n. It seems likely that G_0 will depend upon V_n, however, while K, from its dependence upon patch size distribution, will vary at random from time to time. Therefore, this equation cannot be relied upon to predict arcback rate for various values of V_n, unless the latter is changed rapidly, without permitting arcback rate stabilization, and unless the effect of V_n on G_0 is determined.

6. Other Arcback Phenomena Explained by Patch Theory

It is easy to explain both the rising and falling portions of Fig. 7 by means of the patch theory. As stated before, patches are formed by ion bombardment. Thus, first application of high voltage to an anode finds no patches present, and a low arcback rate. (If patches are present due to previous tests, the arcback rate will be high from the moment high voltage is applied. This is often observed.) As an insulating film is built up, arcbacks become more frequent until a certain time, when the rate of destruction or carbonization of patches begins to exceed the rate of formation. The curve of backfire rate will then fall.

Backfire-critical temperatures can also be explained readily on the basis of the patch theory. It was first observed some years ago,[2] and later confirmed by many investigators, that arcback rate begins to rise rapidly as the temperature of the tested anode is raised beyond 300 to 400°C. After going through extremely high values, this rate falls off rapidly beyond about 550°C. Looking at Eq. (13), it is seen that for low temperatures, G_0 may be as high as the maximum of G, so arcbacks due to patch breakdown would not occur. As the temperature is raised beyond a certain value, G_0 will begin to fall rapidly with increasing temperature, and the backfire rate will rise correspondingly. At still higher temperatures, the conductivity of the patch material will become great enough to prevent G from ever exceeding G_0, and again patch arcbacks disappear.

IV. CONCLUSION

The state of arcback investigation has reached a point where more detailed analyses of the mechanisms responsible for the phenomenon must be made. Recent work has shown that such analyses have to be based on experiments made under transient, rather than static, conditions of inverse current. An experimental procedure has been devised for obtaining such data, and employed in studying the behavior of a small, steel-tank rectifier. Evidence points to insulating patches on the anode surface as the principal cause of arcbacks in the tested rectifier, and many of the characteristics of the patches, deduced by matching arcback theory and test results, are such as would be expected from the hypothecated source of the insulating material. The effect of anode voltage on arcbacks due to patches has been discussed and the conclusions expressed in the form of an equation for arcback probability, which is satisfied by the experimental data.

The author would like to express appreciation to Dr. R. C. Mason, of the University of Pittsburgh and Westinghouse Electric, for helpful encouragement and criticism; and to Dr. Slepian, of Westinghouse, for permission to quote Westinghouse reports. Thanks are due likewise to the engineering staff and administration of West Virginia University, for facilities and encouragement.

Innovations in Instruments

Insulation Tubing for Low Temperatures

A new tubing with resistance to brittleness down to −50°C has been developed by the Fibron Division of Irvington Varnish and Insulator Company. This transparent tubing, known as Transflex, was made especially to secure continued, effective insulation on aircraft flying at high altitudes; and it has already been utilized by such companies as Douglas Aircraft and Curtiss-Wright. Its toughness and rubber-like qualities make it useful for a wide variety of other industrial and electrical applications. For instance, the transparency of Transflex permits quick location of wire breaks and ready identification of wires which have been snaked through it.

Transflex is a Fibronized tubing available from Size No. 14 to $\frac{3}{8}$-inch inside diameter; and it is extremely flexible as shown by the accompanying photograph. Its tensile strength is 3000 pounds per square inch. Its dielectric strength (conducted on a tubing with a wall thickness of approximately 0.020″) is 850 vpm when dry and 815 vpm when wet.

Other characteristics of Transflex tubing are: water absorption, 0.4 percent in weight after 24 hours immersion; Wemco oil test (48 hours at 100°C), not attacked; allowable continuous operating temperature, 150°F (66°C).

★

Mass Spectrometer for Gas Analysis

For industrial research, refineries, and chemical plants a mass spectrometer is announced by the Westinghouse Electric and Manufacturing Company. The unit is essentially a high vacuum tube containing electrodes, filament, slit system, and an electron collector. The gas or vapor to be studied is subjected to bombardment by a narrowly defined beam of electrons in the order of 10^{-6} ampere. The pressure of gas in the ionization chamber, where the bombardment takes place, is about 10^{-4} mm of mercury or lower. The ions thus formed are accelerated through two narrow parallel slits in two parallel plates at a potential difference of from 100 to 1000 volts. The ions emerge from the second slit as a narrowly defined beam of very nearly the same energy. This beam is then deflected by a uniform magnetic field designed to sort the ions according to their mass-to-charge ratio. Thus the spectrometer gives directly information about the relative abundance of different kinds of molecular ion fragments formed when the molecules of a particular kind are struck by electrons of known energy.

For quantitative indication of the gas to be measured, the ions strike a metal cup connected to ground through a very high resistance. The voltage developed across this resistor is fed to the grid of an electrometer tube. This amplifies the current so it can be read with a sensitive galvanometer.

The spectrometer has been used in studying patterns of organic molecules and in determining the purity of gas samples. Sensitivity in the case of air is one part in 100,000. Separation of mass 108 from mass 109 has been made.

Entire assembly is enclosed by steel panels having a black crackle finish except for the control panels which are Micarta. Panels are hinged for accessibility to all parts. The unit is mounted on a rubber-tired truck for complete portability. Only outside connections required are 110-volts a.c. and water connections for cooling the pumps.

★

Motion Pictures Available

Subjects of nation-wide interest are listed in the General Electric Company's colorfully illustrated 1942 motion picture catalog. Defense, x-ray, railroads, lighting, five of the famous "Excursions in Science," and a life of Thomas A. Edison are among the educational and commercial films offered. A variety of industrial films shows behind-the-scene workings of some of the country's most vital industries. Both sound and silent types are available, and several of the sound films are in full color. All are listed in the 16-mm size, and most of them also in 35-mm.

These motion pictures are free (except for shipping fees) to organized groups such as schools, churches, and social, civic, and business organizations in the U. S. Instructions for ordering prints are contained in the catalog GES-402G, which may be obtained by writing to the Visual Instruction Section, Publicity Department, General Electric Company, Schenectady, New York.

★

Acknowledgment

In the announcement in the March issue of the *Journal of Applied Physics* concerning the index for chemical analysis by x-ray diffraction, inadvertently the name of the Dow Chemical Company was omitted. This company has been most generous in publishing its data and in making available to the A.S.T.M. Committee its unpublished data.